PRESSURE DROP DUE TO THE PNEUMATIC CONVEYANCE OF GRAINS AND FORAGES

Thesis for the Degree of M. S.
MICHIGAN STATE UNIVERSITY

Jack Wilbur Crane
1956

PRESSURE DROP DUE TO THE PNEUMATIC CONVEYANCE OF GRAINS AND FORAGES

By

Jack W. Crane

AN ABSTRACT

Submitted Jointly to the Colleges of Engineering and Agriculture
Michigan State University of Agriculture and
Applied Science in partial fulfillment of
the requirements for the degree of

MASTER OF SCIENCE

Department of Agricultural Engineering

1956

Approved by H. F. McColly

4/20/56
J

Until recent years the only important use being made of pneumatic conveying systems on the farm was for filling vertical silos and granaries. Both of these applications involved only short conveying distances, usually less than 45 feet. Due to the short conveying length, an impeller blower was generally used. In most instances, and particularly in the case of grains, the individual particles received their energy, not from the air stream, but from the blower blades. This indicates that the static pressure drop within the pipe is not an important consideration in the design of such a system. However, mechanization in the materials handling field has brought about the use of pneumatic conveying systems for transporting grains and forages from their storage location to the feed parlor. This type of system could possibly involve several hundred feet of pipe including elbows and lengths of varying inclinations. An impeller blower would not prove adequate for such a system. Therefore, it would be necessary to convert to a truly pneumatic system in which the particles are introduced ahead of the blower and obtain their energy from the air stream. In this type of a system, it would be very important for the design engineer to be able to predict the static pressure drop for any situation in which the system might be used. The object of this research was to present equations which could be used to predict the pressure drop in a system, dependent only on the following variables:

1. Material being conveyed.
2. Solid flow rate.
3. Air velocity.
4. Pipe diameter.

5. Pipe length.

6. Pipe inclination.

Throughout the years, the problem of homogeneous fluid flow has been investigated, both experimentally and analytically, in a very thorough manner. However, there has been little attention given to pneumatic conveyance of solids. Almost all the work completed to date has been on an experimental basis with only a few investigators presenting a sound theoretical base for their experimental results. The few analytical developments which are available at the present time are of limited use, as they were set up for specific, and not general, situations. Pinkus (30) presented a very convincing theory for the case of horizontal flow, and his experiments with sand proved the validity of his initial assumptions. The theoretical analysis presented in this report was based on the same initial assumptions, however, it has been extended to include pipes of any inclination, thus making the resultant equations of more value to the design engineer. These equations have been derived, as is presented in the Appendix, and their validity has been proved for soft white winter wheat being conveyed in a 3.89 inch I.D. tube.

The equations, as well as the experimental results, indicate that the pressure drop due to the solids increased as the pipe inclination increased, with throughput and air velocity remaining constant. Also, the drop due to the solids increased as the air velocity decreased and the pipe angle increased.

It was observed during the experiment that the minimum air velocity which will carry wheat particles in a horizontal pipe was 65 feet per second. In a vertical pipe this velocity was 70 feet per second.

The maximum throughput of wheat in a 3.89 inch diameter pipe, which will allow smooth continuous operation, was approximately 57.82 pounds per minute.

PRESSURE DROP DUE TO THE PNEUMATIC CONVEYANCE OF GRAINS AND FORAGES

By

Jack W. Crane

A THESIS

Submitted Jointly to the Colleges of Engineering and Agriculture
Michigan State University of Agriculture and
Applied Science in partial fulfillment of
the requirements for the degree of

MASTER OF SCIENCE

Department of Agricultural Engineering

1956

ACKNOWLEDGEMENTS

The author wishes to express his sincere thanks to Doctor W. M. Carleton for his inspiring guidance and helpful suggestions during the investigation upon which this thesis is based.

He also wishes to thank Professor H. F. Mc Colly for his many helpful suggestions.

Grateful acknowledgement is due to Doctor A. W. Farrall, Head of the Department of Agricultural Engineering, for granting the Graduate Research Assistantship which enabled the author to complete this work.

The author sincerely appreciates the financial assistance of the New Holland Machinery Company of New Holland, Pennsylvania, which made this investigation possible.

Thanks are also due to the authors wife, Marilyn Crane, for her technical assistance on the subject of specialized photography. The many hours of secretarial work which she gave are also much appreciated.

TABLE OF CONTENTS

LIST OF FIGURES

INTRODUCTION

Reason for study

Pneumatic conveying systems have long been recognized as a labor-saving method of transporting solid particles. They were not generally introduced on the farm, however, until recent years, with the exception of the impeller blower used to fill vertical silos with various types of forages. Other than this one application, it was felt that pneumatic conveying systems, as used at that time, were too expensive and immobile for farm use. However, with the introduction of an impeller blower which could be used on grains, without fear of excessive damage, the number of these systems on farms steadily increased.

The impeller system does have one distinct disadvantage when conveying material which is susceptible to injury by impact. Since most of the energy is imparted to the particle by the impeller wheel, the particle has no immediate source of energy to draw upon to replenish that lost throughout the piping system. This means that the transporting distance is limited by the energy loss of the particle. If the system contains bends or long lengths of horizontal pipe where energy losses are great, the maximum transporting distance will be very short unless it is possible to operate the impeller wheel at relatively high speeds.

Mechanization in the materials handling field has brought about the use of pneumatic blowers as a source of energy for transferring grains and forages from the storage location to the feed parlor. Since a large portion of the conveying pipe will be in a horizontal or inclined position, with a large number of elbows, an impeller type system would not be suitable. However, the use of a truly pneumatic conveying system

offers interesting possibilities. Therefore, the remaining discussion will pertain only to the latter.

Objectives

The objectives of this research include: (a) theoretical derivation of an equation for the pressure drop, in pipes of any inclination, due to the friction of the solid phase and (b) experimental determination of the friction factors for various types of particles. With the above information, it will be possible to calculate the total pressure drop by assuming it to be composed of three parts:

1. Drop due to the friction of the solid phase.
2. Drop due to the air friction.
3. Drop due to the static head of the solids.

The static head component will vary from zero for horizontal pipes to a maximum value for vertical pipes.

The velocity of the particles within the pipe proved to be a very important parameter in the development of the pressure drop equation. Two expressions for the solids' velocity will be derived and tested. One assumes the coefficient of particle resistance as a constant, while the other assumes it is a function of Reynolds number.

After the above equations have been established, it will be necessary to verify the theoretical derivations by actual experimentation. The results of each investigation will be completely described in this study.

Limitations of the study

If unlimited time were available, it would be desirable to experimentally measure the pressure drop, dependent upon the following variables: velocity of the particles, solid flow rate, pipe length, pipe diameter,

and pipe inclination. However, due to the limited time of study, only one pipe diameter will be used to test the validity of the initial assumptions. Before the equations developed can be assumed generally correct, the effect of the other variable must be determined.

REVIEW OF LITERATURE

Throughout the years, the problem of homogeneous fluid flow has been investigated, both experimentally and analytically, in a very thorough manner. However, there has been little attention given to pneumatic conveyance of solids. Almost all the work completed to date has been on an experimental basis with only a few investigators presenting a sound theoretical base for their experimental results. The few analytical developments which are available at the present time are of limited use because they were set up for specific, and not general, situations.

Segler (32) gives the results of accomplishments, during the past twenty years, in the field of pneumatic grain conveying as applied on farms. This book covers the general field thoroughly; however, the design data presented are derived primarily from experimental results. Vogt and White (37) were partially successful in their attempt to derive expressions for pressure drops from the solid and fluid properties of the system. Experimental results were obtained from tests of the following particles: steel shot, clover seed, wheat, and sand. Hariu and Molstad (20) analyzed the pressure drop in vertical pipes. However, as was pointed out by the authors, the pressure drop due to the initial particle acceleration was accidentally included in their experimental data, thus obscuring results obtained from test runs with sand particles. Pinkus (30) presented a very convincing theory for the case of horizontal flow, and his experiments with sand particles proved the validity of his initial assumptions. An attempt will be made during this research project to alter and further extend his theory to grains and forages in pipes of varying inclinations. Lapple and Shepherd (23) developed equations for

calculating paths taken by particles undergoing accelerated motion. However, the value of this article is limited because the equations developed pertain only to an unconfined media. Chatley (8) in calculating the power requirements of a grain conveyor, recognized that the energy lost due to friction between solids and pipe wall should be accounted for in the energy balance, but states that no information is available for estimating this. Belden and Kassel (3) analyzed the pressure drop in vertical tubes in a manner similar to that of Vogt and White (37). Belden and Kassel verified their initial assumptions by transporting sand particles of various sizes in vertical pipes. Jennings (21) developed equations relating the acceleration of a particle to its limiting velocity in vertical transport. Dallavalle (10) presents an analysis of the air velocities required to support and carry particles of oats, wheat, and corn. He also presents a review of Cramp's work (9) relating the horizontal and vertical pressure drop due to the transportation of grain particles. Davis (11 and 12) developed equations which relate the air velocity required to lift and suspend particles of varying shape, size and density. Longhouse, Brown, Simmons and Albright (25) attempted to adapt a pneumatic transporting method used by the chemical industry to farm grains. Although their period of study was short, it was stated that the fluidization process looked promising. The bulk of the literature can be summarized by the following statements:

As previously mentioned, very little theoretical work has been completed on the subject of solid particles in fluid suspension. The large majority of that available emanates from work with catalytic cracking systems in the chemical industry. The bulk of the experimental

data has been developed from the horizontal and vertical transporting of farm grains. No data, experimental or analytical, could be found on the subject of transportation in inclined pipes, or truly pneumatic transportation of forages.

THEORY

The following primary symbols and subscripts apply to all equations developed in this study.

I. Primary symbols:

d - diameter of particle (feet)

D - diameter of duct (feet)

H - frictional head (feet of H_2O)

h - frictional head (inches of H_2O)

f - friction factor (dimensionless)

ρ - density (#/ft.^{3})

ρ_s - dispersed solids' density (#/ft.^{3} of pipe)

V - volume (feet^3)

μ - absolute viscosity (#/ft. sec.)

v - velocity (ft./sec.)

t - time (seconds)

s - distance (feet)

RN - Reynolds number (dimensionless)

P - pressure (#/ft.^{2})

N - quantity or number

m - mass of particle (# sec.^{2}/ft.)

L - length (feet)

G_s - solids' mass flow (#/ft.^{2}sec.)

g - constant of gravitational acceleration (ft./sec.^{2})

W - weight (#)

a - acceleration (ft./sec.^{2})

F_L - lift force (#)

F_D - drag force (#)

Θ - pipe angle from the horizontal (degrees)

A - area $(ft.)^2$

Q - flow rate $(ft.^3/sec.)$

II. Subscripts:

a - air

D - duct

ds - dispersed solids

f_s - solids friction factor

sh - static head

sf - solids friction

s - solids

p - particle

The following theoretical analysis will use as its base the work accomplished by Pinkus (30) and Hariu and Molstad (20). Pinkus investigated the pressure drop in horizontal pipes due to the flow of solid catalysts in a pneumatic system. Hariu and Molstad investigated the same phenomenon in vertical pipes, but used a somewhat different theoretical approach. Both of these investigations developed from work with catalytic-cracking systems in the chemical industry. Their interest was focused on particles of much smaller diameter than those encountered in agricultural pneumatic systems; however, the same type of theoretical analysis should apply in either case.

Four basic equations will be presented in this section. Three of

F_D - drag force (#)

Θ - pipe angle from the horizontal (degrees)

A - area $(ft.)^2$

Q - flow rate $(ft.^3/sec.)$

II. Subscripts:

a - air

D - duct

ds - dispersed solids

f_s - solids friction factor

sh - static head

sf - solids friction

s - solids

p - particle

The following theoretical analysis will use as its base the work accomplished by Pinkus (30) and Hariu and Molstad (20). Pinkus investigated the pressure drop in horizontal pipes due to the flow of solid catalysts in a pneumatic system. Hariu and Molstad investigated the same phenomenon in vertical pipes, but used a somewhat different theoretical approach. Both of these investigations developed from work with catalytic-cracking systems in the chemical industry. Their interest was focused on particles of much smaller diameter than those encountered in agricultural pneumatic systems; however, the same type of theoretical analysis should apply in either case.

Four basic equations will be presented in this section. Three of

F_D - drag force (#)

Θ - pipe angle from the horizontal (degrees)

A - area $(ft.)^2$

Q - flow rate $(ft.^3/sec.)$

II. Subscripts:

a - air

D - duct

ds - dispersed solids

f_s - solids friction factor

sh - static head

sf - solids friction

s - solids

p - particle

The following theoretical analysis will use as its base the work accomplished by Pinkus (30) and Hariu and Molstad (20). Pinkus investigated the pressure drop in horizontal pipes due to the flow of solid catalysts in a pneumatic system. Hariu and Molstad investigated the same phenomenon in vertical pipes, but used a somewhat different theoretical approach. Both of these investigations developed from work with catalytic-cracking systems in the chemical industry. Their interest was focused on particles of much smaller diameter than those encountered in agricultural pneumatic systems; however, the same type of theoretical analysis should apply in either case.

Four basic equations will be presented in this section. Three of

them will be of practical use to the designer, while the other will be used only to obtain the solids' friction factor (f_s). It is necessary to determine this constant since it appears as a variable in each of the other three expressions. These equations will later be proved or disproved by the experimental data obtained.

"f_s" will be experimentally determined from the following expression:

$$f_s = \frac{D\left[\rho_a C A_p (v_a - v_s)^2 - 2 g v_p \rho_p \operatorname{Sin} \theta\right]}{V_p \rho_p v_s^2} \qquad (5)$$

A complete derivation of this constant is given in the Appendix under Section I.

As can be seen from equation 5 the velocity of the solids is a very important parameter in the experimental determination of "f_s". This can be determined from measurements of the mass flow rate (Gs) and the density of the dispersed solids (ρ_{ds}). The relationship which enables this calculation to be made is as follows:

$$v_s = \frac{G_s}{\rho_{ds}}$$

Dimensionally the equation becomes:

$$\frac{\text{ft.}}{\text{sec.}} = \frac{\text{lb./ ft.}^2 \text{ sec.}}{\text{lb./ft}^3}$$

This expression will be used extensively throughout the analysis.

The following equation will be used to predict the total pressure drop in a given length of pipe.

$$\Delta H = \frac{f_s v_s L_D G_s}{2 D g \rho_{H_2O}} + \frac{G_s L_D \sin \Theta}{v_s \rho_{H_2O}} + \frac{f_a L_D v_a^2 \rho_a}{2 D g \rho_{H_2O}} \qquad (6)$$

The derivation of this equation is given in the Appendix under Section I.

Assuming that the solids' friction factor (f_s) has been determined experimentally, the only other unknown preventing the practical use of equation 6 is that of the velocity of the solids. Two expressions for "v_s" will be presented here. The derivation of these expressions will be found respectively in Sections II and III of the Appendix. The range over which each of these expressions is valid is shown by Figure I. This figure shows an experimental plot of "C" (drag coefficient) versus "RN" (Reynolds number) as presented by Dallavalle (10). In effect, this curve permits the force due to the air stream, exerted on a particle to be calculated for any given slip velocity. The two other curves shown are assumptions made to derive the two expressions for the particle's velocity. One assumes "C" as a constant equal to 0.44, while the other assumes "C" as a function of "RN" and equal to $0.4 + \frac{40.}{RN}$. The range over which the assumed curves approximate the experimental curves, and therefore the range over which the assumptions are valid, is as follows:

1. Assuming "C" as a constant, the range of "RN" is between 10^3 and $10^{4.5}$.
2. Assuming "C" as a function of "RN" and equal to $0.4 + \frac{40.}{RN}$, the range of "RN" is from $10^{0.5}$ to $10^{4.25}$.

The latter case should encompass the entire range of velocities

Fig. 1

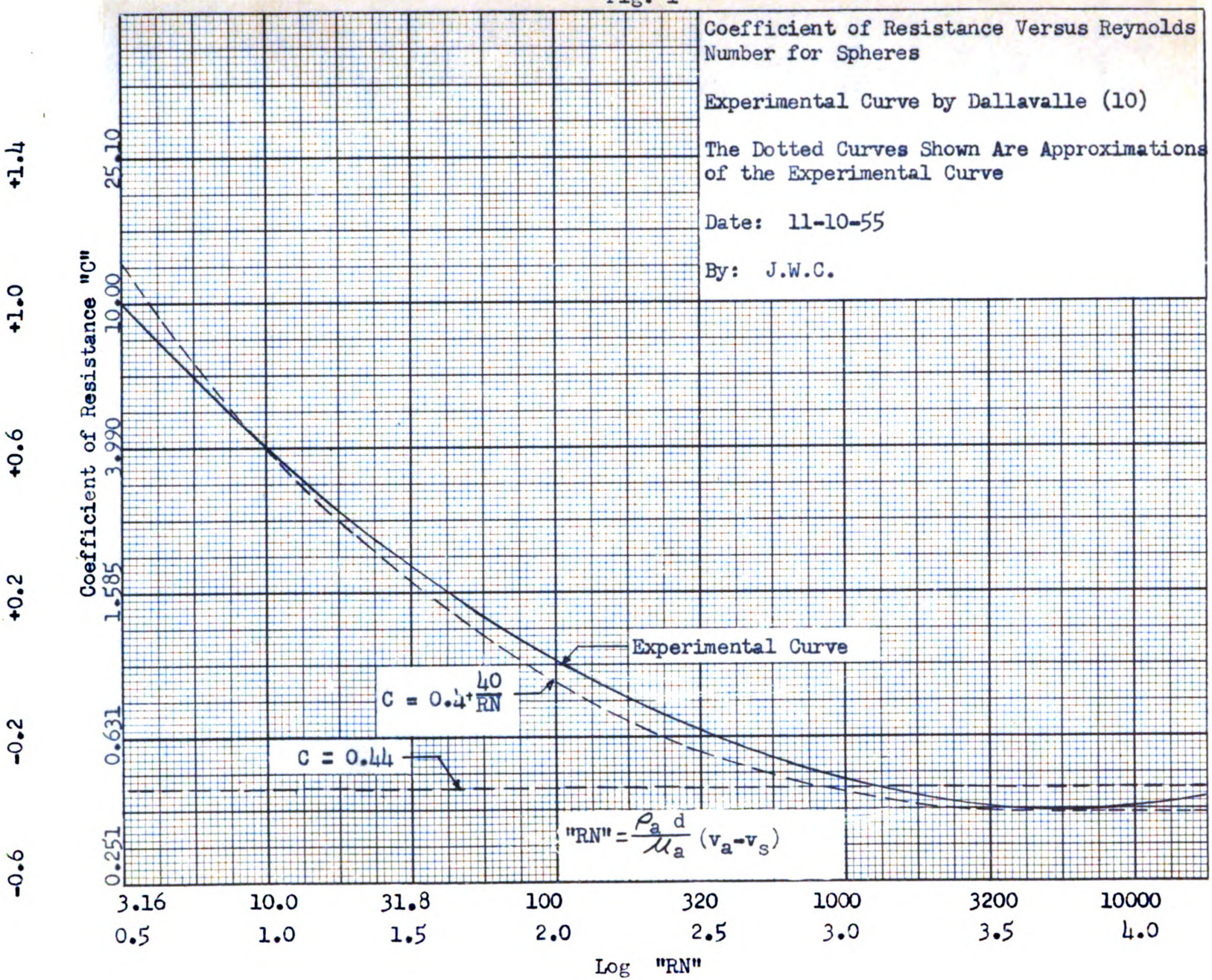
Coefficient of Resistance Versus Reynolds Number for Spheres
Experimental Curve by Dallavalle (10)
The Dotted Curves Shown Are Approximations of the Experimental Curve
Date: 11-10-55
By: J.W.C.
Log "C" = Log $\frac{2 g F}{\rho_a (v_a - v_s)^2 A_p}$
Coefficient of Resistance "C"
25.10
10.00
3.990
1.585
0.631
0.251
-0.6
-0.2
+0.2
+0.6
+1.0
+1.4
Experimental Curve
$C = 0.4 + \frac{40}{RN}$
$C = 0.44$
"RN" = $\frac{\rho_a d}{\mu_a} (v_a - v_s)$
3.16
10.0
31.8
100
320
1000
3200
10000
0.5
1.0
1.5
2.0
2.5
3.0
3.5
4.0
Log "RN"

found in farm pneumatic conveying systems.

The two expressions for the velocity of the particles are as follows:

(1) Assuming "C" equals a constant:

$$v_s = \frac{D\left[\rho_a C A_p v_a^2 - 2 m g^2 \operatorname{Sin}\theta\right]}{\rho_a C A_p v_a D \sqrt{m g D}\sqrt{\rho_a C A_p (2 g D \operatorname{Sin}\theta f_s v_a^2) - 2 m g^2 f_s \operatorname{Sin}\theta}} \qquad (7)$$

(2) Assuming "C" = f (RN) = $0.4 \frac{40}{RN}$

$$v_s = \frac{-2 C_3}{C_2 - \sqrt{C_2^2 - 4 C_3 C_1}} \qquad (8)$$

The constants in equation 8 are:

$$C_1 = \frac{0.2 A_p \rho_a}{m g} - \frac{f_s}{2 D}$$

$$C_2 = -\left[\frac{0.4 A_p v_a \rho_a}{m g} + \frac{20 A_p \mu_a}{m g d}\right]$$

$$C_3 = \frac{0.2 A_p \rho_a v_a^2}{m g} + \frac{20 A_p \mu_a v_a}{m g d} - g \operatorname{Sin}\theta$$

Since equation 7 is valid over only a small range of "RN", the use of the more general expression given by equation 8 is recommended.

It is now possible for the engineer, using equations 6 and 8, to calculate the pressure drop in any straight section of pipe where steady state conditions prevail (acceleration of the particles equals zero) knowing only the design specifications.

APPARATUS

After the theoretical analysis was completed, it was necessary to construct a test apparatus which could be used to prove or disprove the equations derived. Since the individual measurements which must be made during a test cycle consume appreciable time, it was felt that a continuous system would have a distinct advantage over the type in which it was necessary to recharge the hopper manually. It was also necessary to design the system so that the test section could be adjusted to any angle between 0^{o} and 90^{o}. This was accomplished by placing a slip joint between two 90^{o} elbows as shown in the layout of the test apparatus (Fig. 2). The pipe used throughout the system, with the exception of the 90^{o} elbows, was four inch (outside diameter) aluminum irrigation pipe. This particular diameter was chosen for its ease of handling, low cost, and availability. Any diameter, within a reasonable working range, would function equally well since this variable is included in the development of the pressure drop equations. One possible source of error in the system is the variation in the friction factor which would be present between aluminum tubing and the steel tubing, the latter being used in most actual pneumatic systems. This error is assumed to be negligible, since after each type of tubing becomes internally polished, the two friction factors will be very nearly equal. Even if there were an appreciable difference, the resulting error in the experimentally determined friction factor (f_s) would be small. This is evident when the three subdivisions of the total pressure drop are examined. As stated in the Theory Section of this report, these errors are:

1. That due to the air alone.
2. That due to the particles striking each other and the pipe wall.
3. That due to the solids' static head.

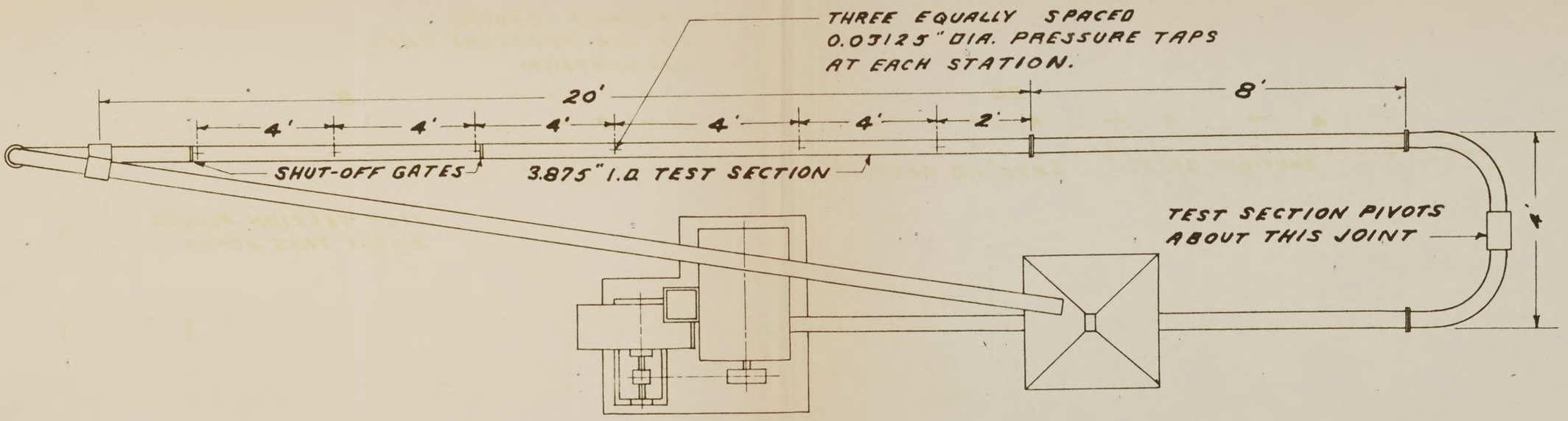

FIG. 2 EXPERIMENTAL PNEUMATIC SYSTEM USED TO MEASURE PRESSURE DROPS

The first component can be determined for any type of system since, as was previously mentioned, the problem of homogeneous flow has been thoroughly investigated.

The third component does not depend upon any friction factor.

The second part of the second component is the only source of error due to the use of a different tube material.

The blower used with the system was of the low-pressure type with radial, forward-curved blades. While backward-curved blades would have improved the efficiency slightly, the former type has two distinct advantages, these being:

1. A lower shaft speed for a given capacity.
2. Less variation in air velocity if the resistance of the system is varied.

The diameter of the fan was 20 inches. Its maximum capacity, in terms of static head, was 17 inches of water at a shaft speed of 2800 R.P.M.

A variable speed electric motor in the three to five H.P. range would have been an ideal source of power for the blower. However, since this was not available, a portable 30 H.P. internal combustion engine was used. In an actual installation, where variation in blower speed is not necessary, an electric motor would be the most practical power unit.

The quantity of air flowing through the pipe was measured by a thin plate orifice placed in the system approximately two feet before the solids' inlet. This orifice constricted the pipe area by 19.4%. The physical dimensions of the orifice, as well as the orifice coefficient, were taken from reference 29. The laws applying to the flow of liquids through orifices hold only if the liquid is incompressible. Therefore,

if the fluid flowing is air, some correction factor must be included in the orifice equation if the results are to be accurate. To determine the magnitude of this correction factor for this specific situation, the assumption was made that the orifice pressure differential would never exceed ten inches of water. This assumption proved overly sufficient when the actual testing began. This gives an absolute pressure ratio $\frac{P_1}{P_2} = \frac{400}{410}$ equal to 0.975. The numerator of this fraction represents standard absolute pressure in inches of water. The compressibility correction factor therefore, varies from 0.98, for a 0.00 inch pressure differential (Ref. #29). Since this factor was so nearly unity, it was neglected in the derivation of the orifice equation.

The equation for the velocity of the air is as follows:

$$v = \frac{65.6\ C}{\sqrt{\left[\frac{D_1}{D_2}\right]^4 - 1}} \sqrt{\Delta h} \qquad (14)$$

Where:

v velocity-ft/sec.

D pipe diameter - ft.

h static head in inches of water

1 and 2 are, respectively, locations before and at the orifice.

This equation was derived assuming an atmospheric pressure of 29.92 inches of Hg and a temperature of 50° Fahrenheit.

For this specific situation, equation 13 further simplifies to:

$$v = 44.25 \sqrt{\Delta h} \qquad (15)$$

This expression was used to construct the graph in Fig. 3.

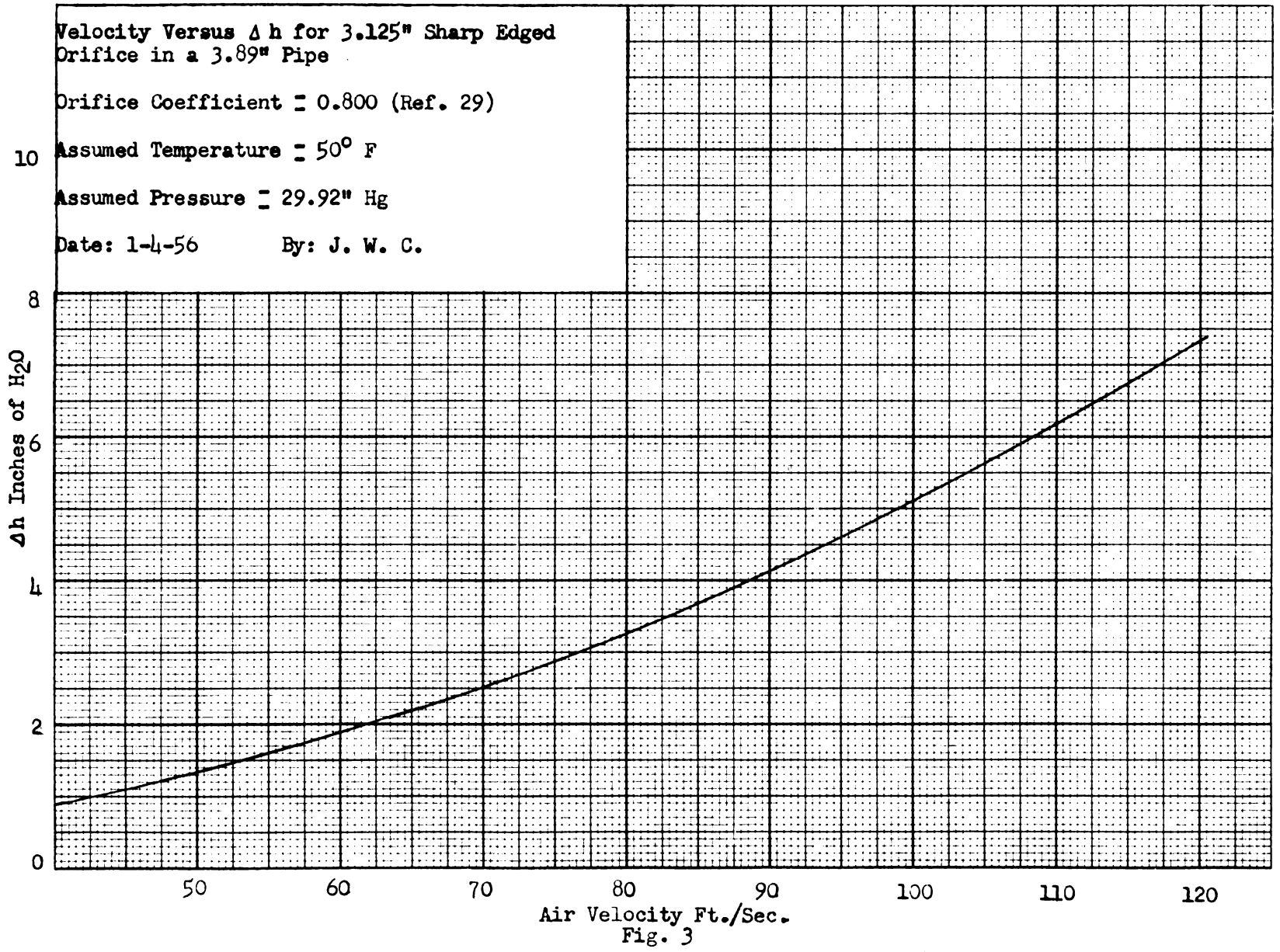
Velocity Versus Δ h for 3.125" Sharp Edged Orifice in a 3.89" Pipe
Orifice Coefficient = 0.800 (Ref. 29)
Assumed Temperature = 50° F
Assumed Pressure = 29.92" Hg
Date: 1-4-56 By: J. W. C.
Δh Inches of H2O
0
2
4
6
8
10
50
60
70
80
90
100
110
120
Air Velocity Ft./Sec.
Fig. 3

As was mentioned earlier, it is essential that the velocity of the particles be known before the value of the solids' friction factor (f_s) can be computed. There are two methods which can be used to determine this value. The first, and perhaps the most obvious, would be to directly measure the velocity of some particle within the pipe. The second method would be to indirectly obtain the velocity by measurement of the mass flow rate (G_s) and the density of the dispersed solids (ρ_{ds}), after which the velocity is computed using the following expression:

$$v_s = \frac{G_s}{\rho_{ds}}$$

This equation is more completely described in the Theory Section of this report.

The first procedure considered involved the use of radioactive tracers. It was thought that if a few particles could be irradiated and mixed with the rest of the mass, their path through the pipe could be traced by a radiation-pickup instrument. If the time could be recorded for a given length of path, the velocity could in turn be computed. However, after discussing the instrumentation problem with Professor Montgomery of the Michigan State University Physics Department, it was decided that while the idea was theoretically feasible, it was financially impractical.

The next method considered involved the use of photography. The basic idea was as follows: A transparent tube, with an attached scale, was to be placed in the actual test section. Then as the particles moved through this section, a camera mounted approximately four feet away exposed a sheet of film for a predetermined time. The average length of

the streaks could be determined from the scale on the transparent tube. The exposure time would be recorded so the velocity could be determined by:

$$v_s = \frac{\text{length of streak}}{\text{shutter speed of camera}}$$

There were two minor sources of error in this system. The first was caused by the possible variation in the depth of field. In other words, the particles which were being photographed could have been on one or the other extremes of the pipe wall (the scale was in the center) which would cause variations in the apparent lengths of the streaks. However, as the distance between the camera and objects increased, the error would decrease. The second source of error lies in changing the surface of the test section which would change its frictional characteristics. However, this change would be relatively small as explained earlier in this section.

A small test set-up shown in Fig. 4 was constructed to determine the feasibility of the method just described.

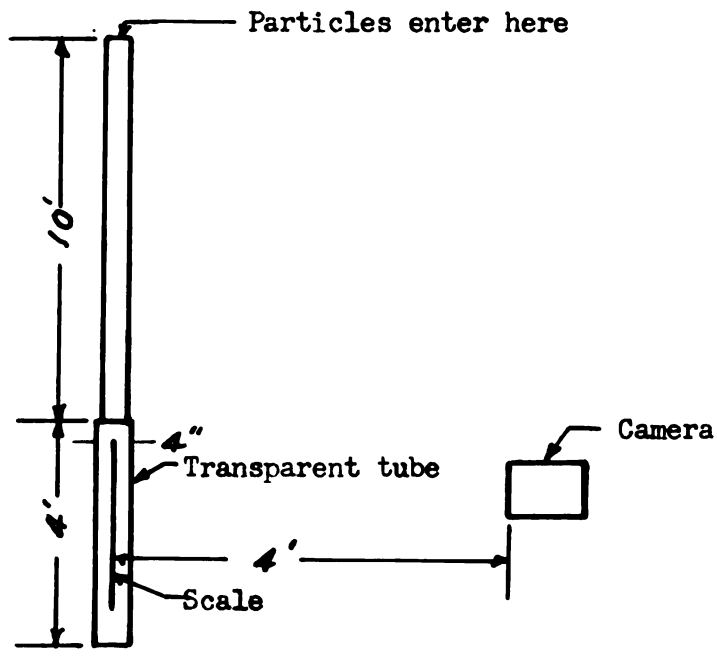

Fig. 4. Test set-up used to determine the solids' velocity by the photographic method.

A speed graphic camera with a focal-plane shutter was used to expose the film. The shutter speed was varied from 1/60 second to 1/400 second. Five #2 photofloods were used as illumination. Photographs were taken with and without a polarizing filter. The use of this filter reduced glare, but also restricted the amount of light passing through the lens.

Particles of beans and wheat were used in these tests. A small number of the individual particles of each type were painted black. This was done with the hope that perhaps the contrasting particle color would produce a well defined streak on the film. This idea proved false as is evident from Fig. 5.

The first series of pictures were taken through a four-inch lucite tube using super panchro press type "B" film. With the photofloods illuminating the plastic tube, the particles were dropped through the upper end, (approximately ten feet above the test section.) Streaks, due to both the natural and painted particles, were easily visible to the naked eye. Sixteen exposures were made with varying shutter speeds and lighting arrangements. Also, since the reading observed on the light meter was measuring only the light around the exterior of the tube, and not that present on the interior, it was necessary to allow more light than the meter recommended. This amount was varied from the correct amount (on the meter) to the maximum allowable on the camera.

Upon development, the negatives gave a perfect picture of everything outside the tube but absolutely nothing was visible on the inside. This indicated insufficient light was penetrating the tube wall. The reason for this was traced to the fact that plastics are excellent

diffusers of light and therefore, while the outside of the tube was well illuminated, the light waves never reached the particles inside the tube in sufficient quantity to allow a picture to be taken.

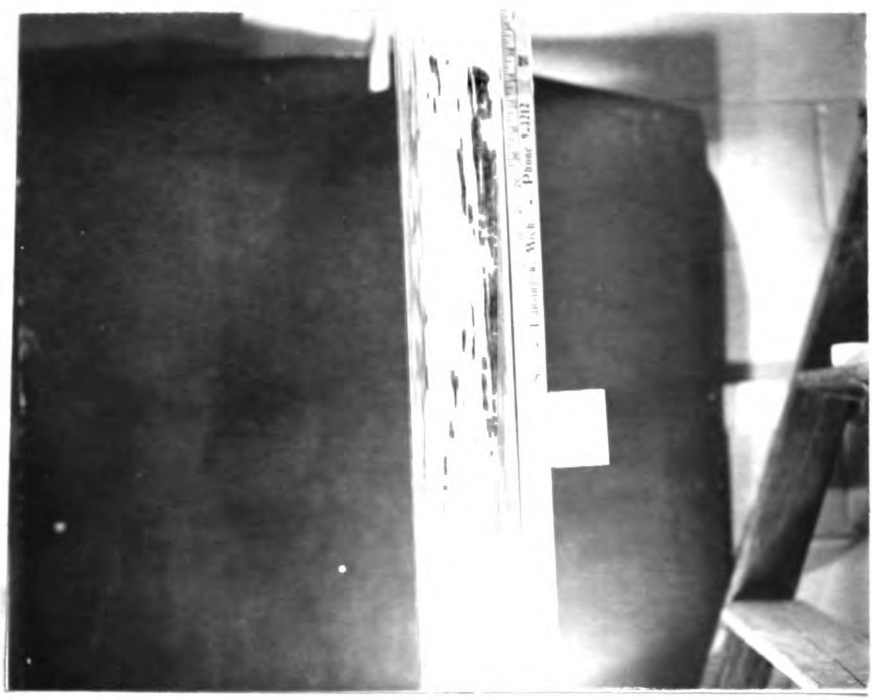

Fig. 5. Natural and painted particles of wheat falling through a 4" I.D. glass tube. Picture taken with Royal-Pan film at a shutter speed of 1/50 sec. and a lens opening of 5.6.

Before the second series of pictures were taken, a four inch glass tube was substituted for the plastic one and special high speed Royal-Pan film was used in the camera.

The development of these films proved that the lighting problem had been solved but in its place had appeared another. This problem is clearly evident in Fig. 5. With a large number of particles in the pipe it is impossible to distinguish between individual streaks. Fig. 6 shows that if the density of particles is very sparse, the method gives excellent results. This again suggests the possibility of attempting to distinguish a few particles from the whole mass. A possible way of accomplishing this would be to paint a few particles with luminous paint and then expose the film in a dark media. This presented more instrumentation problems, however, and it was felt that too much time was being spent on this phase of the project.

The two methods of measuring "v_s" discussed thus far are that of radioactive tracers and photography. While neither of these methods were actually used, they both presented interesting possibilities. However, both have one common defect. It is impossible to accurately measure the average velocity of particles when the system is composed of particles which vary widely in their size range. This problem becomes serious when any type of forage material is being transported through the pipe. This method would, however, work well for uniform size particles such as would be found in the pneumatic conveyance of farm grains.

The method of measuring "v_s" finally decided upon involved the use of the following relationship. As stated earlier in this section, it is:

$$v_s = \frac{G_s}{\rho_{ds}}$$

Fig. 6. Natural colored particles of wheat falling through a 4" I.D. glass tube. The particles are just entering the glass section as is indicated by the lines in the upper part of the photograph. Royal-Pan film was used at a shutter speed of 1/50 sec. and a lens opening of 4.5.

With "G_s" known from initial conditions, and "ρ_{ds}" determined from measurement, the velocity of the solids' can be calculated. The method used to measure the density of the solids in the pipe "ρ_{ds}" was as follows: Two half-round, air-tight, spring-loaded, shut-off valves were placed in the actual test section. These valves, as they are located on the pipe, are shown in Fig. 7. The trigger mechanism of the valves is synchronized to allow the two gates to close instantaneously, thus blocking off a section of the test pipe. An instant later another spring loaded valve stops the inflow of particles at the hopper. Now all that remains is to remove the particles in the blocked portion of the pipe, weigh them, and divide by the volume of the blocked portion of pipe, thus giving "ρ_{ds}".

This system has a distinct advantage over the other two in that it is applicable to any system of particles, uniform or irregular, since it is not dependent upon any one particle but rather on the whole mass.

Assuming the velocity measurement problem solved, the method of entering the particles into the air stream will be discussed.

Three basic methods of introducing solid particles into pneumatic conveying pipes are in general use. These are:

1. The injector feeder, or constricted area type, for low-pressure systems.
2. The auger-feeder for low to medium pressures. Since this type does not provide a complete air seal, it is usually used in conjunction with an injector feeder.
3. The bucket-wheel feeder for high pressure systems.

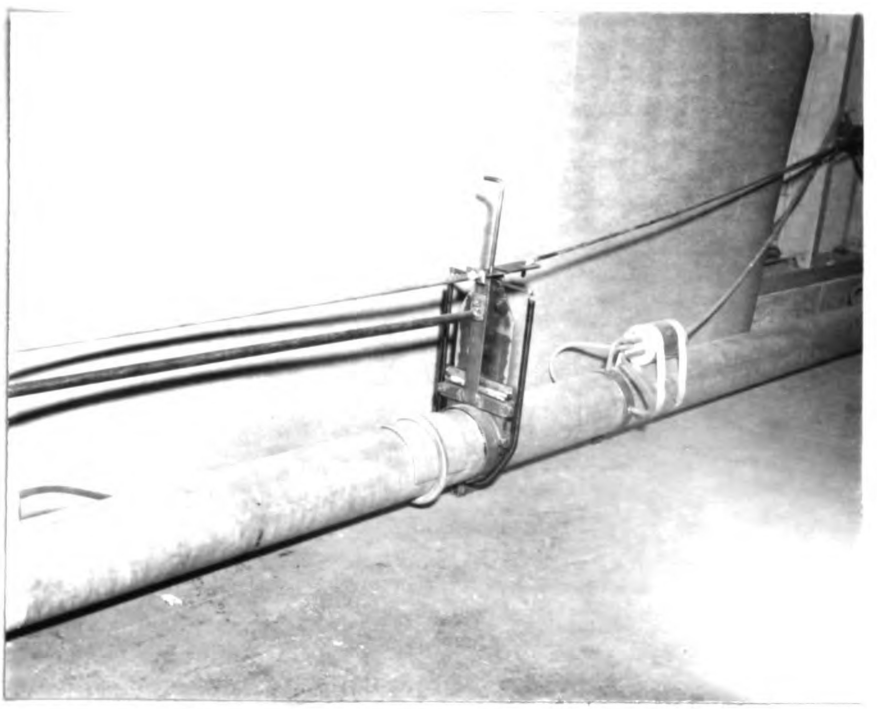

Fig. 7. Method by which each of the two half-round, spring-loaded, shut-off valves are attached to the test pipe.

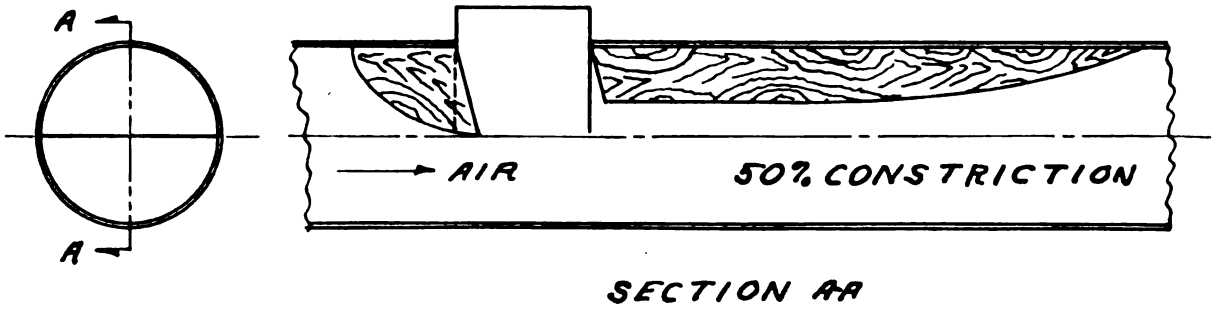

SECTION AA

FIG. 8

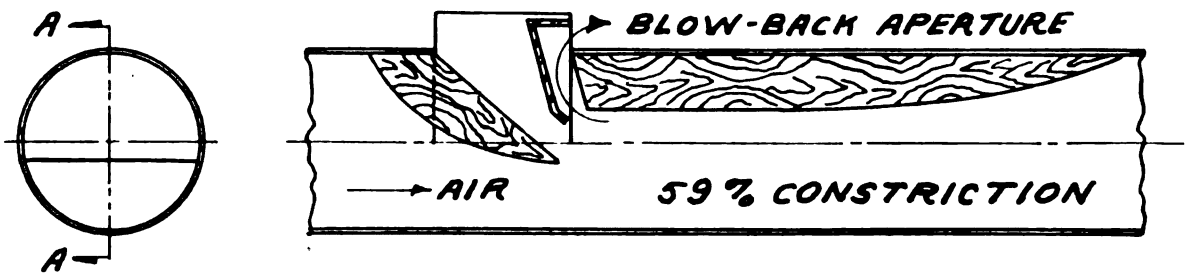

SECTION A-A

FIG. 9

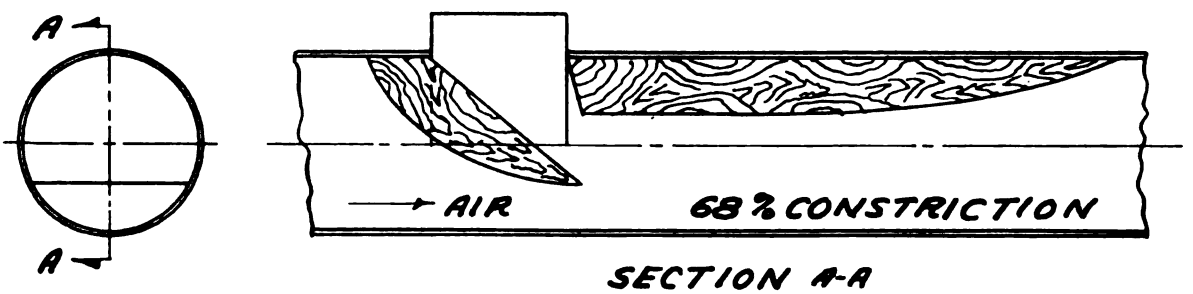

SECTION A-A

FIG. 10

SCALE 3"=1'

INJECTOR FORMS USED

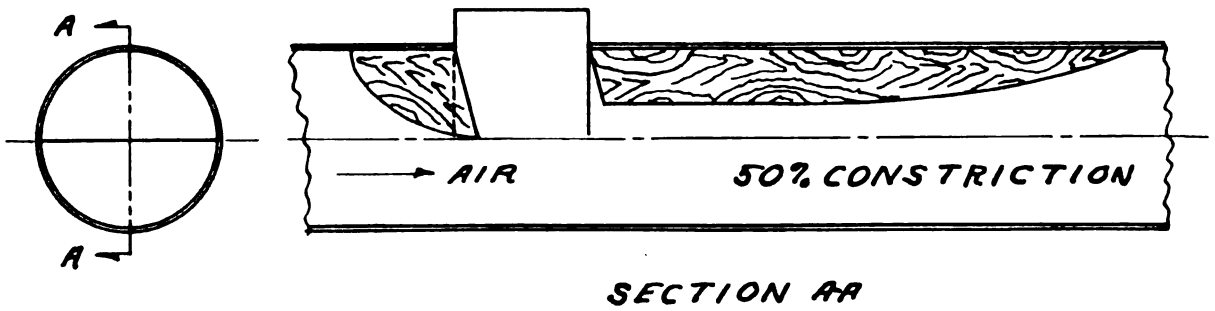

SECTION AA

FIG. 8

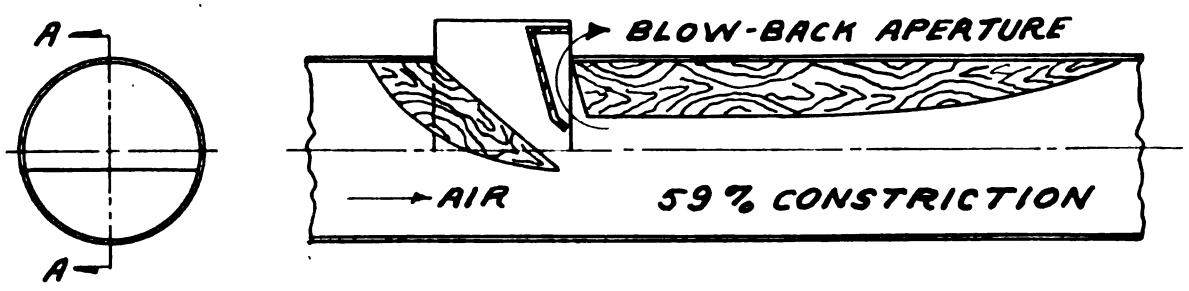

SECTION A-A

FIG. 9

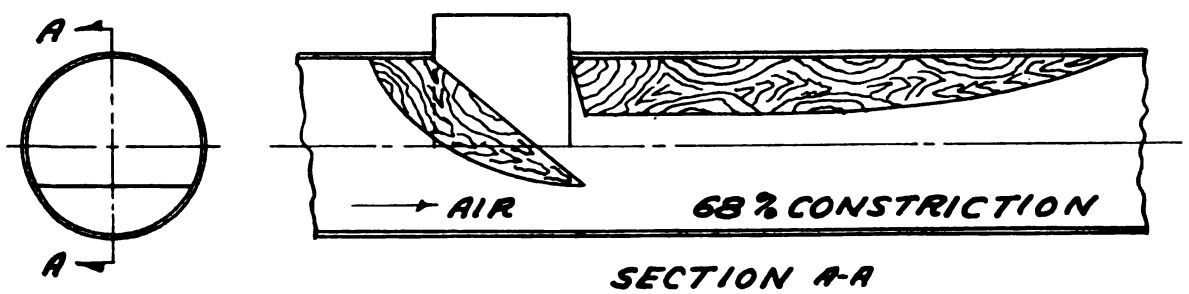

SECTION A-A

FIG. 10

SCALE 3"=1'

INJECTOR FORMS USED

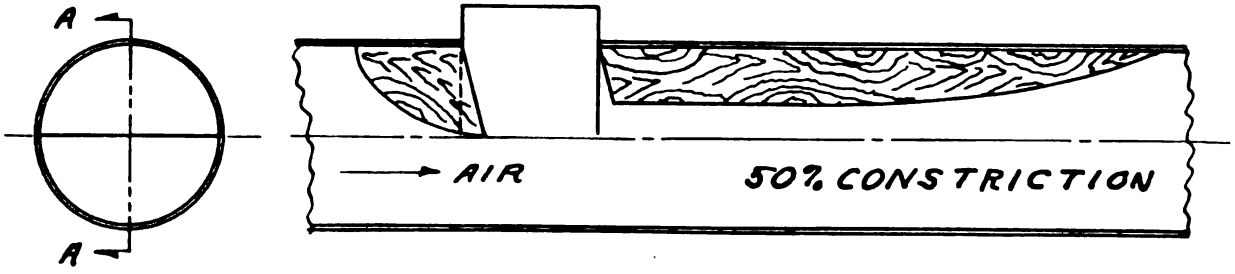

SECTION AA

FIG. 8

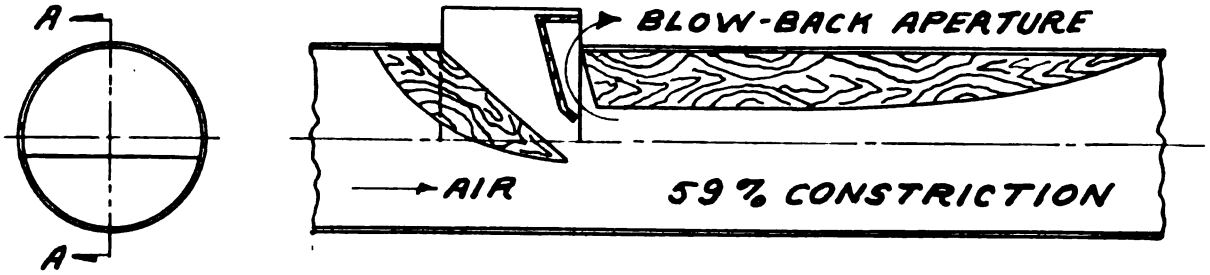

SECTION A-A

FIG. 9

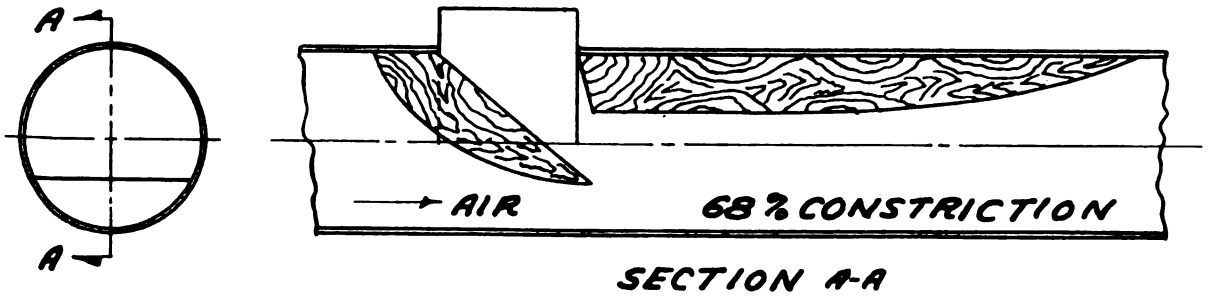

SECTION A-A

FIG. 10

SCALE 3"=1'

INJECTOR FORMS USED

An injector type feeder was first built into the test system. The construction and operation of this feeder is very simple. It operates on the principle that an increase in velocity will cause a decrease in pressure. The velocity increase is accomplished by having a constriction in the pipe line just before the feed inlet which causes the static line pressure to be momentarily transformed into velocity head. This allows the particles to enter the air stream without being blown back by the escaping air. Figs. 8, 9 and 10 show the systems which were used on the test set up. For reasons which will be explained later, none of these set-ups were successful.

An excellent discussion of injector feeders is given by Segler in Ref. 32.

One inherent disadvantage of this type of system is the energy loss due to the transformation of energy from static head to velocity head and subsequently back to static head. This loss varies with the shape of the constriction, but values given by Segler list a 65% loss for an 80% constriction down to a 25% loss for a 50% constriction. (based on the fact that the loss would be 0% for 0% constriction.)

The first type of injector used on the test fixture is shown in Fig. 8. The reduction in area was insufficient, thus allowing considerable blowback and intermittent particle flow.

The next type shown in Fig. 9 provided a greater constriction and also had a blowback aperture. The blowback aperture was installed to allow the air to escape without passing through the incoming particles. This sytem worked much better than the first, but still the flow of particles was intermittent.

Next, an attempt was made to prevent blow back by increasing the pipe constriction to 68% as shown in Fig. 10. When tested this was found to prevent blow back but the energy loss was so great that there was insufficient energy remaining beyond the inlet to carry the particles. This could have been remedied by using a positive displacement blower which would produce higher static pressures than were possible with the existing blower. However, such a blower was not available so the entire idea of an injector feeder was discarded.

It is felt that the principal reason for the failure of the injector system was the size of pipe used. Segler (32) recommends the injector feeder be used on systems where the static pressure is below 10 inches of water and the pipe size is between 6 and 12 inches. The test apparatus met the first requirement, but not the second.

The injector feed has two serious drawbacks when being used in a test apparatus. First, even if the correct pipe constriction is found for a given capacity and pipe length, this will not insure that it would be correct if the two conditions were changed. For example, if no blow back were occurring for a given capacity, and it was decided to increase this capacity, which would increase the resistance, blow back would occur. It would also occur if any change were introduced which would increase the resistance of the system. The quantity of air blown back or drawn in would undoubtedly be insignificant in actual practice but in a test fixture where the volume of air is an important parameter in the theory, it could introduce serious error. If this system had been used, this undesired air movement would have had to have been measured.

The system finally decided upon was a bucket wheel feeder. This

works on the revolving-door principle of always offering an air tight seal between two surfaces, independent of its angular location. A diagram of the bucket wheel used on the test apparatus is shown in Fig. 11 The power for this unit was a 1/3 H.P. electric motor driven through a 40 to 1 worm gear reduction unit. A picture of the set-up is shown in Fig. 12. The aerodynamic efficiency of this system approaches 100 per cent. Segler (32) recommends the use of bucket wheel feeders in medium pressure systems where the static pressure is below 40 inches of water and the pipe diameter is between 4 and 8 inches. The test apparatus falls within both of these limits.

The procedure used to determine the various pressure differentials will be explained in the following discussion.

Static pressure taps were located at four foot intervals along the test section as is shown in the layout drawing (Fig. 2). As described in the review of literature, other investigators have obtained false data by including acceleration losses in the steady state measurements. It is felt that the possibility of introducing this error is completely eliminated by having several stations along the test section instead of the customary one or two. With the pressure taps as shown, the type of flow is immediately evident. If steady state conditions prevail, each of the four stations will register equal pressure differentials. However, if the particles are still undergoing acceleration the pressure differential recorded at each station will become successively smaller as the particle acceleration diminishes, until constant readings are recorded when the particle acceleration is zero. If was found necessary to install an extra eight feet of pipe (Fig. 2) after the first

SHAFT SPEED - 40 RPM

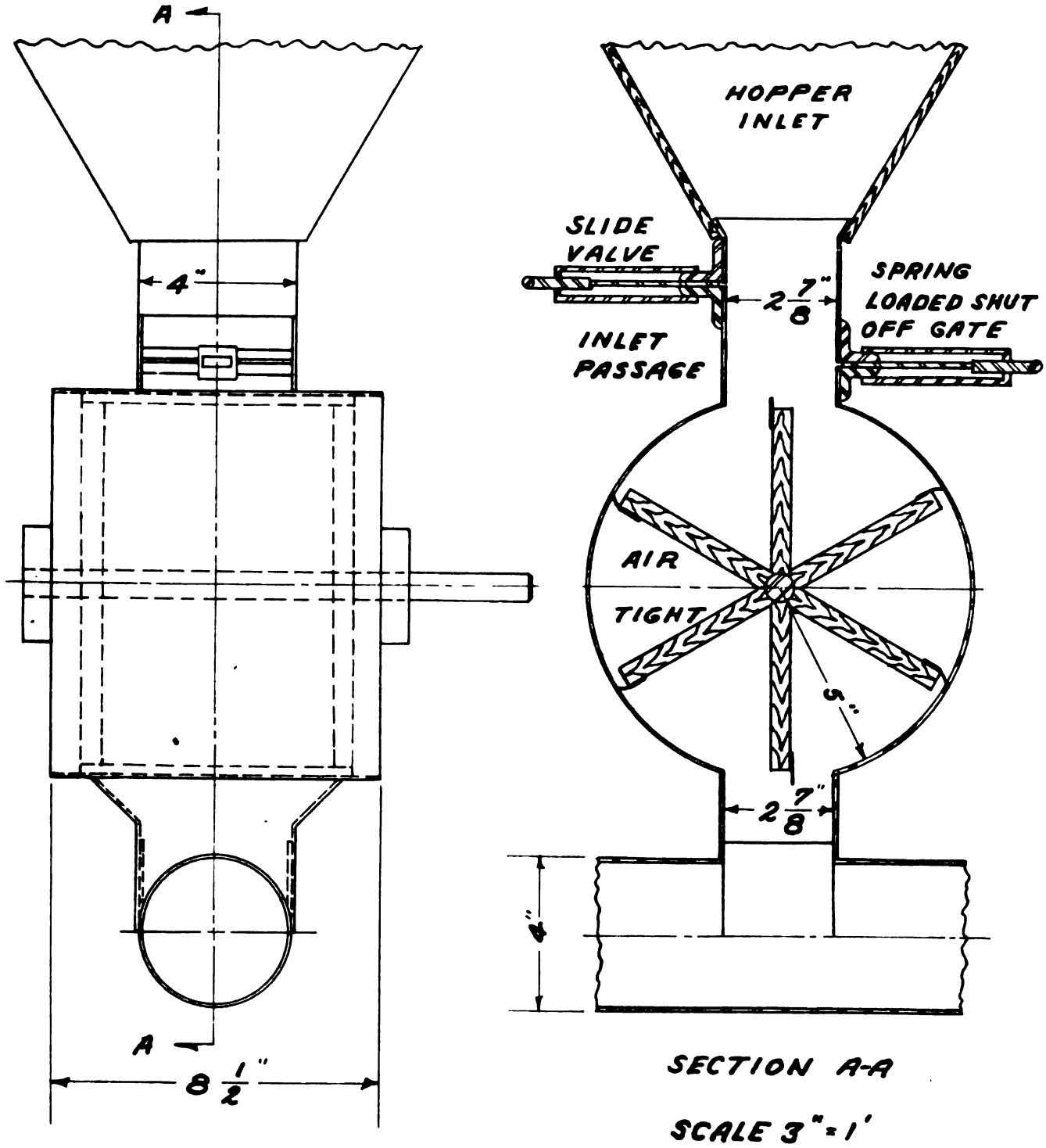

FIG. 11 BUCKET WHEEL FEEDER

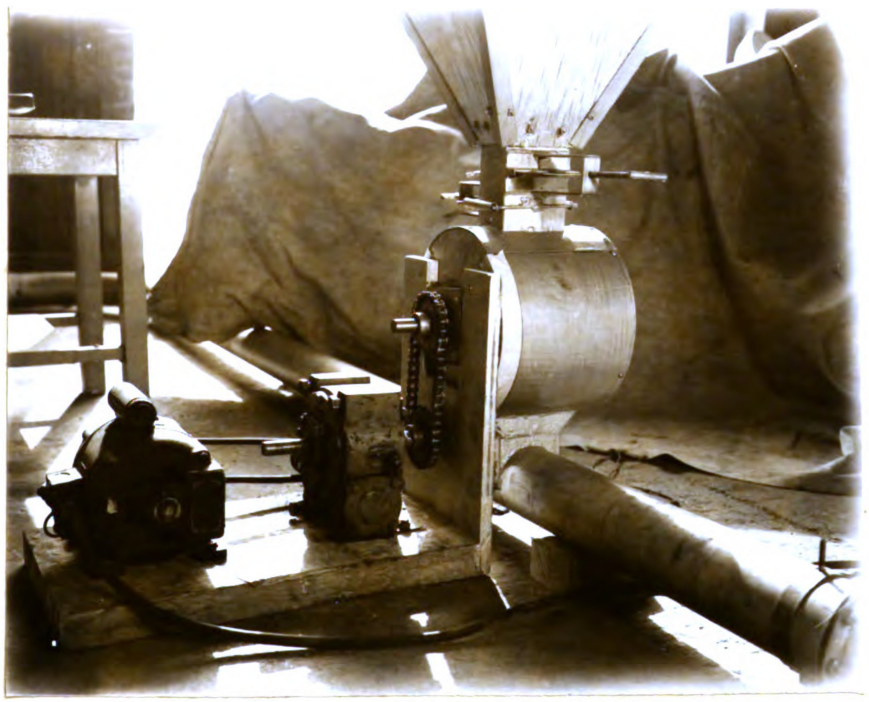

Fig. 12. Drive used to transmit the power output of a 1/3 H.P., 1750 R.P.M. electric motor to the input shaft of the bucket wheel feeder.

180 degree bend to allow the particles to reaccelerate before they entered the test section. Even with this additional pipe, some acceleration could still be recorded at the first two stations. The stations within the test section are shown in Fig. 13.

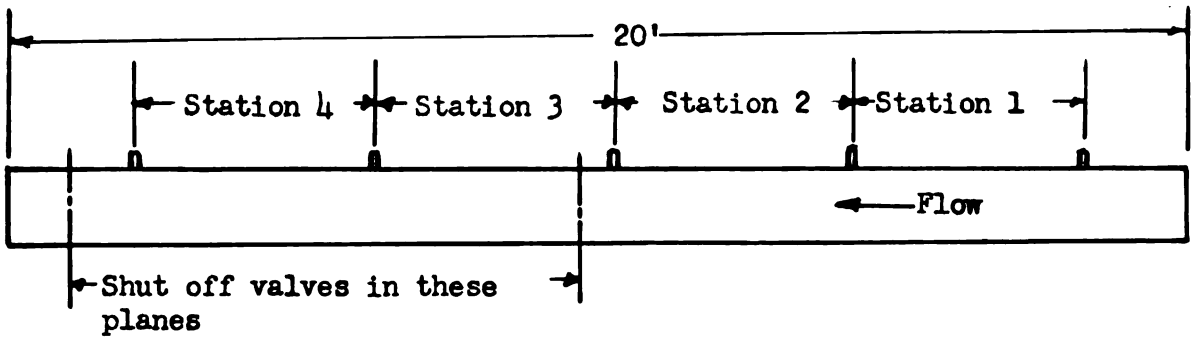

Fig. 13. Location of the individual stations within the test section.

Three individual pressure taps were made at the junction of each station. The actual hole through the pipe wall was 0.03125 inches in diameter. Each of these individual taps were in turn connected to a dampening chamber from which one outlet led to one side of an inclined well type manometer. A photgraph of one of the five systems of taps is shown Fig. 14. Extreme care was exercised in removing the burr from the inside of the pipe after the drilling operation. Had any projections remained around the pressure tap, the internal static head would have been locally converted to velocity head, therefore giving incorrect results.

Two manometers were used, in conjunction with the control panel, shown in Fig. 15 to record all pressure differentials. One was used continuously to register the orifice pressure differential while the other was used to individually indicate the various test station differentials. The control panel made this last set of measurements possible with one manometer by connecting the outlets to successive test stations.

It was found that the manometer reading from the orifice flucuated

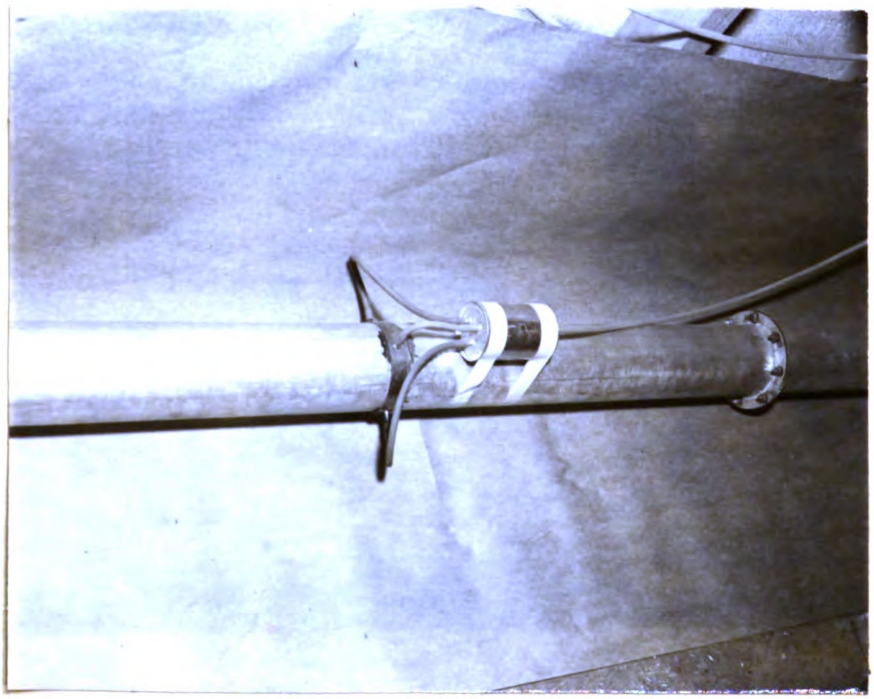

Fig. 14. One of the five systems of pressure taps complete with damping chamber.

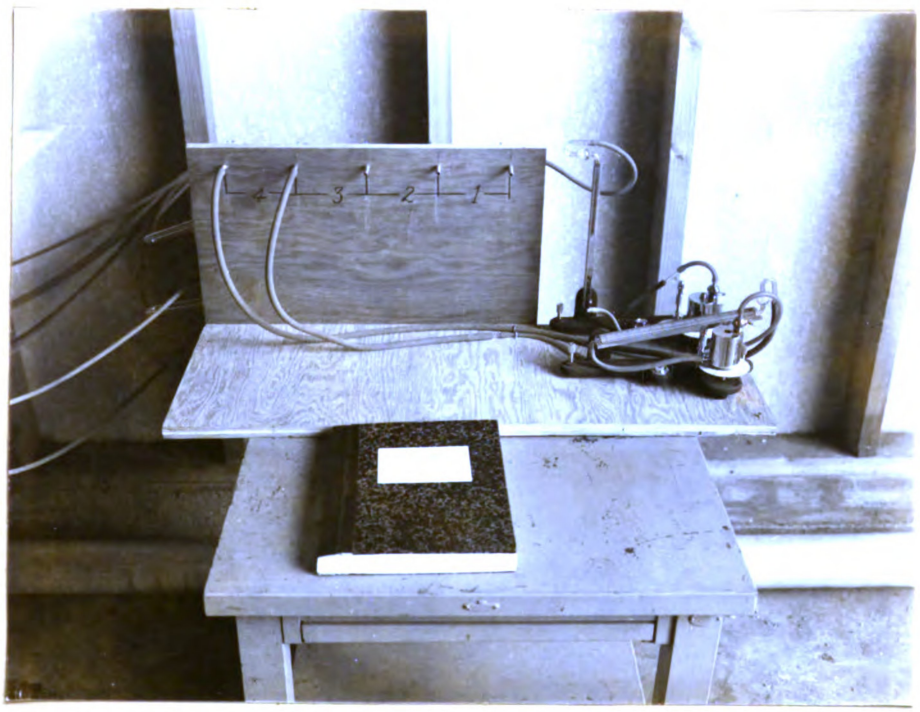

Fig. 15. Control panel used to record all pressure differentials. The individual stations of the test section are shown on corresponding panel taps.

over a small range. These fluctuations did not follow a harmonious pattern but rather were quick, uneven, movements. This situation was remedied by installing a damper in the line extending from each outlet of the manometer. These dampers were steel cylinders approximately eight inches long and four inches in diameter with one end blocked and the other covered by a thin sheet of rubber. Now as the increased pressure, due to a small fluctuation, moved into the damping chamber, the excess energy was absorbed in expanding the rubber sheet rather than moving the column of fluid in the manometer tube.

This concludes the discussion of the test apparatus. To this point, the construction has been completely described, including discussion, and dimensions of the pertinent component parts.

TEST PROCEDURE

Choice of material

Thus far, the theoretical analysis has been completed and the test apparatus which was used to prove or disprove the initial assumptions has been discussed. The next logical step is to explain the test procedure which was followed during the determination of the experimental results.

Assuming that the theory developed was valid, the ultimate objective of this research was to determine friction factors for various grains and solids. It was decided that a complete series of tests should be run on one type of particle before an attempt was made to determine friction factors for other solids. By doing this, the complete theoretical analysis was checked for one type of particle by experimental results. If at any of the intermediate steps the experimental results had shown a substantial and consistant variation from the theoretical results, the initial assumptions, and thus the theoretical analysis would have had to have been assumed incorrect. If this situation had developed, there would have been no point in continuing with the experimental procedure for that, or for any other type of solid, until adjustment was made in the initial assumptions. If this initial test had proved successful, there was still no guarantee that all other types of particles could be examined in a similar manner, since one of the initial assumptions was that "C", the drag coefficient, was based on the shape of the particle. This could have meant that the theoretical analysis would hold for wheat where the particles are relatively uniform and yet not apply to the flow of forages, where the particles not only vary in uniformity but also in density.

The material finally chosen for this initial test was soft white winter wheat. The reasons for this choice are as follows:

1. Availability of the material.
2. Uniformity of the material.
3. Practical use to which data obtained could be put.
4. Ease with which the particles could be injected into the air stream.
5. Stability of the material with successive trips through the blower circuit.

Before the wheat was introduced into the test circuit, it was thoroughly cleaned in a fanning mill. Even with a stable item such as wheat, difficulty in keeping the material free from cracked residue was encountered after it had been blown through the circuit several times. It was felt that the cracking which was observed emanated from the following sources:

1. Binding between the bucket-wheel feeder wall and the individual paddles.
2. Impact with the pipe wall at elbows, etc.
3. Impact with other stationary particles when the grain was blown back into the inlet hopper.

In order to maintain consistant and accurate test results, the wheat was removed from the hopper and again run through the fanning mill when the number of cracked particles appeared to be approximately five per cent. This limit was usually reached after approximately three hours of continuous testing. After the wheat had been cleaned three times it was completely discarded and a new sample was introduced. These samples were all taken from one bin which contained the harvest of one field.

This insured that the physical properties of the wheat would remain the same from sample to sample. The amount of wheat in the hopper for any given test varied from 100 pounds to 125 pounds, only a fraction of this being in the actual test circuit at any given time.

Physical properties of the test material

Since the pressure drop equation developed involved, as variables, the physical properties of the material being conveyed, it was necessary to experimentally determine these properties before the theoretical equations could be checked by the experimental pressure drops obtained. The two basic quantities needed were the average density and the average volume of the individual wheat particles. From these two quantities, the remaining physical properties could be calculated by assuming the shape of each individual particle to be that of a sphere. This assumption is compatible with the curve chosen to represent the drag coefficient (C) as a function of Reynolds' number for the particles.

The actual method used to measure these properties was that of water displacement. Three individual tests were run and the average of these taken as the final results. The wheat for each of these tests was obtained by random sampling from the test hopper. The procedure followed during each of these tests was as follows:

1. Count out 600 wheat kernels.
2. Weigh the kernels.
3. Place them in a 250 milliliter graduate filled with approximately 75 milliliters of water at 60° F.
4. Stir to release all entrapped air.
5. Observe the volume of water displaced.

6. From this data, and by assuming the particles to be spheres, the density, volume per particle, projected area per particle and the weight per particle could be calculated. Values of these properties will be given later.

The use of this approximate method for determining the density of wheat presents two possible sources of error. The first could be caused by the particles absorbing some of the fluid in which they were immersed. This error was kept to a minimum in this experiment by recording the water displaced as soon as possible after the wheat had entered the graduate. The second possible source of error could have been due to confined air in the creases and in the brush of the kernels. This confined air would cause more water to be displaced which would result in a lower density. This error was kept to a minimum by continual agitation of the particles as they were being introduced into the graduate.

The average value obtained for the density of soft white winter wheat was 83.4 #/ft.^{3}. This agreed very well with Zink's (40) results which gave a value of 82.4 #/ft.^{3} for the same type of wheat. It was felt that the small variation was more likely to have been due to actual physical differences between the two samples tested rather than errors due to experimental technique.

Particle flow regulation

The first method used to control the flow of particles from the hopper into the air stream was a simple slide valve. This valve is shown in Fig. 11 and is located just below the hopper. Trouble was encountered with this system when it was desired to obtain a constant flow rate with varying air velocities. This irregular flow was a result of the wheat being metered by a long narrow slot, since under normal con-

ditions the slide valve was only about one-fourth open. This type of system also had the disadvantage of making it almost impossible to duplicate a given flow rate, since only a small movement of the slide caused a large variation in flow rate.

The above problem was solved by making a set of five plates with circular inlets of various diameters. These plates are illustrated in Fig. 16. Any one of these could be conveniently inserted in the slot which the slide valve had occupied with the assurance that any of the five flow rates could be easily duplicated at any future time.

The five flow-regulating plates were all calibrated before the hopper was installed on the test apparatus. The plates were calibrated by mounting the hopper approximately three feet above the ground and catching the outflow for a one minute period. Four of these one minute tests were run on each of the five plates and the results averaged to obtain the final calibration values shown in Fig. 16.

After the plates were calibrated and the hopper installed on the test apparatus, it was still necessary to check the flow rate of the various plates while the system was in operation and to compare these with the values obtained in the previous calibration test. This was accomplished by inserting a flow-deflecting plate in the main pipe line, thus diverting the flow from the pipe into a separate collector before it re-entered the hopper. The weight of material in the collector was recorded for a given unit of time, thus giving the flow rate. This value should compare with the previous calibrations, however, it did not. Also, it was noted that the deviation became larger as the flow rate increased. This observation led to the following hypothesis. As the individual buckets of the bucket wheel feeder moved past the hopper inlet

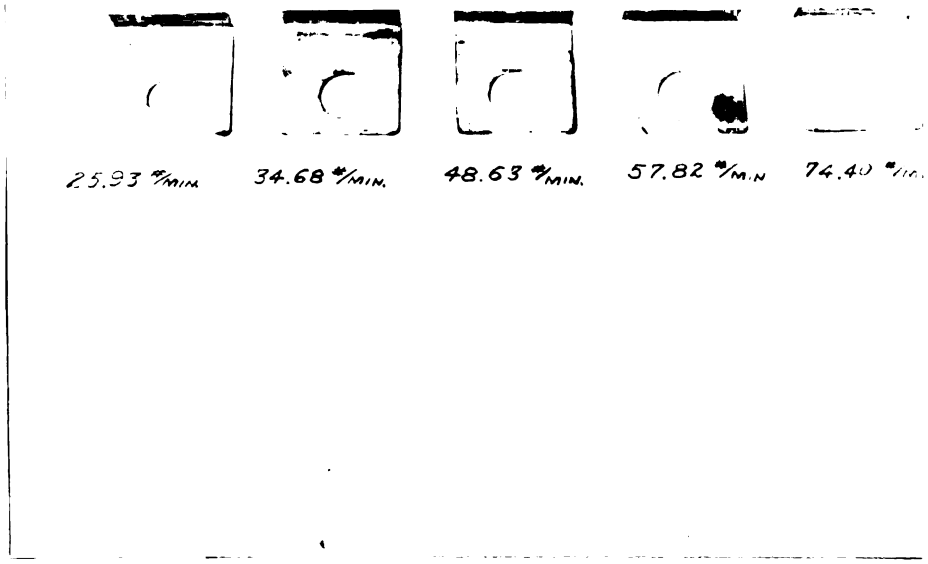

Fig. 16. Calibrated plates used to regulate the solid flow rate.

passage, they released a packet of air which had been picked up as they discharged their load into the pipe system. Also a small amount of air was observed to lead past the bucket wheel paddles. The only outlet for this air was the hole in the calibrated plate through which the wheat particles were flowing. This, of course, would decrease the flow through the calibrated plate. The reason for the larger diviation as the flow rate increased was that the static head within the pipe also increased, thus increasing the amount of air being forced through the calibrated plate.

The above hypothesis was proved correct when a static pressure tap was inserted in the hopper inlet as is shown in Fig. 17. The manometer recorded fluctuating pressures up to six inches of water with the paddle wheel operating. However, with the bucket wheel injector shut off, but with the blower still running, and with an obstruction in the pipe line to maintain a high static pressure, the manometer recorded only a small constant static pressure, which ranged up to approximately one inch of water.

To correct the above situation, it was found necessary to provide a vent in the top of the bucket wheel feeder which would allow the entrapped air to excape before it entered the inlet passage. Two other vents were also provided in the inlet passage to allow for any additional air leakage. Both of the vents are shown in Fig. 17. With these outlets installed, the manometer reading did not go above 0.2 inches of water for any of the five flow rates. Also, when the actual flow rates were again checked, they agreed with the values obtained in the first calibration runs.

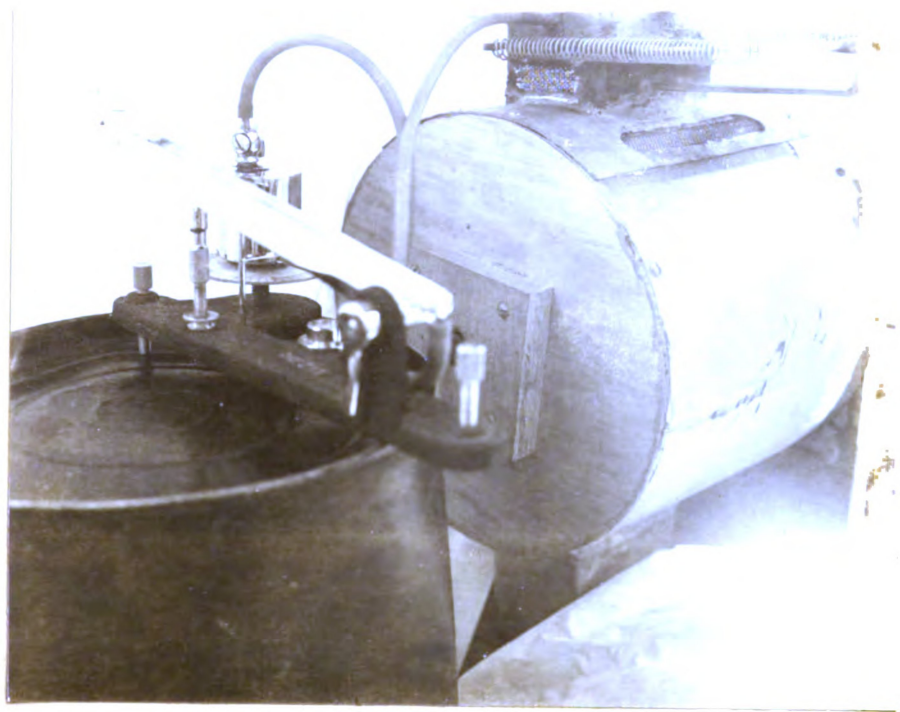

Fig. 17. Bucket wheel feeder showing pressure tap and air vents used to obtain constant flow rates.

Mechanics of test procedure

As was previously mentioned, it was decided to run a complete series of tests on wheat before considering other types of particles. The four principal variables in this test were:

1. Flow rate.
2. Pipe diameter.
3. Pipe inclination.
4. Air velocity.

The first variable was fixed by the size and number of the calibrated plates. The second was fixed in this experiment at 3.89 inches for the inside diameter. Before the material presented in this report can be assumed generally correct, the effect of varying pipe diameter on the solids' friction factor (f_s) must be determined. The effect of the third variable was inspected at pipe angles of 0°, 32.73°, 62.50°, and 90.00°. Fig. 18 and Fig. 19 illustrate the test apparatus at pipe inclinations of 62.50° and 90.00°. The air velocity was varied over as wide a range as was possible with the blower unit used. The minimum air velocity was governed by the point at which the particles ceased to be carried by the air stream. This velocity was approximately 65 feet per second. The maximum air velocity was governed by the output of the blower. This was approximately 110 feet per second.

After the apparatus had been constructed, it was necessary to run the machine until the internal surface of the pipe became sufficiently polished to insure that the pressure drop would be independent of time for any set of conditions. This point was reached after approximately six hours of continuous operation at the maximum possible throughput.

Fig. 18. Test apparatus with a pipe inclination of 62.50°.

Fig. 19. Test apparatus with a pipe inclination of 90.00°.

The next step was to determine the static pressure drop, per foot of pipe, as a function of velocity. This was necessary since a method was desired by which pressure drop due to the solids could be differentiated from the total drop which the manometers would register under actual operating conditions. Now by assuming that the pressure drop due to the air alone remains constant for a given velocity, with or without particles in the pipe, it is possible to obtain the drop due to the solids alone. This was obtained by subtracting the air drop from the total drop observed under actual operating conditions.

The overall picture of the series of tests on wheat in a 3.89" I.D. pipe, which have been completed to date, is as follows:

1. At a pipe angle of 0°, five constant throughputs were tested. At each of these constant throughputs, the air velocity was varied from approximately 65 feet per second to 110 feet per second, and the corresponding pressure drop recorded.
2. At a pipe angle of 32.73°, four constant throughputs were tested with the air velocity varying as at a pipe angle of 0°.
3. At a pipe angle of 62.50°, four constant throughputs were tested with the air velocity varying as at a pipe angle of 0°.
4. At a pipe angle of 90.00°, four constant throughputs were tested with the air velocity varying as at a pipe angle of 0°.

The actual procedure followed during one of the five tests, with the pipe at an angle of 0°, was as follows:

1. The calibrated plate, which would give the desired flow rate, was inserted through the slide valve opening.
2. Next, the spring loaded shut off gates, one of which is shown in Fig. 7, were cocked into firing position.
3. The blower and bucket wheel feeder were then put into motion. At this point, air was blowing through the test circuit but no wheat was being conveyed.
4. To introduce wheat particles into the bucket wheel feeder, and thus into the air stream, the spring loaded shut off gate shown in Fig. 11 was cocked.
5. The blower speed was then adjusted to provide the minimum air velocity required to carry the particles.
6. The pressure drop was checked at each of the four stations shown in Fig. 13. It was found that the pressure drop at station 1 and that at station 3 was less than that at station 2, but the drop at station 3 and 4 were equal. This indicated that the particles were still accelerating as they passed through station 1, but reached their terminal velocity at some point along station 2, thus giving constant pressure drops in stations 3 and 4. This situation prevailed at all throughputs, pipe angles, and air velocities with the exception of the largest throughput at a pipe angle of 90°. In this one case, the particles did not reach their terminal velocity until some point along station 3. With the exception of the latter situation, it was possible to measure the combined pressure drop over stations 3 and 4, thus giving a

larger drop which could be measured more accurately. This drop could be measured to 0.01 of an inch of water by the inclined manometer shown in Fig. 15.

7. As soon as possible after the pressure drop for the combined station 3 plus 4 was recorded, the reading on the manometer connected to the thin plate orifice was recorded. Since a larger range was needed on this measurement, it was necessary to use the manometer tube in an upright position as is shown in Fig. 15. This caused a decrease in the sensitivity of the instrument which prevented variations of less than 0.10 inches of water from being detected.
8. This is the point in the procedure at which a check could be made on the solid flow rate if it were desired to do so. This check is made by inserting a deflecting plate in the main pipe line and weighing the throughput for a given unit of time.
9. The next step in the procedure was to pull the trip releasing the two shut off gates, thus trapping a sample of wheat in the eight foot section of the pipe.
10. Immediately after releasing these gates, the trip on the spring loaded inlet passage gate was released, thus stopping the inflow of particles to the bucket wheel feeder.
11. It was then necessary to remove the entrapped sample of wheat which represented the density of the dispersed solids. This entrapped wheat was removed by a special vacuum device, through an air tight trap within the blocked off section of pipe. This trap, in a closed position, is visible in Fig. 7. Then the

weight of the entrapped wheat was recorded to the nearest 0.01 of a gram. From this it was possible to calculate the density of the dispersed solids, and thus the average velocity of the individual wheat particles.

This ends one complete test cycle for one air velocity. At this point the air velocity was then increased and another test cycle was completed. Approximately 30 of these cycles were completed for each of the various flow rates at each pipe inclination.

Possible sources of error

Two possible sources of error were investigated at this point.

The first is due to the compressibility of the air within the pipe line. If appreciable compression did take place, it would mean that the density of the dispersed solids would not be independent of pipe length, thus steady state conditions would never prevail. If this condition existed, the experimental friction factor (f_s) could not be assumed generally correct. This condition was investigated assuming a pressure drop of 0.10 of an inch of water per foot of pipe for 150 feet of pipe. This gave a total head loss of 15 inches of water. It is shown in the Appendix under Section V that due to the compressibility of the air at this head differential, the velocity of the air at point 2, 150 feet from point 1, will be 0.966 of that at point 1. Even with this large head differential, which would probably never be reached in a farm pneumatic system, the velocity variation is insignificant. The previous statement holds since this loss is only one of three losses in the entire system, and the sum of these three can rarely go above 15 inches of water without exceeding the capacity of the average blower.

The second possible source of error was introduced when the air vents were installed in the bucket wheel feeder to insure a uniform flow rate at all air velocities. It might then have been argued that an appreciable air loss would result from these vents. If this air loss were significant, it would have to be accounted for in the calculation of the experimental friction factor (f_s). By assuming the maximum possible loss to be 11.71 ft.^{3}/min. for an air flow of 500 ft.^{3}/min., the percentage loss is 2.25. The validity of these assumptions is proved in the Appendix under Section VI. This 2.25 per cent loss can be considered insignificant when the accuracy of the orifice coefficient is considered.

EXPERIMENTAL RESULTS

Physical properties of particles tested

The method employed to experimentally determine the physical properties of the soft white winter wheat used in these tests was explained in the previous section. The averages of the results obtained are as follows:

Density per particle "ρ_p"	=	83.4 lb/ft.^{3}
Volume per particle "V_p"	=	0.993×10^{-6} ft.^{3}
Projected area per particle "A_p"	=	120.5×10^{-6} ft.^{2}
Diameter of particle "d"	=	12.39×10^{-3} ft.
Weight per particle "W_p"	=	82.6×10^{-6} lb.

Equation 6 and 7 can be considerably simplified by the introduction of these constants. These equations in simplified form, will be given in the next section.

Pressure drop results

The first actual test which was run, after the pipe had been internally polished, was conducted to determine the pressure drop per foot of pipe when air alone was being conveyed. The results of this test are shown in Fig. 20. The curve shown is actually an average of those obtained for varying atmospheric conditions. A check was run on this curve at the beginning of each day's testing and if deviation was observed, this was taken into account in the analysis of the results. For any given atmospheric condition, the curve resulting was offset a consistent amount from the average curve shown in Fig. 20. The dotted curves in this figure illustrate the maximum and minimum deviation from the average curve.

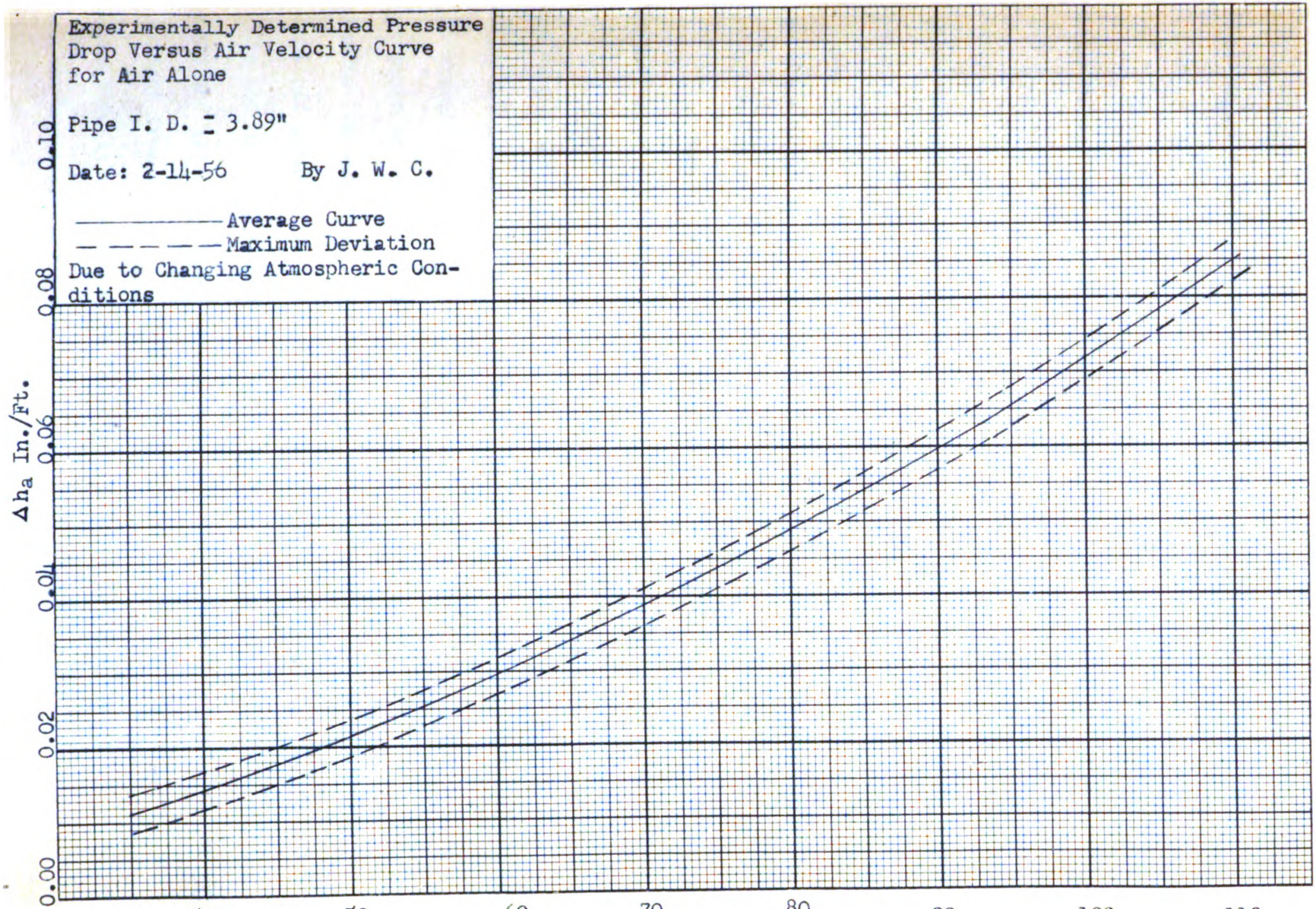
Experimentally Determined Pressure Drop Versus Air Velocity Curve for Air Alone
Pipe I. D. = 3.89"
Date: 2-14-56 By J. W. C.
Average Curve
Maximum Deviation Due to Changing Atmospheric Conditions
Pressure Drop, Per Foot of Pipe, Due Only to the Air
Δh_a In./Ft.
0.00
0.02
0.04
0.06
0.08
0.10
40
50
60
70
80
90
100
110
Air Velocity Ft./Sec.
Fig. 20

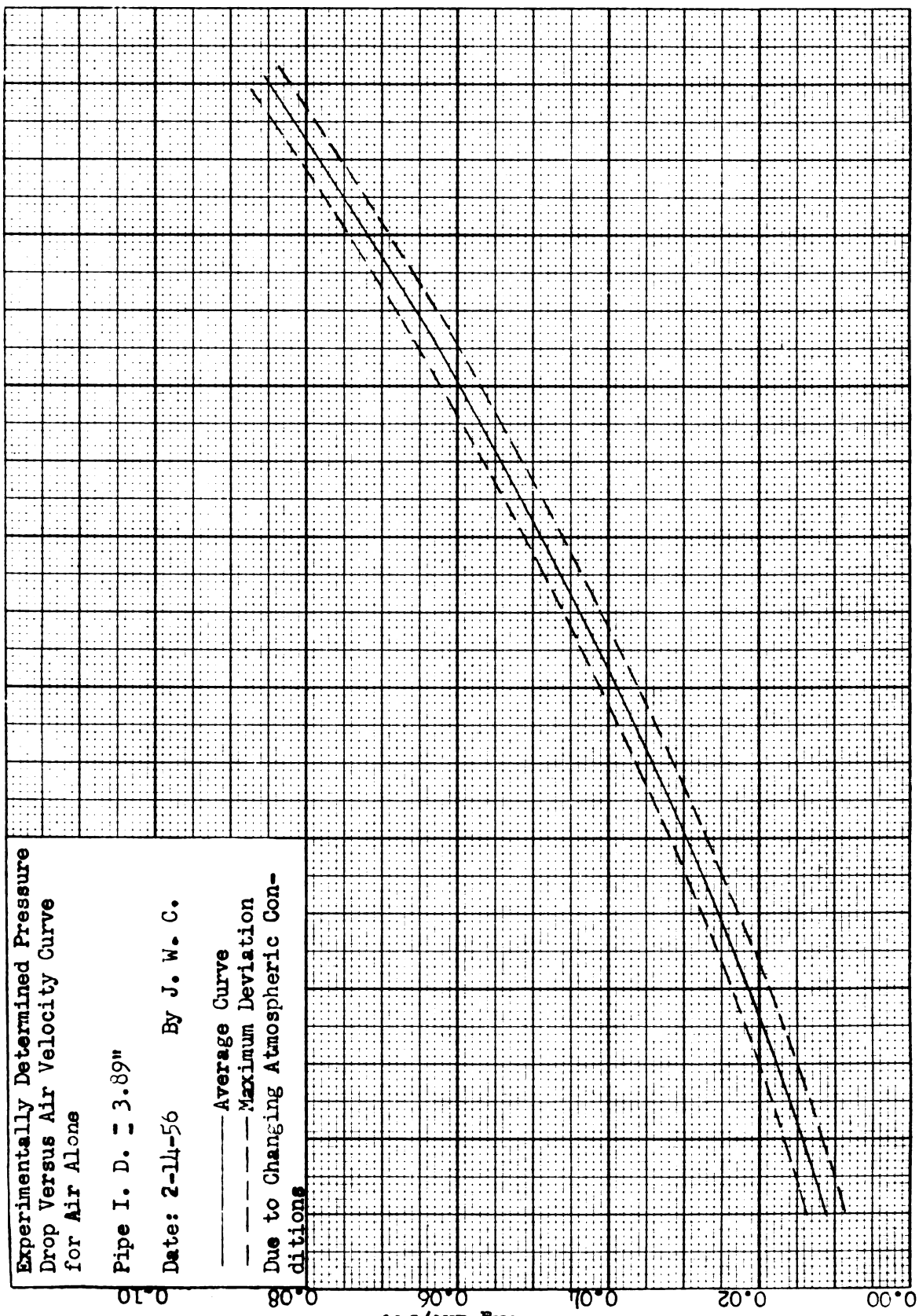

Pressure Drop, Per Foot of Pipe, Due Only to the Air

Fig. 20

It was not possible to obtain the pressure drops, due only to the solid phase, by subtracting the drop, due to air alone, as obtained in Fig. 20, from the total drop observed for a given flow rate and air velocity.

At the beginning of the tests, it was hoped that a graph of particle velocity versus air velocity could be obtained. From this data and by use of equation 5, a graph of solids' friction factor (f_s) versus air velocity could be obtained. Then by assuming "f_s" remained constant for wheat being conveyed at any flow rate, pipe diameter, or pipe inclination, the pressure drop, for any actual condition, could be calculated by the use of equation 6. These calculated values could then be checked by the actual observed pressure drops, thus proving, or disproving, the validity of the initial assumptions leading to equations 5, 6, and 8.

It can be seen from Fig. 21 that the data obtained from the weight of the entrapped solids, which permitted the density of the dispersed solids, and their solids' velocity, to be calculated, proved to be very inaccurate.

There are two possible sources of error which might lead to inconsistent as well as consistent variation in the data obtained. The inconsistent error, which is very evident in Fig. 21, could have been due to the very small quantities of wheat being trapped between the two shut off gates. This weight ran from a low of 18 grams, for low throughputs and high air velocities, to a high of 183 grams, for high throughputs and low air velocities. The consistent error which would not be evident from Fig. 21 could have been caused by one of the shut off gates consistently closing before the other. Both of these errors could have

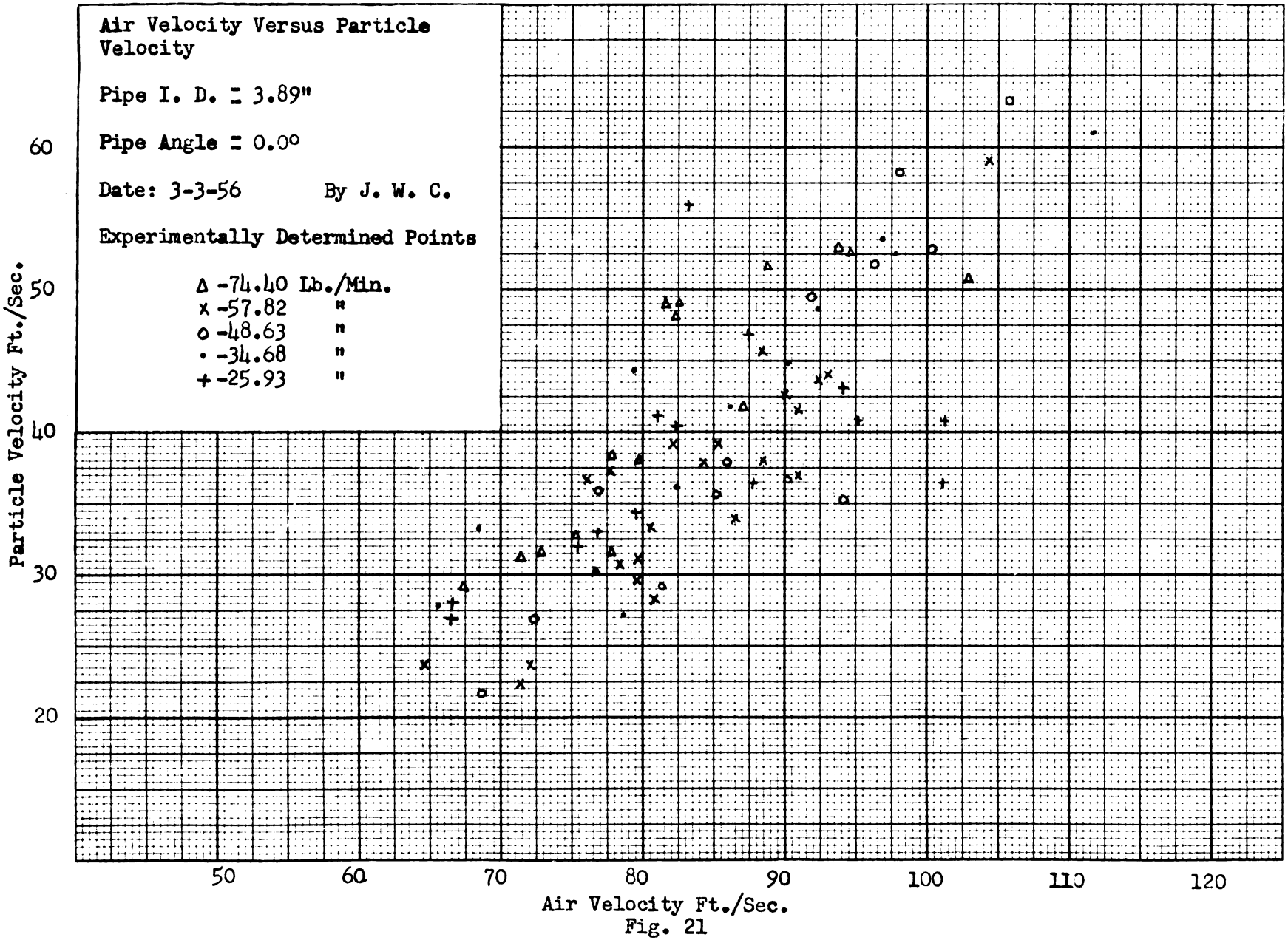
Air Velocity Versus Particle Velocity
Pipe I. D. = 3.89"
Pipe Angle = 0.0°
Date: 3-3-56 By J. W. C.
Experimentally Determined Points
Δ -74.40 Lb./Min.
x -57.82 "
o -48.63 "
• -34.68 "
+ -25.93 "
Particle Velocity Ft./Sec.
60
50
40
30
20
50
60
70
80
90
100
110
120
Air Velocity Ft./Sec.
Fig. 21

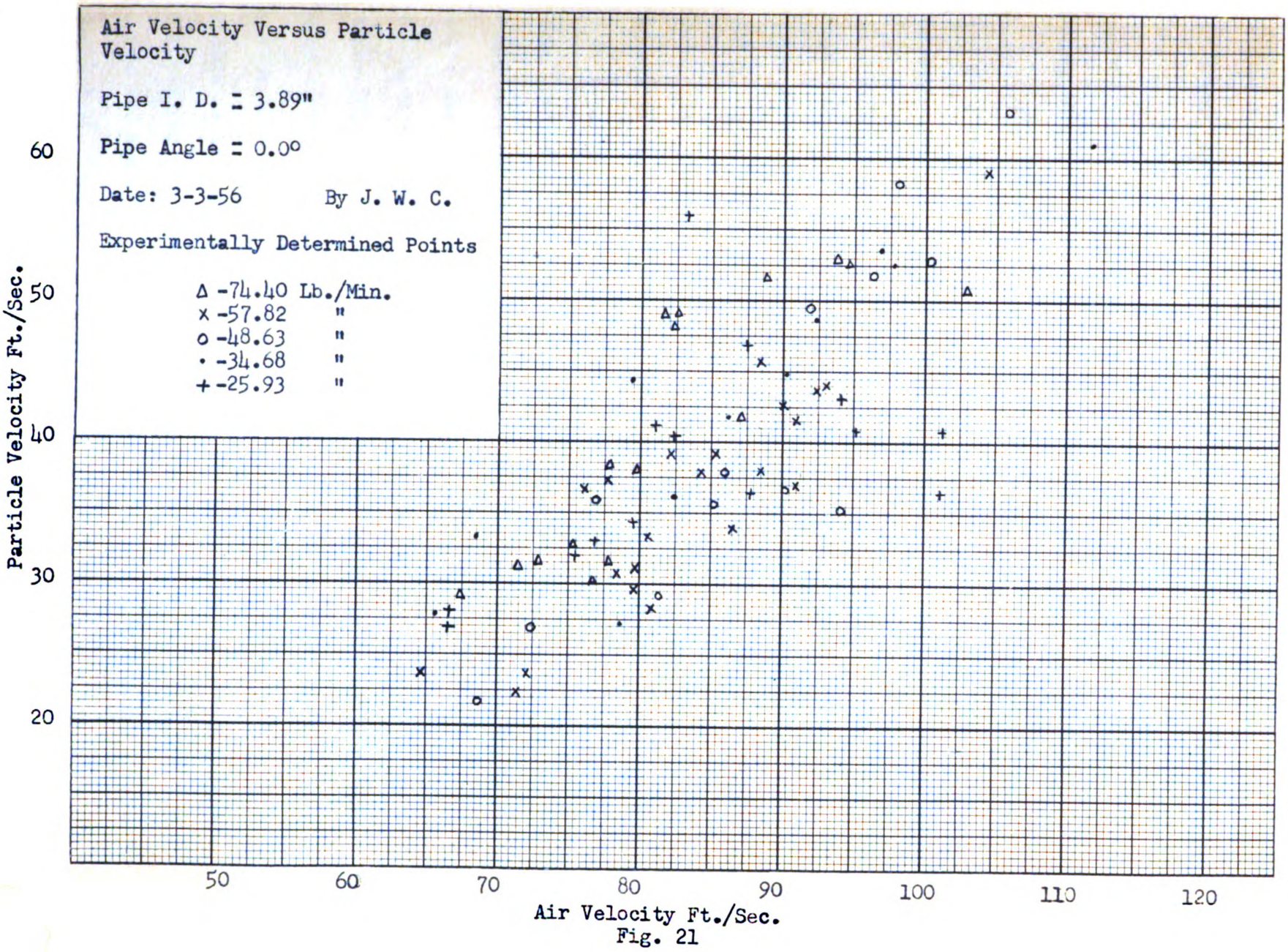
Air Velocity Versus Particle Velocity
Pipe I. D. = 3.89"
Pipe Angle = 0.0°
Date: 3-3-56 By J. W. C.
Experimentally Determined Points
Δ -74.40 Lb./Min.
x -57.82 "
o -48.63 "
• -34.68 "
+ -25.93 "
Particle Velocity Ft./Sec.
60
50
40
30
20
50
60
70
80
90
100
110
120
Air Velocity Ft./Sec.
Fig. 21

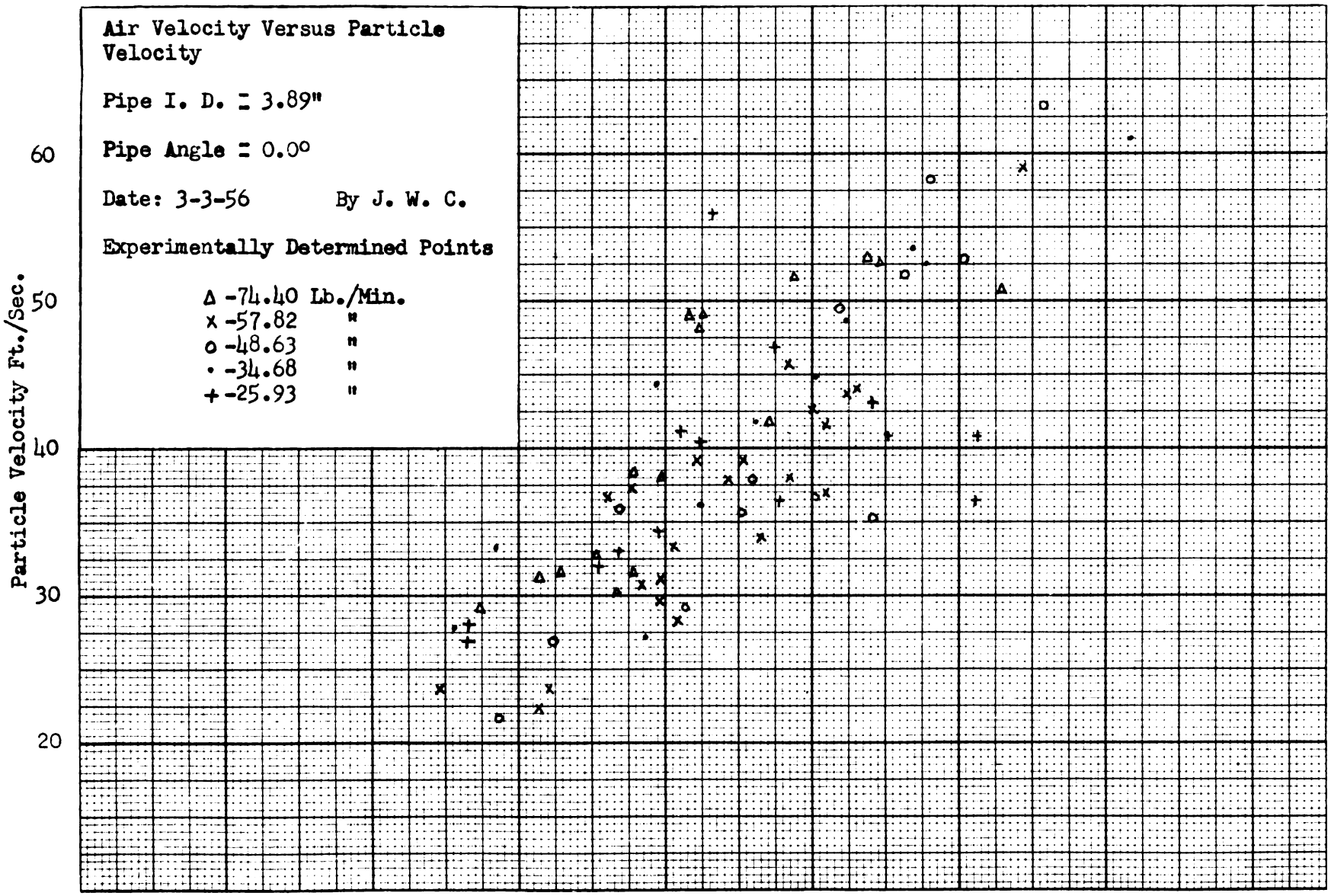
Air Velocity Versus Particle Velocity
Pipe I. D. = 3.89"
Pipe Angle = 0.0°
Date: 3-3-56 By J. W. C.
Experimentally Determined Points
Δ -74.40 Lb./Min.
x -57.82 "
o -48.63 "
• -34.68 "
+ -25.93 "
Particle Velocity Ft./Sec.
60
50
40
30
20
50
60
70
80
90
100
110
120
Air Velocity Ft./Sec.
Fig. 21

been eliminated by the use of a longer test section. It appears that at least 25 feet of pipe between the shut off gates would be necessary to insure accurate results. Rather than rebuilding the test apparatus, another method was devised to determine the graph of solids' velocity versus particle velocity. This method is explained in the following paragraph.

The experimental pressure drops were plotted against air velocity on a graph such as Fig. 25. Next a line of best fit was drawn through each group of points representing one of the five throughputs. (These are not the dotted lines shown in the figure.) From each of the five experimentally determined curves, it was possible to calculate a curve of air velocity versus particle velocity. This curve was compatible with the experimentally determined points for that one throughput. Theoretically, the five pressure drop versus air velocity curves should transpose into one identical curve on the graph of air velocity versus particle velocity. The method of calculating the latter curve from the former is as follows: Equation 6 was solved for "f_s" and set equal to equation 5, thus elinimating "f_s" as a parameter. For any given air velocity and throughput, the only variables left in the above equation were the solids' velocity (v_s) and the coefficient of resistance (C). Now $0.4 + 40/79.7 (v_a - v_s)$ could be substituted for "C", thus leaving a simple quadratic equation in one unknown, "v_s". The five curves, along with the proposed average curve, are shown in Fig. 22. It should be noticed that the average air velocity versus particle velocity curve agrees reasonably well with the experimental points in Fig. 21. There is, however, a consistent offset which may have been due to uneven closing of the shut off gates as explained earlier.

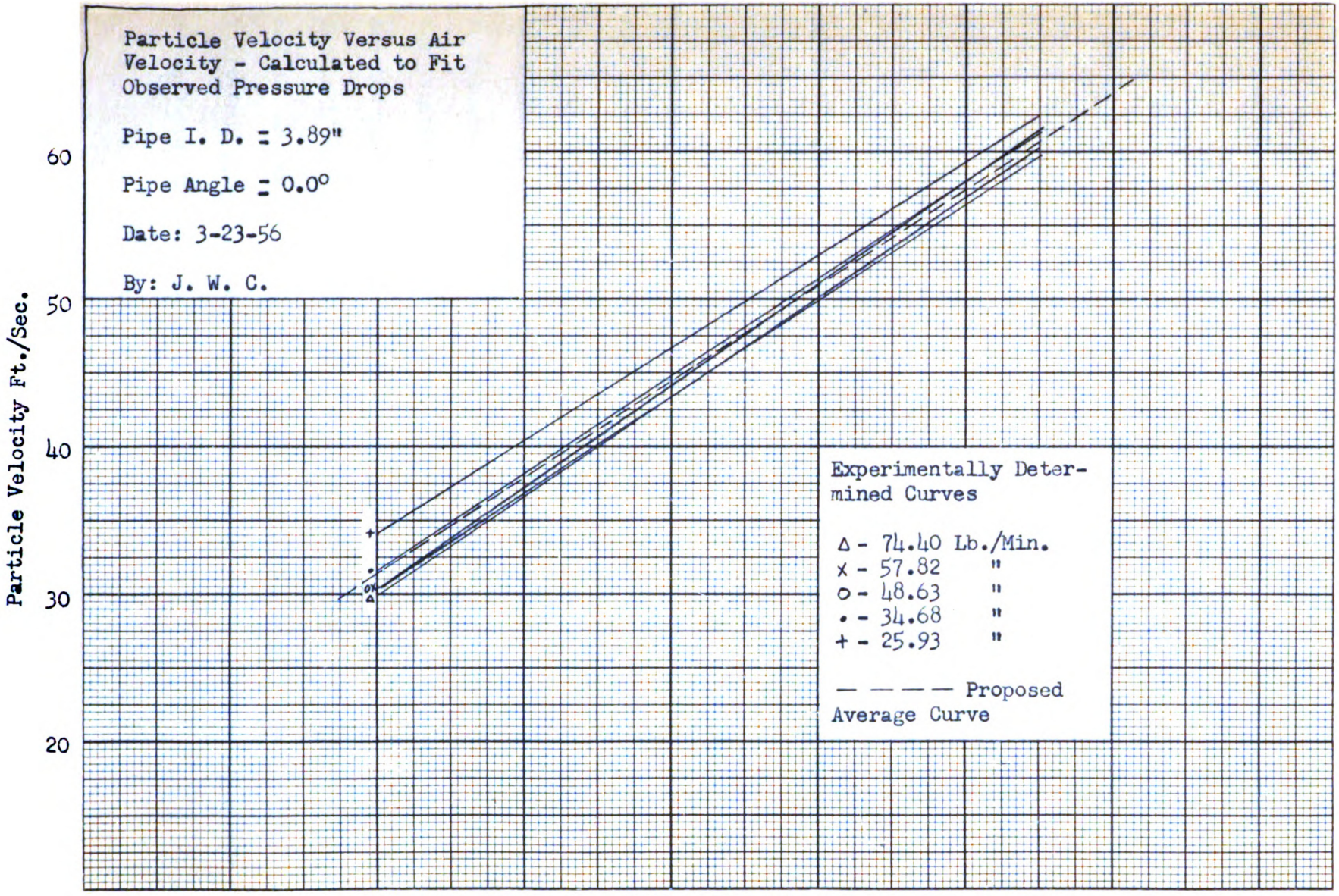
Particle Velocity Versus Air Velocity - Calculated to Fit Observed Pressure Drops
Pipe I. D. = 3.89"
Pipe Angle = 0.0°
Date: 3-23-56
By: J. W. C.
Experimentally Determined Curves
Δ - 74.40 Lb./Min.
x - 57.82 "
o - 48.63 "
• - 34.68 "
+ - 25.93 "
— — — — Proposed Average Curve
Particle Velocity Ft./Sec.
20
30
40
50
60
50
60
70
80
90
100
110
120
Air Velocity Ft./Sec.
Fig. 22

It is now possible by using Fig. 22 and equation 5 to calculate a curve representing "f_s" as a function of the air velocity. This curve is shown in Fig. 23. It is valid for any throughput, pipe angle, or air velocity. This curve is one of the most important results of the research since it makes it possible to predict the pressure loss for any pipe angle, throughput, or air velocity. The validity of the curve will be tested by calculating the pressure drop for various pipe inclinations and then comparing these with the experimentally determined pressure drops.

The first step in the calculation of the pressure drop versus air velocity curve from Fig. 23 was to calculate the velocity of the particles at various pipe inclinations. A comparison of the calculated curves for particle velocity versus air velocity at each pipe inclination is shown in Fig. 24. These curves were calculated from equation 8. As would be expected, the rate of change of "v_s" with respect to "θ" decreases as "θ" approaches 90°.

The curves of Fig. 24, along with equation 6, were next used to calculate the curves of pressure drops versus air velocity which are represented in Figs. 25, 26, 27, and 28. These four curves represent the relative compatibility between the experimentally determined points and the calculated curves, which were based on the solids' friction factor (f_s), given by Fig. 23. The other four graphs, Figs. 29, 30, 31, and 32, are merely another way of representing the data shown in the first four graphs. These will be very useful in the discussion of the results presented on the following two pages.

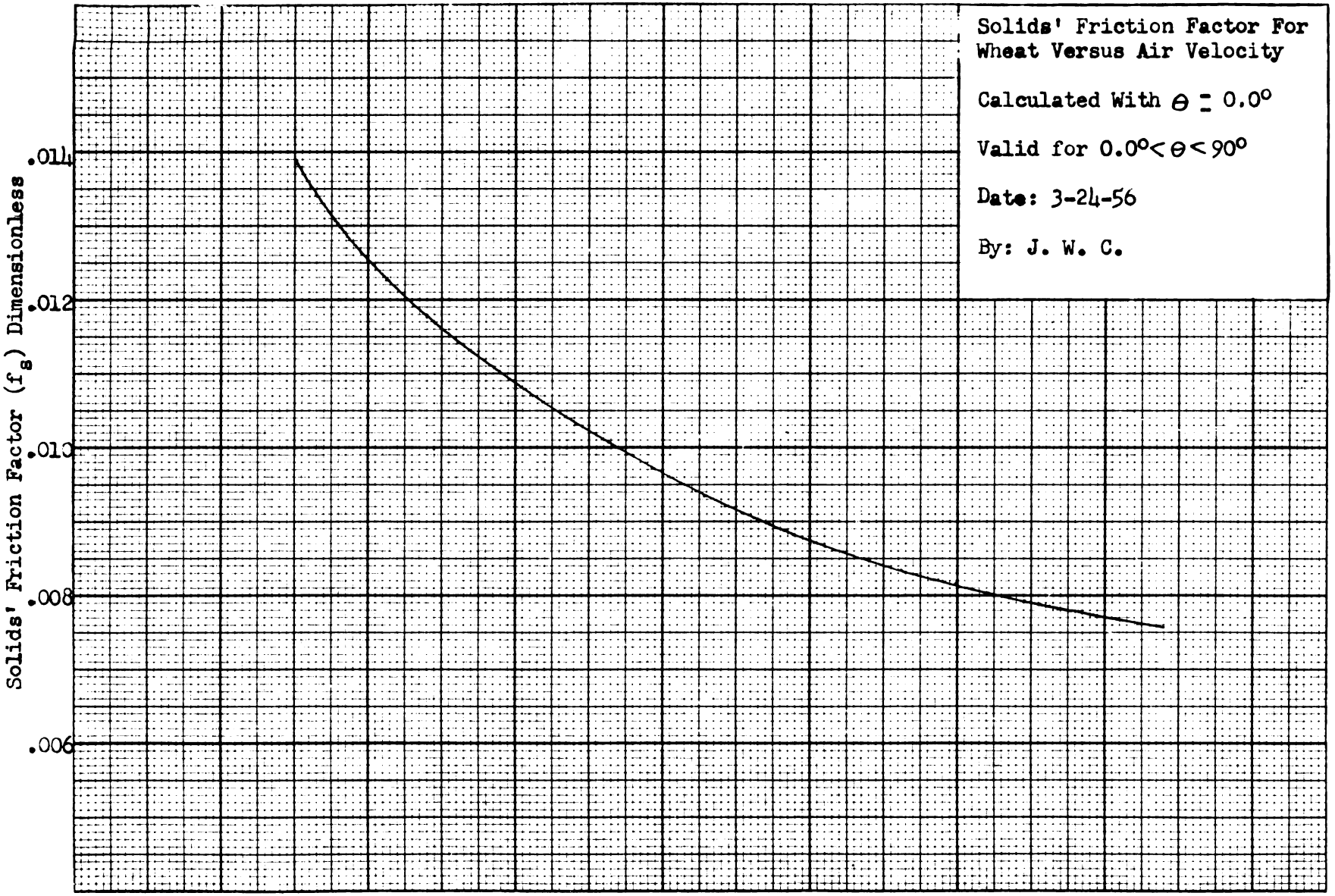
Solids' Friction Factor For Wheat Versus Air Velocity
Calculated With θ = 0.0°
Valid for 0.0° < θ < 90°
Date: 3-24-56
By: J. W. C.
Solids' Friction Factor (f_s) Dimensionless
.014
.012
.010
.008
.006
50
60
70
80
90
100
110
120
Air Velocity Ft./Sec.

Fig. 23

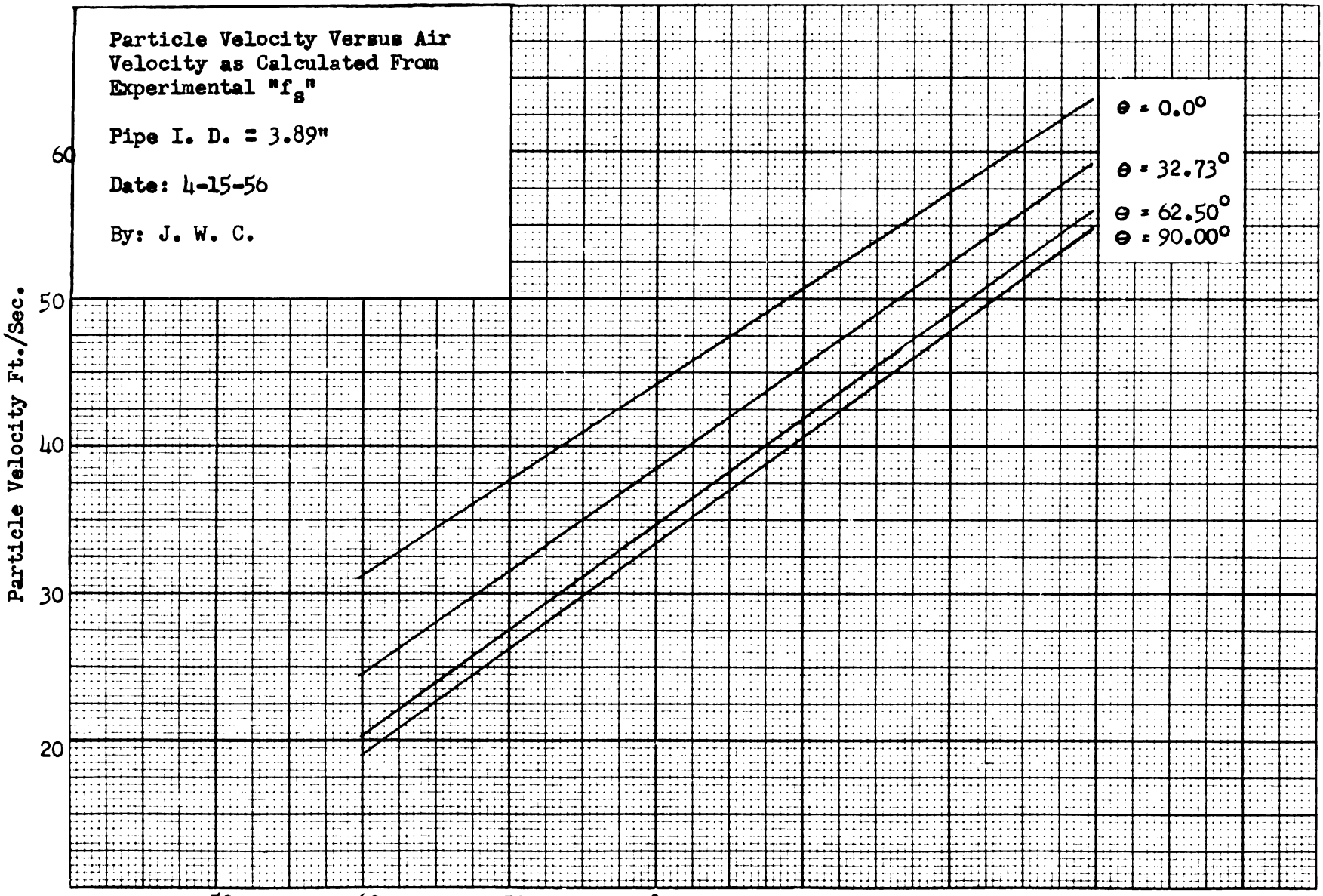
Particle Velocity Versus Air Velocity as Calculated From Experimental "f_s"
Pipe I. D. = 3.89"
Date: 4-15-56
By: J. W. C.
θ = 0.0°
θ = 32.73°
θ = 62.50°
θ = 90.00°
Particle Velocity Ft./Sec.
60
50
40
30
20
50
60
70
80
90
100
110
120
Air Velocity Ft./Sec.

Fig. 24

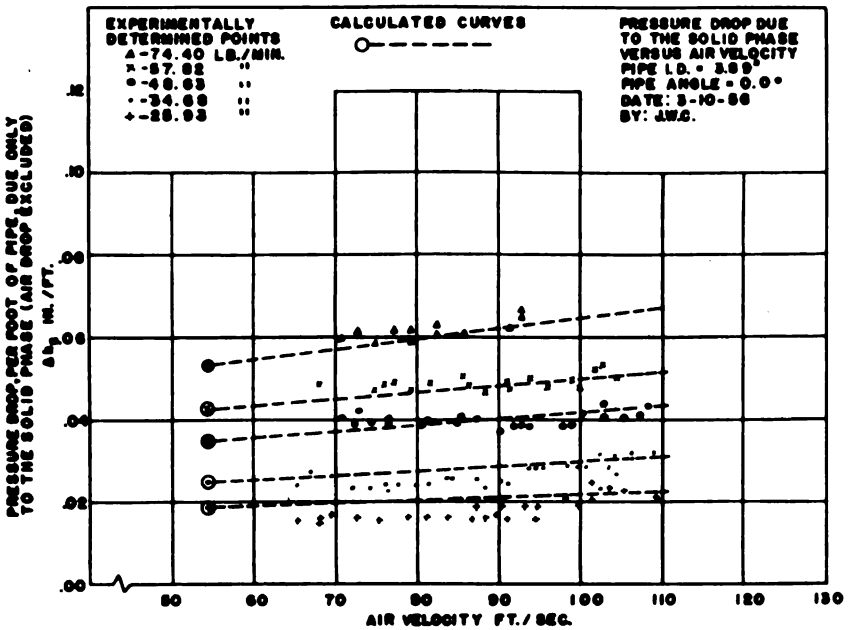

FIGURE NO. 25

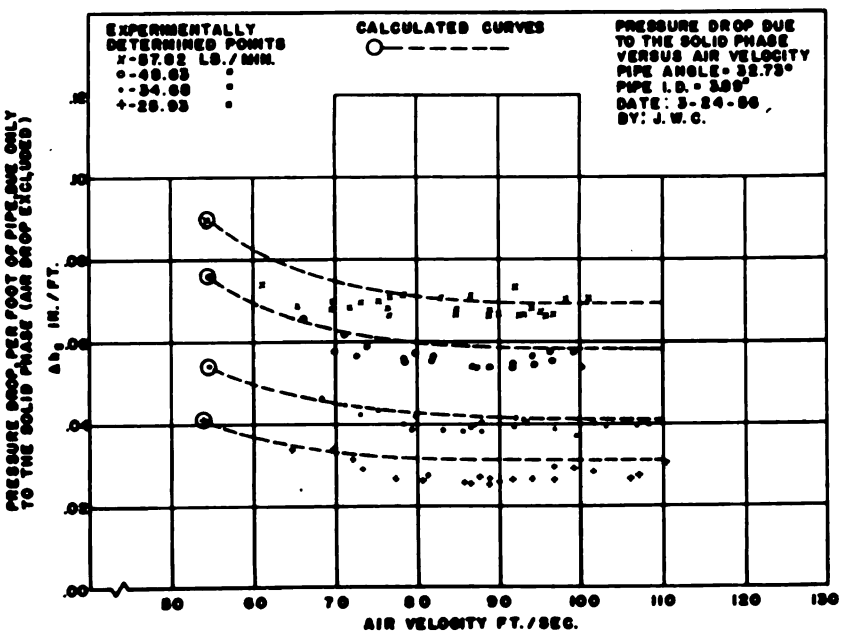

FIGURE NO. 26

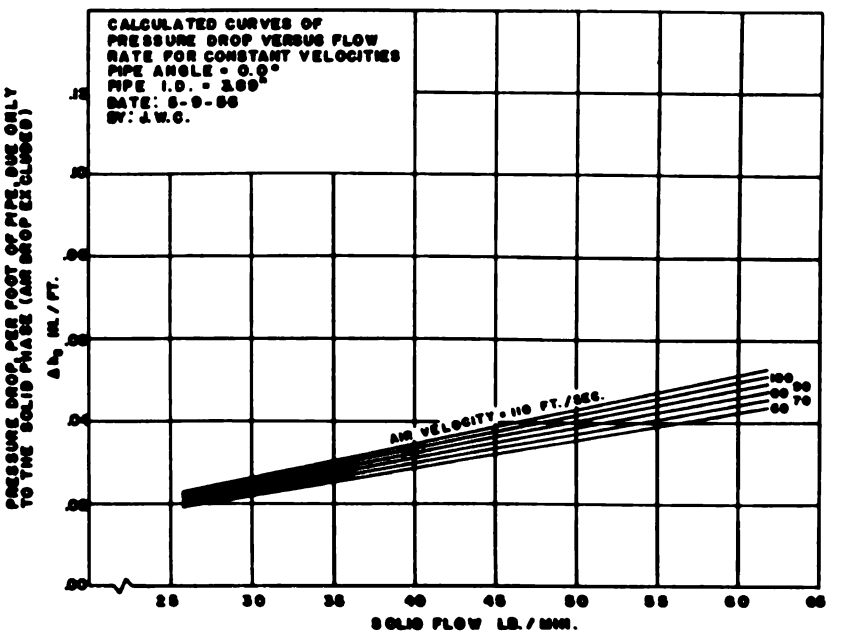

FIGURE NO. 29

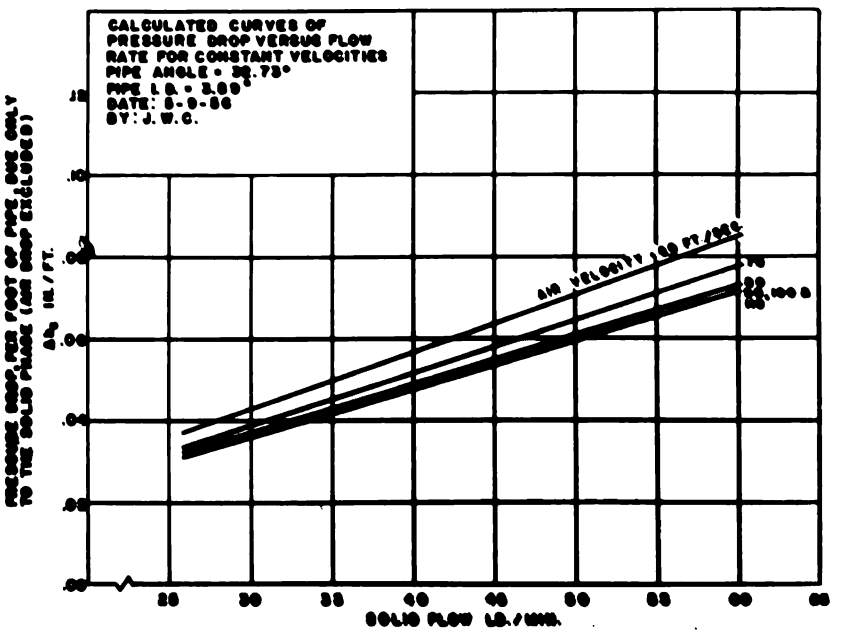

FIGURE NO. 30

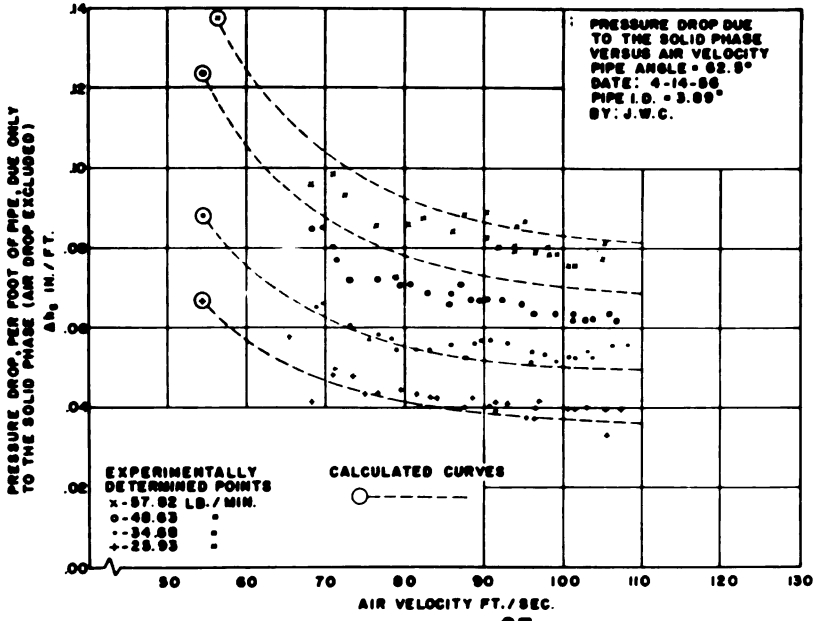

FIGURE NO. 27

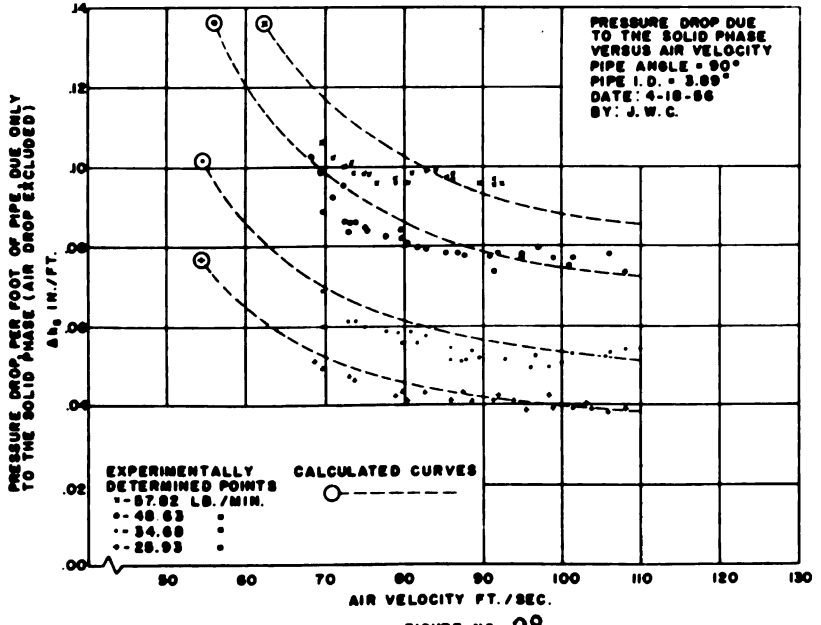

FIGURE NO. 28

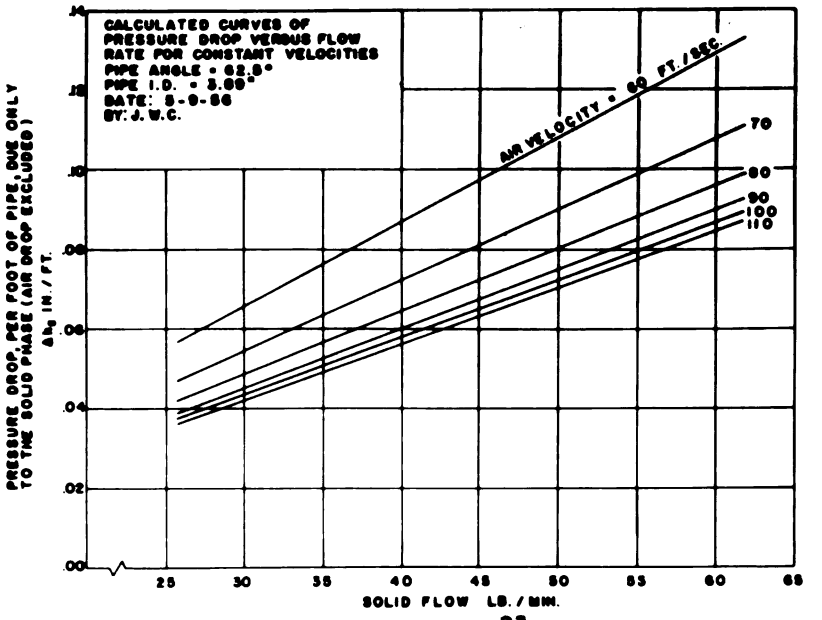

FIGURE NO. 31

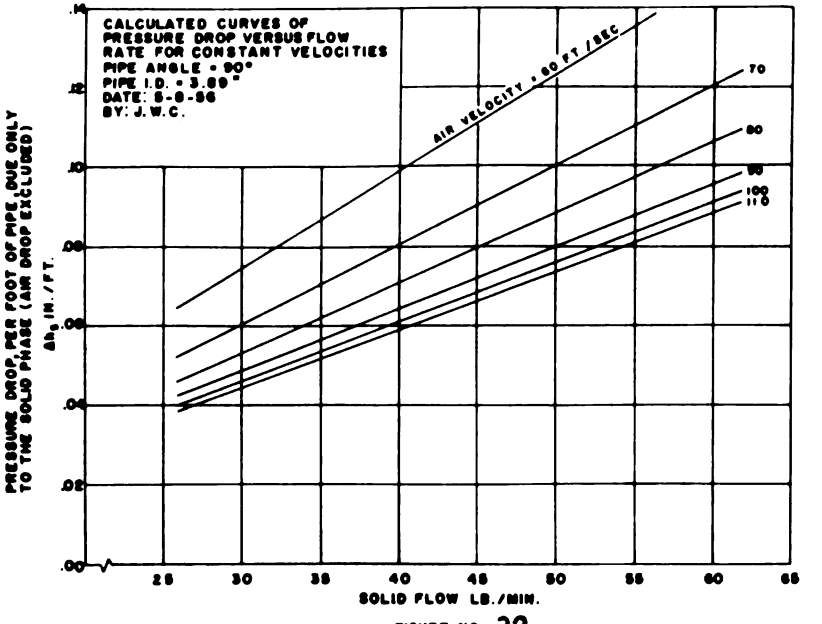

FIGURE NO. 32

The first point which warrants discussion is the degree of accuracy with which the theoretical curves, shown in Figs. 25, 26, 27, and 28, match the experimentally determined points. As was previously mentioned, the experimental points in Fig. 25 were used as a basis for determining the solids' friction factor (f_s) which was in turn used to calculate the remaining curves for various pipe inclinations. For this reason, Fig. 25 can not be used as a basis for comparison. Also it should be noted that five throughputs were analyzed in Fig. 25, but that only four were considered in the remaining three figures. The reason for this is as follows: With a blower of the type used on the test apparatus, which is similar to ones used in actual practice, the throughput is limited by the pressure drop within the pipe line. It will be noticed that as the pipe angle was increased, the pressure drop per foot of pipe increased rapidly. While the blower could handle 74.40 lb./min. with the pipe in a horizontal position, it could not supply the additional energy needed when the pipe angle was increased. Thus, when a throughput of 74.40 lb./min. was attempted, at any angle other than 0°, very inconsistent pressure drop readings were recorded, indicating intermittent particle flow. For this reason, these results were not recorded. Also, it will be noticed that the velocity range possible with the blower used becomes smaller as the throughput increases.

The experimental points in Figs. 26, 27, and 28 agree reasonably well with the calculated curves. The largest deviation occured in Fig. 28, with a throughput of 57.82 lb./min. As the velocity was decreased from 100 ft./sec. to 90 ft./ sec., the experimental points fell

directly on the curve, but with a further decrease to 70 ft./sec., the points failed to follow the changing slope of the theoretical curve. This one test was duplicated five times with similar results in each case. The maximum deviation of these points from the theoretical curve was 9.1 per cent, but since this deviation was not evident at the other three throughputs, it was neglected.

By inspection of equation 6, it can be seen that the static head component of pressure drop varies from zero for horizontal pipes to a maximum for vertical pipes. This same phenomenon is evident in Figs. 25, 26, 27, and 28. For a change in pipe angle from 0^{o} to 90^{o}, there is an accompanying increase in the pressure drop, for a constant throughput, of over 100 per cent. There is a drop in particle velocity of approximately 20 per cent over this same range; thus it can be argued that the drop due to the friction of the solid phase could not account for the increase in pressure drop. Since the drop due to the air friction does not change for a given velocity, the only other component which could have increased was the drop due to the solids' static head. This is analogous to water flowing through a pipe line. Neglecting fluid friction, the static head is zero if the pipe is horizontal and increases as a function of the sine of "Θ" as the inclination increases. In a pneumatic conveying system, the total increase in static head is composed of two components. The first is due to the phenonenon mentioned above. The second is common only to systems which have solid particles suspended in a fluid of low specific gravity. In such a system, as the pipe angle increases, the velocity of the particles decrease. This decrease in velocity causes the density of the dispersed

solids to increase, thus increasing the static head. This is illustrated in Fig. 33. It should be understood that even though the curve representing a variable particle velocity seems to have a greater effect on "ρ_{ds}" than the curve representing pipe inclination, such is not the case. While the curves in Fig. 33 are illustrative, they do not represent an actual situation. If a pipe were varied from 0^{o} to 90^{o}, thus transversing the entire pipe inclination curve, the particle velocity would decrease, but only over a small portion of the particle velocity curve. Thus the direct increase in pipe inclination accounts for the largest part of the increase in the density of the dispersed solids.

The continual decrease in the slope of the curve, from a pipe angle of 0^{o} to 90^{o} in Figs. 25, 26, 27, and 28, is also due to the static head component of pressure loss. At a pipe angle of 0^{o}, the pressure loss and air velocity possess a linear relationship, which is compatible with the theory developed. As the pipe angle increases, the pressure loss increases at a faster rate for low air velocities than it does for high air velocities. Fig. 34 represents the two components of pressure loss which, when added, give the second curve from the top, represented in Fig. 28. It can be seen from this figure that the static head component of the total pressure drop due to the solids is much larger at low air velocities. The reason for this is as follows: For a given throughput, the density of the particles within the pipe (ρ_{ds}) is directly related to the air velocity. At low air velocities, the density of the dispersed solids would be high. For high air velocities, the opposite would be true. This is represented graphically in Fig. 34. Since the static head loss is directly proportional to the weight of

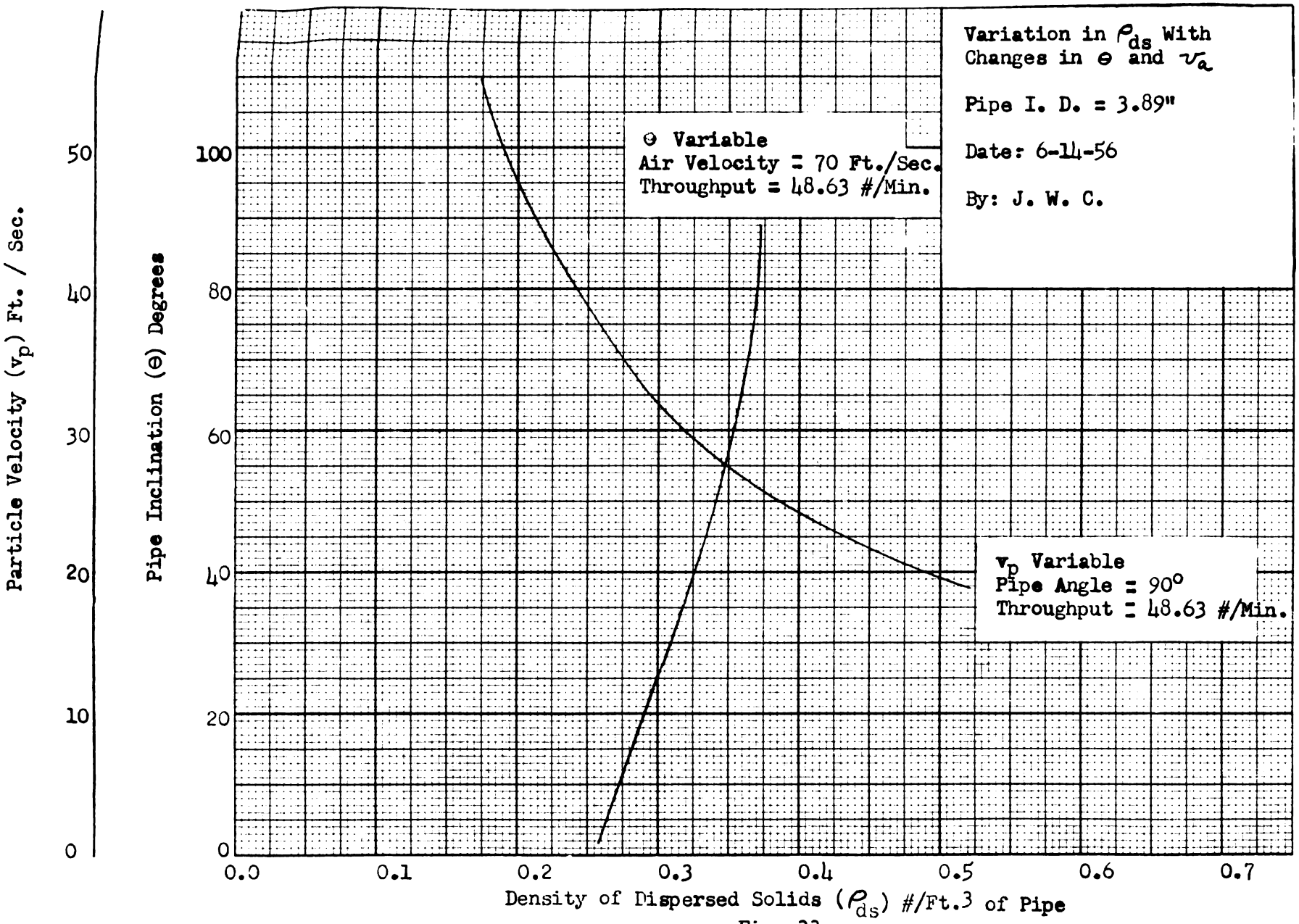
Variation in ρ_{ds} With Changes in θ and v_a
Pipe I. D. = 3.89"
Date: 6-14-56
By: J. W. C.
θ Variable
Air Velocity = 70 Ft./Sec.
Throughput = 48.63 #/Min.
v_p Variable
Pipe Angle = 90°
Throughput = 48.63 #/Min.
Particle Velocity (v_p) Ft. / Sec.
0
10
20
30
40
50
Pipe Inclination (θ) Degrees
0
20
40
60
80
100
0.0
0.1
0.2
0.3
0.4
0.5
0.6
0.7
Density of Dispersed Solids (ρ_{ds}) #/Ft.3 of Pipe

Fig. 33

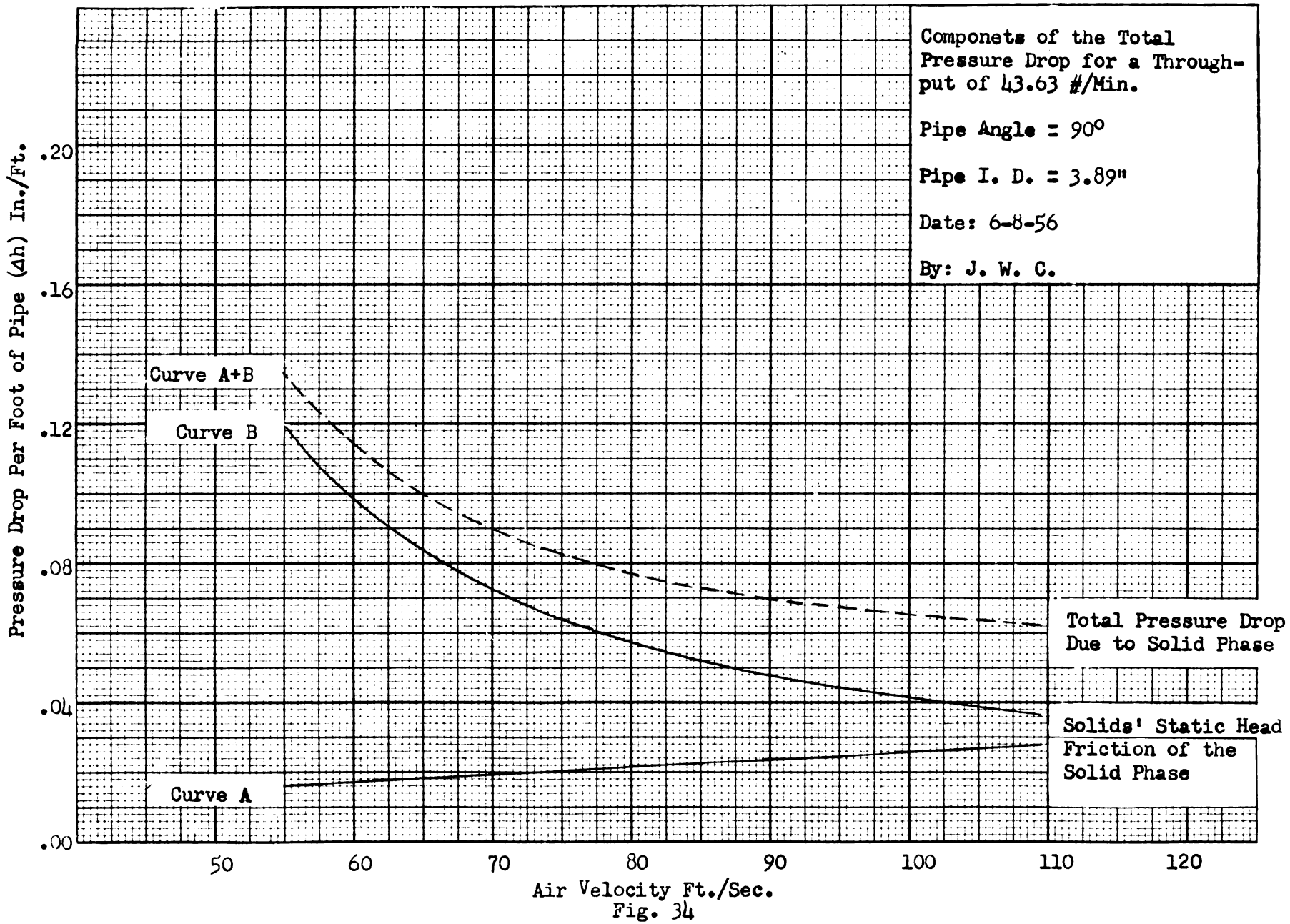
Componets of the Total Pressure Drop for a Throughput of 43.63 #/Min.
Pipe Angle = 90°
Pipe I. D. = 3.89"
Date: 6-8-56
By: J. W. C.
Curve A+B
Curve B
Curve A
Total Pressure Drop Due to Solid Phase
Solids' Static Head
Friction of the Solid Phase
Pressure Drop Per Foot of Pipe (Δh) In./Ft.
.20
.16
.12
.08
.04
.00
50
60
70
80
90
100
110
120
Air Velocity Ft./Sec.
Fig. 34

solids per unit volume of pipe, the head loss would be greater at low air velocities, as is indicated in Fig. 34. Theoretically, curve "B" in Fig. 34 would approach the abscissa asymptoticly as the air velocity approached infinity.

Thur far in this discussion, the reasons for the results which are presented in Figs. 25, 26, 27, and 28 have been discussed. The following paragraphs will deal with the data presented in Figs. 29, 30, 31, and 32, which were obtained directly from Figs. 25, 26, 27 and 28.

The graphs of throughput versus pressure drop emphasize several points which are not obvious at first glance in Figs. 25, 26, 27, and 28. If it were desired to specify an air velocity from Fig. 29 for a given throughput, which would result in a minimum pressure drop, the lower curve, representing an air velocity of 60 ft./sec. would be chosen. If the same thing were desired, but Fig. 32 were used, the curve representing an air velocity of 110 ft./sec. would be chosen. This points out that the trend of these curves is completely reversed in changing the pipe inclination from 0° to 90°. This reversal is caused by change in the slope from positive, in Fig. 25, to negative, in Fig. 28. It should be noticed that at the two smaller pipe inclinations, the pressure drop for a given throughput does not vary excessively with air velocity. However, at the two larger pipe angles, the pressure drop is significantly dependent upon the air velocity.

It can be observed from Figs. 29, 30, 31, and 32 that the slope of the curves increase as the pipe inclination varies from 0° to 90°. This is caused by the increase in the pressure drop differential, between any two constant throughput curves, as the pipe angle increases. This cause is evident if a comparison is made between Fig. 25 and Fig. 28.

Another point which is very well illustrated by Fig. 32 is that the slope of the individual curves, for one pipe angle, increases as air velocity decreases. This can be explained by the use of Fig. 28. As the air velocity increases, the pressure differential, between any two of the constant throughput curves, decreases, thus causing the slope of the lines in Fig. 32 to increase. The reason for this increase can be traced directly to the increase in the static head loss as the air velocity decreases. This trend, of course, reverses direction at some angle between 0° and 32.73° where the slope of the curves in Fig. 25 reach zero and become negative as it is in Fig. 26.

An analysis of Figs. 30, 31, and 32 gives the impression that it is more economical, from a power standpoint, to maintain a very high air velocity. While it is not the object of this research to discuss power requirements, the above statement warrants a brief explanation. The statement is true only from the standpoint of head loss due to the presence of the solid phase. When the entire power requirement is considered, the situation reverses direction. The explanation of this reversal lies in the fact that the horse-power required to move air alone is proportional to the cube of the fan R.P.M. Thus, while it is advantageous to operative at high velocities from the standpoint of energy loss due to the presence of the solid phase, this advantage is more than offset by the additional power input required to increase the air velocity. Another argument for operating at low air velocities is that less damage will result from impact of the particles with the pipe wall as they round corners in the pipe line, or are deflected at the pipe outlet.

This concludes the discussion of the results presented in the eight graphs on pages 61 and 62. The next two items to be discussed are the two tables in Fig. 35 and 36. These two tables, one representing the lowest and the other the highest throughput tested, are presented to give a quick comparison of the inter-relation between throughput, pipe inclination and air velocity.

From either Fig. 35 or 36, it is possible to make the following pressure drop comparisons for soft white winter wheat being conveyed, at a constant rate, through a 3.89 inch I.D. tube.

1. Hold air velocity constant and vary the pipe angle.
2. Hold pipe angle constant and vary the air velocity.
3. Vary both air velocity and pipe inclination.

In addition, by varying the throughput, a comparison of the effect of this variable on the resultant pressure drop can be made.

Δh_s (in./ft.) For a throughput of 25.93 #/min.

Air Velocity ft./sec.	Pipe Inclination			
	0.0°	32.73°	62.5°	90.0°
60	0.0190	0.0369	0.0570	0.0645
70	0.0200	0.0333	0.0470	0.0522
80	0.0208	0.0320	0.0420	0.0458
90	0.0213	0.0312	0.0390	0.0421
100	0.0220	0.0310	0.0374	0.0400
110	0.0228	0.0310	0.0363	0.0385

Fig. 35. Effect of pipe inclination and air velocity on pressure drop due to the solid phase (air drop excluded).

Δh_s (in./ft.) For a throughput of 57.82 #/min.

Air Velocity ft./sec.	Pipe Inclination			
	0.0°	32.73°	62.5°	90.0°
60	0.0433	0.0826	0.1256	0.1436
70	0.0450	0.0754	0.1045	0.1168
80	0.0469	0.0711	0.0930	0.1030
90	0.0484	0.0696	0.0864	0.0935
100	0.0500	0.0697	0.0832	0.0884
110	0.0519	0.0698	0.0816	0.0856

Fig. 36. Effect of pipe inclination and air velocity on pressure drop due to the solid phase (air drop excluded).

SUMMARY AND CONCLUSIONS

Equations have been derived which enable the design engineer to calculate the pressure drop, due to the conveyance of solid particles, for any pneumatic conveying system. For any specific condition, the equations depend only on the experimentally determined friction factor (f_s). These equations were presented under the Theory Section and were derived in the Appendix.

The design and construction of the test apparatus is illustrated under the Apparatus Section. The procedure followed during the tests and the results of these tests are given in the next two sections.

The figures on pages 59, 61, and 62 represent the most important data presented. Fig. 23 represents the experimental friction factor (f_s) which was used to calculate the graphs shown on pages 61 and 62. These graphs represent a comparison between the experimental and theoretical results. It is felt that these two agree closely enough to assume that the equations developed are valid, over the range tested, for wheat flowing in a 3.89 inch pipe. As previously mentioned, these equations were developed on the basis of initial assumptions set forth by Hariu and Molstad (20) and Pinkus (30). While the equations developed have proved valid for various throughputs, pipe inclinations, and air velocities, they can not be assumed generally applicable until their validity is proved in a larger diameter pipe.

Specific equations for soft white winter wheat

The two equations which are of most use to the design engineer are 6 and 8. Restating these equations:

$$v_s = \frac{-2C_3}{C_2 - \sqrt{C_2^2 - 4C_1C_3}} \qquad (8)$$

Where:

$$C_1 = \frac{0.2 A_p P_a}{m g} - \frac{f_s}{2D}$$

$$C_2 = \frac{-0.04 A_p P_a v_a}{m g} - \frac{2D A_p \mu_a}{m g d}$$

$$C_3 = \frac{0.2 A_p P_a v_a^2}{m g} + \frac{2D A_p \mu_a}{m g d} v_a - g \sin\theta$$

And:

$$\Delta H = \frac{f_s v_s L_D G_s}{2D g P_{H_2O}} + \frac{G_s L_D}{v_s P_{H_2O}} \sin\theta + \frac{f_a L_D v_a^2 P_a}{2D g P_{H_2O}} \qquad (6)$$

Now with "f_s" known from Fig. 23 and "v_s" calculated from equation 8, it is possible to predict the pressure loss by the use of equation 6 for steady state flow, in feet of water.

These equations can be considerably simplified for any one type of particle and atmospheric condition. By making use of the physical properties of the soft white winter wheat used in this study and by assuming dry air at a temperature of 50° F., equation 6 and 8 become:

$$v_s = \frac{-2 C_3}{C_2 - \sqrt{C_2^2 - 4 C_1 C_3}} \qquad (8_a)$$

Where:

$$C_1 = 0.0227 - \frac{f_s}{2D}$$

$$C_2 = -0.0454\, v_a - 0.02858$$

$$C_3 = 0.0227\, v_a^2 + 0.02858\, v_a - 32.2 \sin\theta$$

And:

$$\Delta H = (2.49)10^{-4} \frac{f_s v_s G_s L_D}{D} + 0.01604 \frac{G_s}{v_s} L_D \sin\theta + (1.9)10^{-5} \frac{f_a L_D v_a^2}{D} \quad (6_a)$$

The assumptions which limit the use of equations $8_{(a)}$ and $9_{(a)}$ are as follows:

1. The particles being conveyed must be wheat with physical properties similar to those of the wheat used in this experiment.
2. Dry air at a temperature of 50° F.
3. An atmospheric pressure of 14.7 pounds per square inch.
4. The solids' friction factor (f_s) is as given in Fig. 23.

The variation of head loss with changing atmospheric conditions is small, however, if extreme accuracy is desired, the origional equations 6 and 8 should be used. It should also be remembered that the head loss in feet of water, as calculated from equation 6 or $6_{(a)}$ is only one of three of the major pressure losses encountered in an actual pneumatic conveying system. Either of these equations give the pressure drop which results after steady state conditions prevail. By this, it is implied that the particles no longer have any appreciable acceleration. In this experiment, this point occurred approximately 24 feet beyond the 180° bend for all pipe inclinations. There was a slight increase in this distance as the inclination increased. However, since the exact point at which particle acceleration ended was not

important, the values were not recorded. Any one of the pressure drops observed were valid as long as they were recorded beyond this point. The other two types of pressure losses which, while very important, were not investigated in this study are:

1. Pressure loss due to the acceleration of the particles to their steady state velocity.
2. Pressure loss due to any bends or elbows in the pipe line.

An actual example will now be given to illustrate the use of equations 6 and 8. It should be remembered that while the following example assumes that "f_s" is valid for any pipe diameter, this has not been experimentally verified.

Wheat is being conveyed at a rate of 5,500 #/hr., with an air velocity of 75 feet per second, through a six inch diameter tube at an inclination of 40° with the horizontal. Calculate the pressure drop in 60 feet of this tube after steady state conditions prevail (particle acceleration equals zero). The atmospheric conditions under which the system will operate are:

1. Air temperature of 60° F.
2. Air pressure of 14.7 p.s.i.
3. Relative humidity of 50%.

Since these conditions differ from those upon which equations $6_{(a)}$ and $8_{(a)}$ were based, it is necessary to use equations 6 and 8.

Solution:

The method of attack is as follows:

1. Solve equation 8 for the average particle velocity (v_s).
2. Use this value in equation 6 to determine the pressure drop in feet of water.

To solve these equations, the following constants will be needed:

1. Physical properties of the wheat are as given on page 52.
2. v_a = 75 ft./sec.
3. f_a = 0.028 (From Reference 6)
4. f_s = 0.0102 (From Fig.23)
5. μ_a = 12.2 x 10^{-6} #/ft. sec.
6. ρ_a = 0.0763 #/ft.^{3}
7. D = 0.5 ft.
8. L_D = 60 ft.
9. $G_s = \frac{5500}{\pi 0.25^2 \times 3600} = 7.775$ #/ft.^{2} sec.

Calculation of "v_s" from equation 8:

$$v_s = \frac{-2C_3}{C_2 - \sqrt{C_2^2 - 4C_3C_1}}$$

Where:

$$C_1 = \frac{0.2 A_p \rho_a}{mg} - \frac{f_s}{2D}$$

$$C_1 = \frac{(0.2)(120.5 \times 10^{-6})(0.0763)}{82.6 \times 10^{-6}} - \frac{0.0102}{2(0.5)}$$

$$C_1 = 0.01185$$

$$C_2 = -\left[\frac{0.4 A_p v_a \rho_a}{m g} + \frac{20 A_p \mu_a}{m g d}\right]$$

$$C_2 = -\left[\frac{(0.4)(120.5\times10^{-6})(75)(0.0763)}{82.6\times10^{-6}} + \frac{(20)(120.5\times10^{-6})(12.2\times10^{-6})}{(82.6\times10^{-6})(12.39\times10^{-3})}\right]$$

$$C_2 = -3.311$$

$$C_3 = \frac{0.2 A_p \rho_a v_a^2}{m g} + \frac{20 A_p \mu_a v_a}{m g d} - g \sin\theta$$

$$C_3 = \frac{(0.2)(120.5\times10^{-6})(0.0763)(75)^2}{82.6\times10^{-6}} +$$

$$\frac{(20)(120.5\times10^{-6})(12.2\times10^{-6})(75)}{(82.6\times10^{-6})(12.39\times10^{-3})} - 32.2 \sin 40^\circ = 106.46$$

So:

$$v_s = \frac{-(2)(106.46)}{-3.311 - \sqrt{(-3.311)^2 - (4)(106.46)(0.01185}}$$

$$v_s = 37.9 \text{ FT./SEC.}$$

Now calculate ΔH from equation 6:

$$\Delta H = \frac{f_s v_s L_D \sigma_s}{2 D g \rho_{H_2O}} + \frac{\sigma_s L_D}{v_s \rho_{H_2O}} \sin\theta + \frac{f_a L_D v_a^2 \rho_a}{2 D g \rho_{H_2O}}$$

$$\Delta H = \frac{(0.0102)(37.9)(60)(7.775)}{(2)(0.5)(32.2)(62.4)} + \frac{(7.775)(60)\ \mathrm{Sin}\ 40^\circ}{(37.9)(62.4)} +$$

$$\frac{(0.028)(60)(75)^2(0.0763)}{(2)(0.5)(32.2)(62.4)}$$

$$\Delta H = 0.0886 + 0.1265 + 0.358$$

ΔH = 0.5731 feet of water for 60 feet of pipe.

This is the pressure drop which would result after steady state conditions prevail. If an actual systerm were to be designed, the other two types of losses, mentioned earlier, would have to be added to the above figure to obtain the total head loss.

As was brought out in the Review of Literature, very few investigators have studied pressure losses in farm pneumatic systems. Segler (32) does set up an equation which can be used to predict the pressure loss in a horizontal pipe, provided the appropriate friction factor is used. Pressure drops were calculated using Segler's equations for the throughputs shown in Fig. 25, and the values thus obtained were then compared with the theoretical values shown in the figure. The deviation between the two values ranged from 1.7 per cent to 10.1 per cent with the present investigator's values being consistently lower. This is the only check which could be made on the experimental and theoretical results obtained in this experiment, as no reference could be found in which the pressure drop due to solid particles had been investigated at various pipe inclinations between 0° and 90°.

The data presented in the graphs on pages 61 and 62 were completely discussed in the previous section; however, a more condensed discussion will now be presented.

The principal objective of Figs. 25, 26, 27, and 28 was to compare the experimentally determined points. A small consistent deviation is evident at the two highest throughputs in Fig. 26, 27, and 28. At these throughputs, the experimental points seem to fall slightly below the experimental curves. As was mentioned earlier, this deviation is insignificant from a practical standpoint but from a theoretical point of view, an explanation should be offered. This explanation is as follows: The solids' friction factor (f_s) was based on pressure drops observed with the pipe in a horizontal position and then was in turn used to calculate the theoretical curves at the other inclinations. Since the component of pressure drop which "f_s" represents is that of the particles sliding on the pipe wall, it is possible that there was more sliding when the pipe was horizontal than when it was vertical. If this were true, this component of head loss would be less at larger pipe angles than was indicated by "f_s". This explanation seems feasible; however, there is a possibility that it may be incorrect. Actual observation of the flow of particles with the pipe in the horizontal and vertical positions indicated no difference in the uniformity of the density of the dispersed solids. It should be remembered that this was only a visual observation and that there may have been a difference which was not evident to the naked eye.

The two trends which are illustrated in Figs. 25, 26, 27, and 28 should be again emphasized. The first is that the pressure drop

increases as pipe inclination increases. This is due directly to the increasing static head component of pressure loss which is a function of the sine of the pipe angle. The second trend is an increase in pressure drop as the air velocity decreases and the pipe angle increases. This is due to increased density of the solids within the pipe as the air velocity decreases. This in itself would have no effect on the static head component if the pipe were horizontal, since the static head is, by definition, zero. However, it can be seen that if the pipe were at some angle other than 0^{o}, this increased weight of solids per unit volume of pipe would appreciably increase the static head. This same argument can be presented to explain the pressure drop increasing, with an increasing rate, at large pipe angles and low air velocities. If it were possible to increase the air velocity to infinity, the curves in Figs. 26, 27, and 28 would reach a point at which they became linear and possessed a slope equal to the curve in Fig. 25 for any given throughput. This is most evident in Fig. 26 where at high air velocities the curves are again becoming linear.

Figs. 29, 30, 31, and 32 illustrate that there is a linear relationship between pressure drop and flow rate for a given air velocity. As would be expected, the pressure drop increases as flow rate increases for any given air velocity. Also, due to the static head component, the pressure drop is less at higher velocities for pipe angles of 32.73^{o} or greater. A more thorough explanation of this phenomenon is given in the previous section.

Fig. 34 shows the two components which make up the total pressure drop due to the presence of solid particles in the air stream. Fig. 37 shows this curve combined with the pressure drop due to the air alone.

The combined curve represents the total drop which would be present in an actual system under a specific set of conditions. It is evident that there is an optimum velocity at which the total head loss will be a minimum. From a power input standpoint, this still would not be the most economical velocity at which to operate. This velocity can be determined from the H.P. curve in the same figure. In this particular case, an air velocity of approximately 62 feet per second required a minimum H.P. The point of minimum H.P. will always occur near the lowest, if not at the lowest, air velocity which will convey the particles. If the exact point is desired, a graph similar to Fig. 37 can be determined for any specific design requirement by the use of Fig. 23 and equations 6 and 8.

Practical operating range

As was just shown, it is generally desirable to keep the air velocity as low as possible to reduce the power required for operation at a given capacity. In this experiment, the minimum air velocity possible ranged from approximately 65 feet per second for a horizontal pipe to 70 feet per second for a vertical pipe. These figures agree very well with those given by Segler (32) and Kleis (22).

It was stated by both Segler (32) and Kleis (22) that the maximum throughput is almost entirely dependent upon weight, rather than volume. In other words, a given size pipe would convey a greater volume of oats per hour than wheat, the pounds per hour remaining constant. Kleis (22) found that an upper limit for a four inch horizontal pipe was 58.4 pounds per minute. The results of this experiment indicate that it is possible to exceed this value, but the system operated much more smoothly when the throughput was kept below this limit.

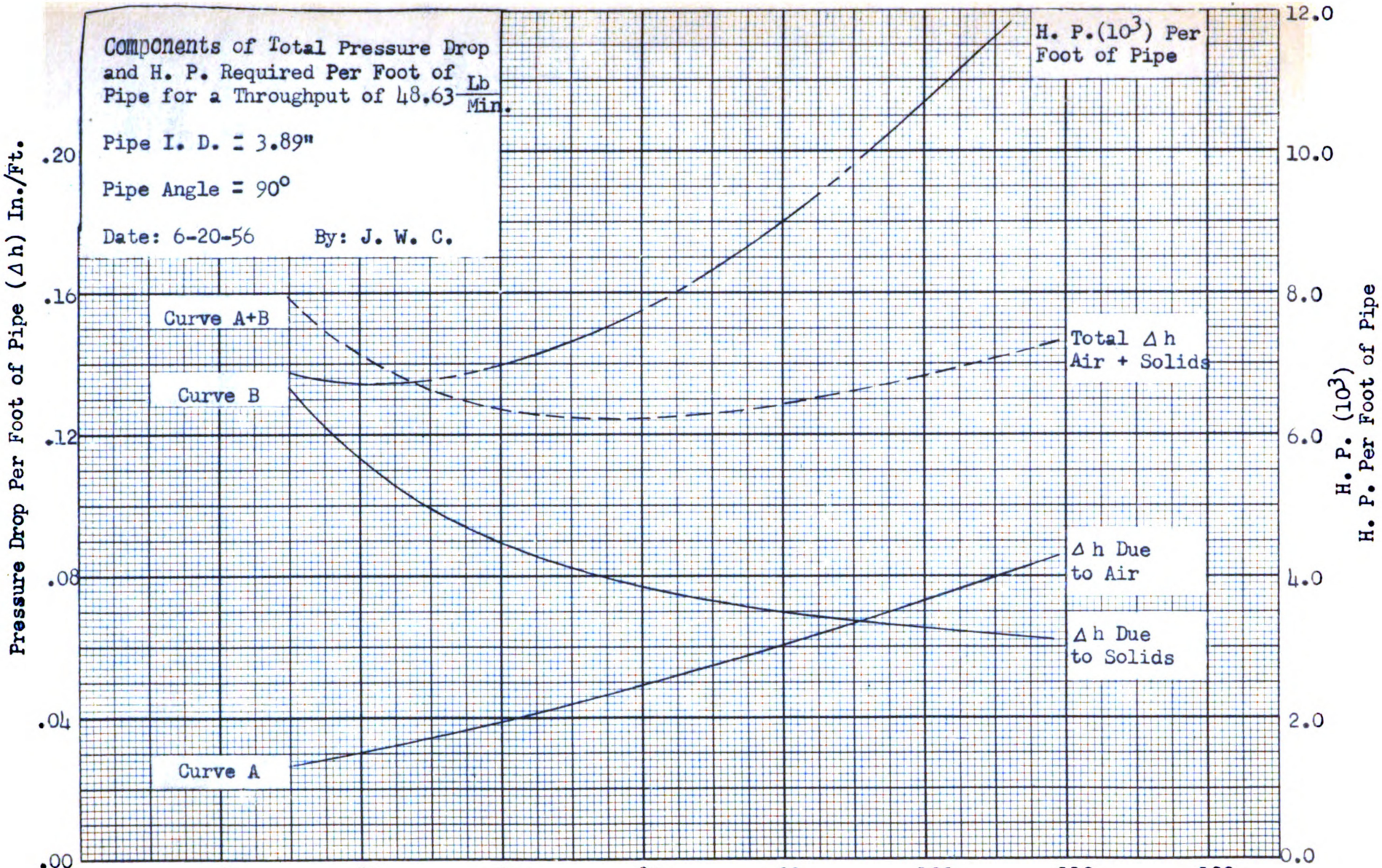
Components of Total Pressure Drop and H. P. Required Per Foot of Pipe for a Throughput of 48.63 Lb/Min.
Pipe I. D. = 3.89"
Pipe Angle = 90°
Date: 6-20-56 By: J. W. C.
H. P.(10³) Per Foot of Pipe
Curve A+B
Curve B
Curve A
Total Δ h Air + Solids
Δ h Due to Air
Δ h Due to Solids
Pressure Drop Per Foot of Pipe (Δ h) In./Ft.
H. P. (10³) H. P. Per Foot of Pipe
.00
.04
.08
.12
.16
.20
0.0
2.0
4.0
6.0
8.0
10.0
12.0
50
60
70
80
90
100
110
120
Air Velocity Ft./Sec.

Fig. 37

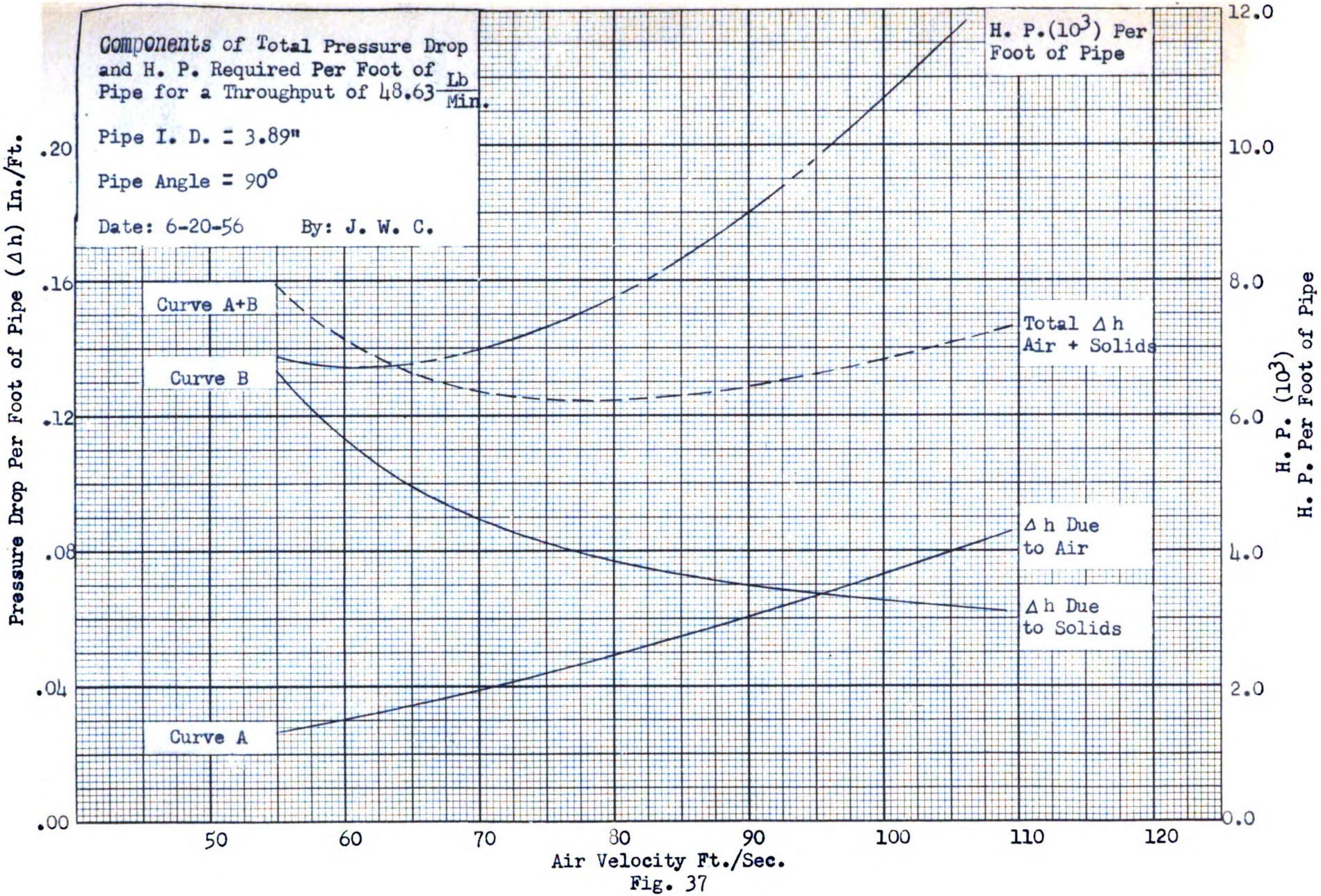
Components of Total Pressure Drop and H. P. Required Per Foot of Pipe for a Throughput of 48.63 Lb/Min.
Pipe I. D. = 3.89"
Pipe Angle = 90°
Date: 6-20-56 By: J. W. C.
H. P.(10³) Per Foot of Pipe
Curve A+B
Curve B
Curve A
Total Δ h Air + Solids
Δ h Due to Air
Δ h Due to Solids
Pressure Drop Per Foot of Pipe (Δ h) In./Ft.
H. P. (10³) H. P. Per Foot of Pipe
.00
.04
.08
.12
.16
.20
0.0
2.0
4.0
6.0
8.0
10.0
12.0
50
60
70
80
90
100
110
120
Air Velocity Ft./Sec.

Fig. 37

The number of feet of pipe which could be included in an actual system depends upon the following:

1. Capacity of the blower.
2. Size of pipe used.
3. Throughput desired.
4. Pipe inclination.
5. Number of elbows and bends.

To determine this value for any specific situation, it is necessary to add the steady state drop, as determined from equation 6, to the inlet drop and the drop due to any elbows which are present. The latter two losses were not investigated during this research.

Possible analysis of silage particles.

If the theoretical analysis, as presented to date, can be proved valid for all common types of farm grains, the next step would be to investigate the possibility of applying the theory to the flow of forages in a truly pneumatic system. This presents many problems, both theoretical and practical. From a theoretical stand point, it would be almost impossible to determine a true solid's velocity since the particles are not uniform. The best method of attack would be to determine a representative "v_s" from the pressure drop data obtained. This method of obtaining "v_s" was completely discussed earlier in this report. The value obtained might be interpreted to represent an average velocity of all the particles in the pipe. The range which this average velocity represents would vary considerably from light to heavy particles.

While most grains approach the shape of a sphere, particles of forages are more closely represented by a cylinder. Since the value

of the coefficient of resistance (C), as used to calculate "f_s" for wheat, was determined from true spheres, it would be necessary to obtain such a graph for cylinders when the analysis is applied to forages.

A serious practical problem, which makes it difficult to obtain experimental results, is the method by which the particles could be introduced into the air stream. Due to the low density of the material, it is necessary that the pipe have a minimum diameter of seven inches. It appears doubtful that the bucket wheel feeder used with grains would work satisfactorily with forages. There is a possibility that with the larger pipe, the injector feeder might operate effectively. However, the most promising possibility seems, at the present time, to be some type of auger-feeder.

From the previous remarks, it can be seen that the problem of truly pneumatic transportation of forages is much more complicated to analyze, both theoretically and practically, than the flow of grains. Another point which should be remembered is that, to data, forages have been transported almost entirely in impeller systems. However, the work of Kleis (22) indicates that in a system where particle damage is not important, thus allowing the blower to operate at a high R.P.M., the particles do receive appreciable energy from the air stream. This indicates that the analysis as presented for truly pneumatic systems, may have some application in impeller systems which use high speed blowers and convey material long distances.

Summary of conclusions

1. The experimental data obtained, to date, indicates the theoretical analysis was valid.

2. Pressure drop due to the solids increased as pipe inclination increased.
3. Pressure drop due to the solids increased as the air velocity decreased and the pipe angle increased.
4. A linear relationship existed between the pressure drop due to the solids and the flow rate, for any given velocity.
5. Pressure drop due to the solids increased as flow rate increased for any given air velocity and pipe inclination.
6. The static head component of pressure drop decreased as air velocity increased.
7. The sliding component of pressure drop increased linearly as air velocity increased.
8. The horse power input to the system was a minimum when the air velocity was as low as possible, this value being determined by the point at which the air ceased to convey the particles.
9. The minimum air velocity which will carry wheat particles in a horizontal pipe was 65 feet per second. In a vertical pipe this velocity was 70 feet per second.
10. The maximum throughput of wheat in the 3.89 inch diameter pipe, which allowed smooth operation, was 57.82 pounds per minute.

RECOMMENDATIONS FOR FUTURE STUDY

1. Check the equations, which were developed, with pipe of varying diameters.

To date, the theoretical equations have been proved for wheat flowing through a 3.89 inch diameter pipe of varying inclinations. The next logical step is to test the validity of these equations for a larger pipe. If they hold for the latter case, they can be assumed applicable to any farm grain. This leads to the next step which is to calculate friction factors for various other types of grain.

2. Determine "f_s" values for different grains.

After the validity of the equations has been proved for larger diameter pipes, friction factors can be calculated for other types of grain. These values could be computed directly from pressure drop data obtained with either the large or small pipe, since the equations have proved valid for any pipe diameter. It is suggested that the smaller pipe be used because of ease of handling, etc. Actually, only one pipe inclination is needed to obtain enough data to plot a "f_s" curve; however, it is recommended that the data thus obtained be checked at some other pipe inclination.

3. Investigate pressure losses due to forages.

As was mentioned earlier, this is a very difficult problem since forage particles not only vary in size, but also in density, within any one lot. Then if various lots are considered, the length of cut will vary, thus introducing another variable. It is felt that if a friction factor were determined, it would be at best only an approximation.

4 - Study the design of an inlet which could be used to introduce forage particles into the air stream of a truly pneumatic system.

It was mentioned earlier that the best possibility, to date, was the use of an auger-feeder. This, however, requires additional construction and extra power source, both of which are undesirable. A method is needed by which the desired capacity could be effieiently handled.

5 - Study the relationship between pressure drop in a high speed impeller system and a truly pneumatic system.

In a low speed impeller system of the type discussed in the Introduction of this study, the particles receive most of their energy directly from the impeller wheel; therefore, pressure drop is not an important parameter in the design of such a system. In a high speed impeller system, the particles still receive appreciable energy from the impeller wheel, but they also can obtain energy from the air stream to replenish that lost throughout the piping system. This indicates that the pressure loss, per foot of pipe, would have a direct effect upon the distance the particles could be conveyed for a given blower. It is possible that after a reasonable length of pipe, this pressure loss could be calculated from the equations developed in this report.

6 - Establish an exact method of determining particle velocity.

Determining the particle velocity has been a major problem confronting all who have investigated pressure losses due to the pneumatic conveyance of solid particles. Since it is an important parameter in the development of any type of theoretical pressure loss equation, its value must be determined. Three possible methods of

determining "v_s" were discussed in the Apparatus section of this study. The shut-off gates finally decided upon proved rather inaccurate. This made it necessary to calculate "v_s" from the pressure drop values, which is perfectly valid, but cuts down the number of variables left to check the theoretical equations from two to one. If it would have been possible to experimentally determine "v_s" at one inclination, the value for any other inclination could have been calculated and compared with the experimental results.

Some method is needed which would permit the determination of an average "v_s" without interruption of the flow within the pipe. This would allow the readings to be taken much faster and also more accurately.

7 - Investigate losses with various elbow radii.

Segler (32) has made a brief study of this subject, however, the possibilities are by no means completely exhausted. Segler (32) discusses the paths followed by the individual particles as they travel around 90° bends of various radii. He presented the internal wear of the pipe wall as proof of his statements.

It would seem advantageous to obtain a glass elbow and run these same tests while recording the motion of the particles with a high speed camera. From these observations, perhaps further theoretical work could be accomplished.

8 - Study acceleration losses immediately following bends.

Segler (32) gives data which allows the pressure drop in certain size elbows to be represented by the drop in an equivalent length of straight pipe. After expressing a given elbow in terms of equivalent feet of pipe, equation 6 and 8 can be used to predict the pressure loss.

Since the data that Segler (32) presents is limited, it is felt that more work is needed for elbows of other configurations. Data of this kind is essential in the actual design of a pneumatic system since equation 6 and 8 are not valid for sections of pipe in which the particles are being accelerated.

9. Determine a method by which inlet losses could be reduced.

Segler (32) gives a very thorough coverage to the subject of pressure losses with various types of inlets. He expresses these losses, as he did for elbows, in terms of equivalent feet of straight pipe. His data shows that these losses are an appreciable percentage of the total pressure loss. It is therefore felt that it would be advantageous to design an inlet which would reduce these losses.

The principal inlet loss occurs because the particles have no initial velocity, parallel to the pipe wall, at the instant they enter the air stream. If a small impeller could be used to accelerate the particles to their terminal velocity, before they enter the air stream, the inlet acceleration drop could be neglected, thus reducing the total head required considerably.

APPENDIX

So that the body of this report may be kept as clear as possible, the derivations of the principal equations have been omitted in the theoretical analysis and presented in this Appendix.

The first three sections will be devoted to the derivation of the pressure drop equations.

Due to the complex nature of the system to be analyzed, it was necessary to make the following simplifying assumptions before proceeding with the pressure drop analysis:

1. The component of velocity perpendicular to the pipe wall will be small relative to that parallel to the wall.
2. The total pressure drop along any section of pipe, after steady state conditions are reached ($a_p = 0$), is made up of three components, these being:
   a. That due to the air alone. This is assumed to remain constant with or without particles in the air stream.
   b. That due to the particles striking each other and the pipe wall.
   c. That due to the solids' static head.
3. The coefficient of resistance, as applied to freely falling bodies, can be applied to particles moving in an air stream.
4. A friction equation of the Fanning or Darcy-Weisbach type will account for the energy loss due to impact between the individual particles and the pipe wall.

The equation of motion will be developed from the following free body diamgram of a single particle. This particle is experiencing an upward acceleration due to an air stream, whose direction is tangent to the path of motion at the instant considered.

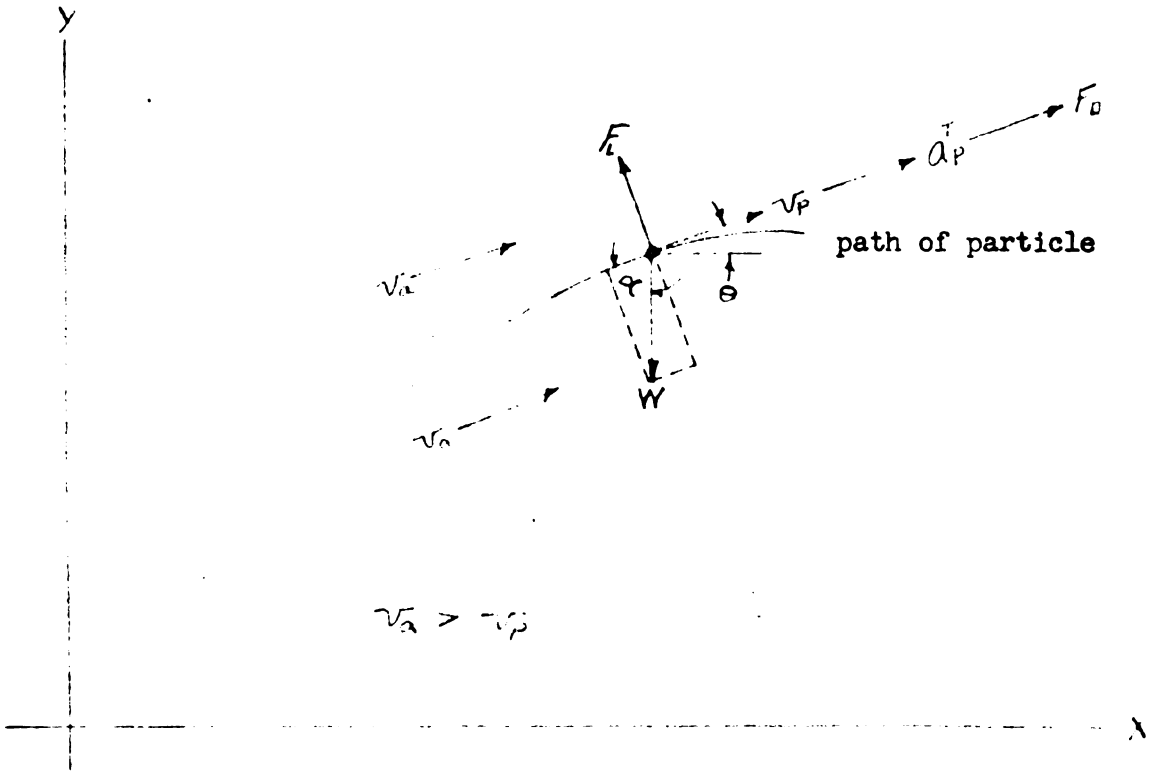

Fig. 38. Free body diagram of a single particle experiencing an upward acceleration due to an air stream, whose direction is tangent to the path of motion.

Section I

Derivations of equations 5 and 6 are as follows:

Applying Newton's Law ($\Sigma F = ma$) to the system in Fig. 38, and summing the forces in the tangential direction gives:

$$\Sigma F_{(Tan)} = F_D - W\left(\frac{\rho_p - \rho_a}{\rho_p}\right) Cos.\ \alpha$$

Expressing α in terms of θ:

$$\alpha = 90 - \theta$$

$$Cos.\alpha = Cos\,(90 - \theta)$$

$$Cos.\alpha = Sin.\ \theta$$

Giving:

$$\Sigma F_{(Tan)} = F_D - W\left(\frac{\rho_p - \rho_a}{\rho_p}\right) Sin.\ \theta = ma \qquad (1)$$

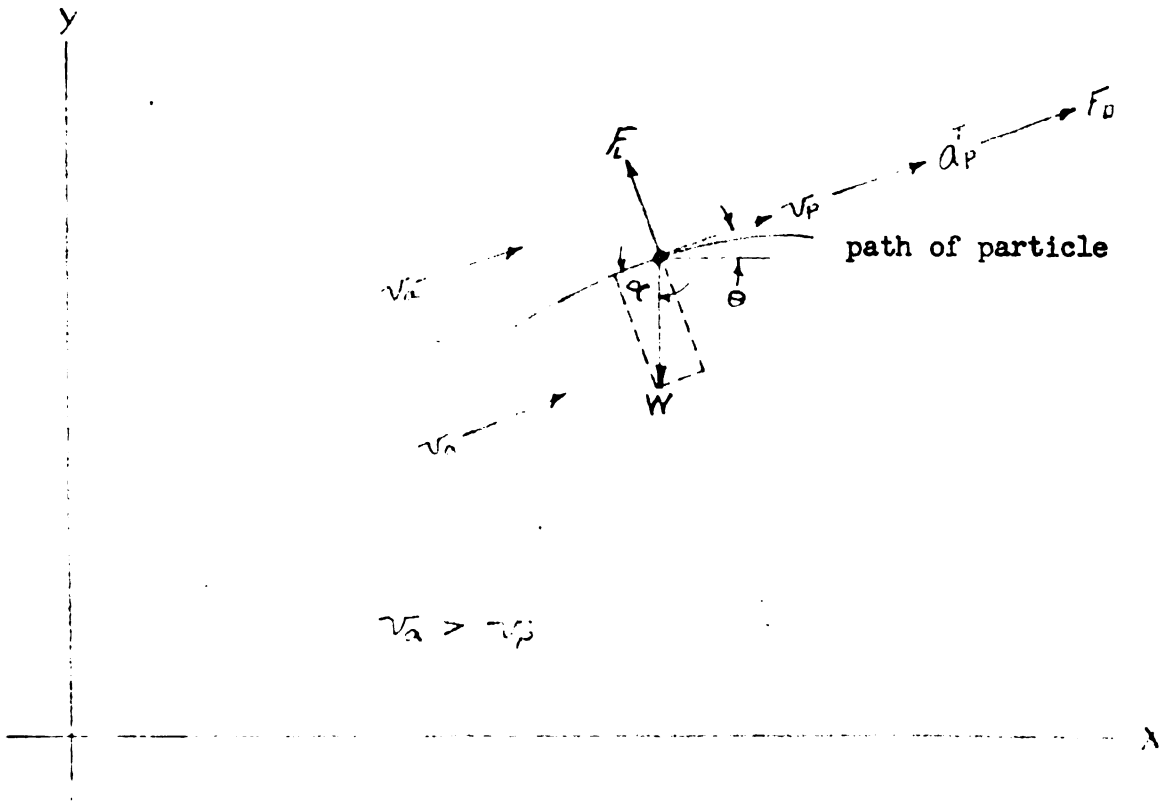

Fig. 38. Free body diagram of a single particle experiencing an upward acceleration due to an air stream, whose direction is tangent to the path of motion.

Section I

Derivations of equations 5 and 6 are as follows:

Applying Newton's Law ($\Sigma F = ma$) to the system in Fig. 38, and summing the forces in the tangential direction gives:

$$\Sigma F_{(Tan)} = F_D - W\left(\frac{\rho_p - \rho_a}{\rho_p}\right) Cos.\ \alpha$$

Expressing α in terms of θ:

$$\alpha = 90 - \theta$$

$$Cos.\ \alpha = Cos\ (90 - \theta)$$

$$Cos.\ \alpha = Sin.\ \theta$$

Giving:

$$\Sigma F_{(Tan)} = F_D - W\left(\frac{\rho_p - \rho_a}{\rho_p}\right) Sin.\ \theta = ma \qquad (1)$$

F_D, as defined by Goldstein for free falling spheres, is equal to $\frac{\rho_a v^2 C A}{2g}$. This will also apply to a system where the air is moving, as well as the particle, if the relative velocity $v_{a/s} = (v_a - v_s)$ is substituted for "v". Equation 1 now becomes:

$$\frac{\rho_a (v_a - v_s)^2}{2g} C A_p - mg\left(\frac{\rho_p - \rho_a}{\rho_p}\right) \sin\theta = m \frac{dv_s}{dt} \qquad (2)$$

This equation would hold for one particle in an air stream, but if several particles are simultaneously in the stream, an additional term must be included to account for energy lost due to collisions with other particles. In addition, if the particles are enclosed in a pipe, this term must account for losses due to sliding on the pipe wall.

Following the suggestions of other investigators, the Darcy-Weisbach friction equation will be added to account for these extra losses encountered in actual pneumatic transporting systems.

$$H = \frac{f_s L_D v_s^2}{2Dg}$$

Rearranging this so it will represent the force exerted per particle (F):

$$\Delta P = \frac{f_s L_D v_s^2}{2Dg} \rho_{ds}$$

Now multiplying both sides by A_p gives:

$$(\Delta P) A_p = \frac{f_s L_D v_s^2}{2Dg} \rho_{ds} A_p$$

$L_D \rho_{ds}$ = pounds of solids per square foot of pipe cross-section. This multiplied by the area of one particle gives weight "W" of that particle. Therefore, the above equation can be written as:

$$F = \frac{f_s v_s^2}{2D} \frac{W}{g}$$

$$F = \frac{f_s v_s^2}{2D} m$$

Adding this term to those of equation 2 gives the complete differential equation of motion for the system.

$$\frac{dv_s}{dt} = \frac{\rho_a (v_a - v_s)^2}{2mg} C A_p - g\left(\frac{\rho_s - \rho_a}{\rho_s}\right) \sin\theta - \frac{f_s v_s^2}{2D} \qquad (3)$$

When steady state conditions prevail ($\frac{dv_s}{dt} = 0$), equation 3 can be re-written in the following form:

$$\frac{\rho_a (v_a - v_s)^2}{2g} C A_p = mg\left(\frac{\rho_s - \rho_a}{\rho_s}\right) \sin\theta + \frac{f_s v_s^2}{2D} n. \qquad (4)$$

Since for grains and forages the term ($\frac{\rho_s - \rho_a}{\rho_s}$) is very nearly unity, it will be neglected in the remaining pressure drop calculations.

It can be seen from this force balance that the energy loss due to solids' friction plus that due to the static head will be equal to that supplied by the drag correlation.

Converting each of the force terms in equation 4 into equivalent expressions for pressure drop per unit of mass flow results in the following expressions:

1. For the impact between particles and the tube wall the Darcy-Weisback friction equation gives:

$$\Delta H_{fs} = \frac{f_s L_D v_s^2}{2Dg} \frac{\rho_{ds}}{\rho_{H_2O}}$$

Expressing this as drop per unit of mass flow by using $G_s = \rho_{ds} v_s$ gives:

$$\frac{\Delta H_{fs}}{L G_s} = \frac{f_s v_s}{2Dg \rho_{H_2O}}$$

ΔH_{fs} is in terms of feet of H_2O.

2. For the static head expression:

$$\Delta H_{sh} = \frac{\rho_{ds}}{\rho_{H_2O}} L \sin\theta$$

Expressing this as drop per unit of mass flow gives:

$$\frac{\Delta H_{sh}}{L G_s} = \frac{\sin\theta}{\rho_{H_2O} v_s}$$

From the two previous expressions, it can be seen that the pressure drop is a linear function of both the solids' velocity and flow rate. The validity of this expression will be tested by analyzing the experimental data.

3. From the drag correlation:

$$F_{(Per\ Particle)} = \frac{\rho_a C A_p (v_a - v_s)^2}{2g}$$

The number of particles present in "L" feet of pipe will be equal to:

$$N = \frac{Total\ W}{W\ per\ Particle} = \frac{\rho_s V_D}{W_p} = \frac{G_s}{v_s} \frac{A_D L_D}{W_p}$$

$$N = \frac{G_s A_D L_D}{v_s V_p \rho_p}$$

So the total force exerted on the solids in "L" feet of pipe is:

$$F_{(TOT.)} = \frac{\rho C A_t (v_a - v_s)^2}{2g} \left(\frac{G_s A_D L_D}{v_s V_p \rho_p} \right)$$

Changing to drop per unit of mass flow:

$$\frac{F_{(TOT)}}{L_D A_C} = \frac{\#}{ft.^2 ft.} = \frac{\rho_a C A_p (v_a - v_s)^2}{2g} \left(\frac{G_s}{v_s V_p \rho_p} \right)$$

$$\frac{\Delta H_s}{L_D G_s} = \frac{\rho_a C A_p (v_a - v_s)^2}{\rho_{H_2O}\, 2g\, v_s V_p \rho_p}$$

Substituting these equivalent expressions into the force equation 4 gives:

$$\frac{\rho_a C A_p (v_a - v_s)^2}{\rho_{H_2O}\, 2g\, v_s V_p \rho_p} = \frac{Sin\ \theta}{\rho_{H_2O}\, v_s} + \frac{f_s v_s}{2Dg\, \rho_{H_2O}}$$

Solving this equation for "f_s" gives:

$$\frac{\rho_a C A_p (v_a - v_s)^2}{\rho_{H_2O}\, 2g\, v_s V_p \rho_p} = \frac{2Dg\, Sin\,\theta + f_s v_s^2}{2Dg\, v_s \rho_{H_2O}}$$

$$D\rho_a C A_p (v_a - v_s)^2 = V_p \rho_p 2Dg\, Sin\,\theta + V_p \rho_p f_s v_s^2$$

$$f_s = \frac{D\left[f_a C A_p (v_a - v_s)^2 - 2g V_p \rho_p \sin\theta\right]}{V_p \rho_p v_s^2} \qquad (5)$$

This expression will be used to experimentally determine "f_s" from the observed data.

As previously mentioned, the total head loss for a given length of pipe (assuming steady state flow exists) is made up of three parts.

$$\Delta H = \Delta H_{sf} + \Delta H_{sh} + \Delta H_a$$

If the steady state condition has not been attained, another term must be added to account for the pressure loss during the acceleration period. This term will amount to an appreciable percentage of the total drop near the inlet.

$$\Delta H = \frac{f_s v_s L_D G_s}{2Dg \rho_{H_2O}} + \frac{G_s}{v_s \rho_{H_2O}} L_D \sin\theta + \frac{f_a L_D v_a^2 \rho_a}{2Dg \rho_{H_2O}} \qquad (6)$$

(ΔH is in feet of H_2O).

"f_s" is the experimentally determined value of the solids' friction. "f_a" is the value of Darcy-Weisback friction factor for the flow of air through pipes. The equivalent Fanning friction factors would be one fourth as large as those used in the Darcy-Weisback equation.

Section II

The derivation of equation 7 is as follows:

Restating equation 3:

$$\frac{dv_s}{dt} = \frac{\rho_a (v_a - v_s)^2}{2mg} C A_p - g\left(\frac{\rho_s - \rho_a}{\rho_s}\right) \sin\theta - \frac{f_s v_s^2}{2D} \qquad (3)$$

This differential equation will now be solved for "v_s" in terms of the other variables.

Letting:

$$\frac{\rho_a C A_p}{2mg} = x$$

$$\frac{f_s}{2D} = Y$$

$$3\left(\frac{\rho_s - \rho_a}{\rho_s}\right) \sin\theta = Z$$

Substituting into 3 gives:

$$\frac{dv_s}{dt} = X(v_a - v_s)^2 - Z - Y v_s^2$$

Separating variables yields:

$$dt = \frac{dv_s}{X v_a^2 - 2X v_a v_s + (X-Y) v_s^2 - Z}$$

Since "v_a" is constant during the acceleration period, the following substitutions can be made:

$$K_1 = X v_a^2 - Z$$

$$K_2 = 2X v_a$$

$$K_3 = (X - Y)$$

Substituting these expressions into the above equation:

$$dt = \frac{dv_s}{K_3 v_s^2 - K_2 v_s + K_1}$$

Integrating both sides yields:

$$t = \frac{1}{\sqrt{-4K_1K_3 + K_2^2}} \ln \frac{2K_3 v_s - K_2 - \sqrt{-4K_1K_3 + K_2^2}}{2K_3 v_s + K_2 + \sqrt{-4K_1K_3 + K_2^2}} + C$$

Replacing the second set of constants with the first gives:

$$\sqrt{-4K_1K_3 + K_2^2} = \sqrt{-4(X v_a^2 - Z)(X - Y) + 4X^2 v_a^2}$$

$$= 2\sqrt{-(X^2 v_a^2 - ZX - YX v_a^2 + ZY) + X^2 v_a^2}$$

$$= 2\sqrt{ZX + YX v_a^2 - ZY}$$

The expression for "t" now becomes:

$$t = \left[\frac{1}{2\sqrt{ZX + YX v_a^2 - ZY}}\right] \left[\ln \frac{2(X-Y)v_s - 2X v_a - 2\sqrt{ZX + YX v_a^2 - ZY}}{2(X-Y)v_s - 2X v_a + 2\sqrt{ZX + YX v_a^2 - ZY}}\right] + C$$

Since the initial conditions are $v_s = 0$ when $t = 0$, the constant of integration (C) is equal to:

$$C = \frac{-1}{2\sqrt{ZX - YX v_a^2 - ZY}} \ln \frac{-2X v_a - 2\sqrt{ZX + YX v_a^2 - ZY}}{-2X v_a + 2\sqrt{ZX + YX v_a^2 - ZY}}$$

Replacing "C" with its equivalent expression yields:

$$t = \left[\frac{1}{2\sqrt{ZX + YX v_a^2 - ZY}}\right] \left[\ln \frac{2(X-Y)v_s - 2X v_a - 2\sqrt{ZX + YX v_a^2 - ZY}}{2(X-Y)v_s - 2X v_a + 2\sqrt{ZX + YX v_a^2 - ZY}} - \ln \frac{-2X v_a - 2\sqrt{ZX + YX v_a^2 - ZY}}{-2X v_a + 2\sqrt{ZX + YX v_a^2 - ZY}}\right]$$

Making use of the following logarithmic idenity ($\ln A - \ln B = \ln \frac{A}{B}$) the equation for "t" becomes:

$$t = \left[\frac{1}{2\sqrt{ZX + YX v_a^2 - ZY}}\right] \ln \left[\frac{2(X-Y)v_s - 2X v_a - 2\sqrt{ZX + YX v_a^2 - ZY}}{2(X-Y)v_s - 2X v_a + 2\sqrt{ZX + YX v_a^2 - ZY}} \left[\frac{-2X v_a - 2\sqrt{ZX + YX v_a^2 - ZY}}{-2X v_a + 2\sqrt{ZX + YX v_a^2 - ZY}}\right]\right]$$

To facilitate the simplification of the previous expression, let:

$$K_4 = [illegible]$$

$$K_5 = 2 \, [illegible] \, v_a$$

$$K_6 = \sqrt{Z X + Y X v_a^2 - Z Y}$$

$$t = \frac{1}{2K_6} \ln \left[\frac{K_4 - K_5 - 2K_6}{K_4 - K_5 + 2K_6}\right] \left[\frac{-K_5 + 2K_6}{-K_5 - 2K_6}\right]$$

$$t = \frac{1}{2K_6} \ln \frac{[illegible] K_5 + K_4 2K_6 - 2K_6^2 + K_5^2}{-K_4 [illegible] - 2K_5^2 + K_5^2 - K_4 K_5}$$

Clearing this expression of K_4 and K_5:

$$t = \frac{1}{2K_6} \ln \frac{-2(X-Y) v_s 2 X v_a + 2(X-Y) v_s K_6 [illegible]}{-2(X-Y) [illegible] K_6 - 4(Z X + Y X v_a^2 - Z Y) + [illegible]}$$

$$\frac{4(Z X + Y X v_a^2 - Z Y) + 4 X^2 v_a^2}{4 X^2 v_a^2 [illegible] (X-Y) v_s 2 X v_a}$$

$$t = \frac{1}{2K_6} \ln \frac{v_s\left[-(X-Y) X v_a + (X-Y) K_6\right] - Z(X-Y) + (X-Y) v_a^2 X}{v_s\left[-(X-Y) K_6 - (X-Y) X v_a\right] - Z(X-Y) + (X-Y) v_a^2 X}$$

$$t = \frac{1}{2K_6} \ln \frac{v_s\left[K_6 - X v_a\right] - Z + v_a^2 X}{v_s\left[-K_6 - X v_a\right] - Z + v_a^2 X}$$

$$t = \frac{1}{2K_6} \ln \frac{v_a^2 X - Z - v_s (X v_a - K_6)}{v_a^2 X - Z - v_s (X v_a + K_6)}$$

Clearing this expression and transposing into exponential form gives:

$$\frac{1}{e^{-K_6 t 2}}\left[v_a X - Z - v_s (X v_a + K_6)\right] = v_a^2 X - Z - v_s (X v_a - K_6)$$

$$\frac{v_a^2 X}{e^{-2K_6 t}} - \frac{Z}{e^{-2K_6 t}} - \frac{v_s X v_a}{e^{-2K_6 t}} - \frac{v_s K_5}{e^{-2K_6 t}} - v_a^2 X + Z + v_s X v_a - v_s K_6 = 0$$

Solving for "v_s":

$$v_s\left(\frac{X v_a}{e^{-2K_6T}} - \frac{K_6}{e^{-2K_6T}} + X v_a - K_6\right) = -\frac{v_a^2 X}{e^{-2K_6T}} + \frac{Z}{e^{-2K_6T}} + v_a^2 X - Z$$

$$v_s\left(\frac{e^{-2K_6T} X v_a - K_6 e^{-2K_6T} - X v_a K_6}{e^{-2K_6T}}\right) = \frac{Z - v_a^2 X + e^{-2K_6T} v_a^2 X - Z e^{-2K_6T}}{e^{-2K_6T}}$$

$$v_s = \frac{Z - v_a^2 X + e^{-2K_6T} v_a^2 X - Z e^{-2K_6T}}{X v_a e^{-2K_6T} - K_6 e^{-2K_6T} - X v_a - K_6}$$

Simplifying this expression:

$$v_s = \frac{X v_a^2 (e^{-2K_6T} - 1) + Z - Z e^{-2K_6T}}{e^{-2K_6T}(X v_a - K_6) - X v_a - K_6}$$

$$v_s = \frac{-\left[v_a^2 X (1 - e^{-2K_6T}) - Z + e^{-2K_6T} Z\right]}{-\left[X v_a + K_6 - e^{-2K_6T}(X v_a - K_6)\right]}$$

$$\lim_{t \to \infty} v_s \quad \frac{v_a^2 X - Z}{X v_a + \sqrt{ZX + YX v_a^2 - ZY}}$$

Removing the constants :

$$v_s = \frac{\frac{v_a^2 \rho_a C A_p}{2mg} - g\left(\frac{\rho_s - \rho_a}{\rho_s}\right) \sin\theta}{\frac{\rho_a C A_p v_a}{2mg} + \sqrt{\frac{\rho_a C A_p g}{2mg}\left(\frac{\rho_s - \rho_a}{\rho_s}\right)\sin\theta + \frac{v_a^2 f_s \rho_a C A_p}{202mg} - g\left(\frac{\rho_s - \rho_a}{\rho_s}\right)\frac{f_s}{20}\sin\theta}}$$

As mentioned in the development of the pressure drop equations, the value of $\left(\frac{\rho_s - \rho_a}{\rho_s}\right)$ will be almost unity and hence will be neglected in the remaining calculations.

$$v_s = \frac{\frac{v_a^2 \rho_a C A_p}{2mg} - g \sin\theta}{\frac{\rho_a C A_p v_a}{2mg} + \sqrt{\frac{\rho_a C A_p}{2m}\sin\theta + \frac{v_a^2 f_s \rho_a C A_p}{202mg} - \frac{g f_s}{20}\sin\theta}}$$

$$V_s = \frac{\frac{V_a^2 \rho_a C A_p - 2 m g^2 \sin\theta}{2 m g}}{\frac{\rho_a C A_p V_a}{2 m g} + \frac{\sqrt{2 g L \rho_a C A_p \sin\theta + V_a^2 f_s \rho_a C A_p - 2 m g^2 f_s \sin\theta}}{2\sqrt{m g D}}}$$

$$V_s = \frac{\frac{V_a^2 \rho_a C A_p - 2 m g^2 \sin\theta}{2 m g}}{\frac{\rho_a C A_p V_a L + \sqrt{m g L}\sqrt{2 g L \rho_a C A_p \sin\theta + V_a^2 f_s \rho_a C A_p - 2 m g^2 f_s \sin\theta}}{2 m g D}}$$

$$V_s = \frac{D(\rho_a C A_p V_a^2 - 2 m g^2 \sin\theta)}{\rho_a C A_p V_a D + \sqrt{m g D}\sqrt{\rho_a C A_p (2 g L \sin\theta + f_s V_a^2) - 2 m g^2 f_s \sin\theta}} \quad (7)$$

Derived assuming "C" equals a constant. Valid for RN between 10^3 and $10^{4.5}$.

Section III

The derivation of equation 8, in which "C", as a function of "RN", equals $0.4 + \frac{24}{RN}$, is as follows:

Restating equation 3:

$$\frac{dV_s}{dt} = \frac{C \rho_a A_p (V_a - V_s)^2}{2 m g} - g\left(\frac{\rho_s - \rho_a}{\rho_s}\right)\sin\theta - \frac{f_s V_s^2}{2 L} \quad (3)$$

Again disregarding the $\left(\frac{\rho_s - \rho_a}{\rho_s}\right)$ term for this application, and letting:

$$\frac{A_p \rho_a}{2 m g} = r$$

$$\frac{f_s}{2 D} = Y$$

$$g \sin\theta = Z$$

Let $RN = X V_{a/s}$ where $X = \frac{d \rho_a}{\mu_a}$

Substituting this into the expression for "C" yields:

$$C = 0.4 + \frac{40}{X(V_a - V_s)}$$

Now replacing the terms in equation 3 with these notations:

$$\frac{dV_s}{dt} = \left[0.4 + \frac{40}{X(V_a - V_s)}\right] r(V_a - V_s)^2 - Y V_s^2 - Z$$

$$\frac{dV_s}{dt} = 0.4\, r(V_a - V_s)^2 + \frac{r}{X} 40 (V_a - V_s) - Y V_s^2 - Z$$

$$\frac{dV_s}{dt} = 0.4\, r V_s^2 - 0.8\, r V_a V_s + 0.4\, r V_s^2 + \frac{r}{X} 40 V_a - \frac{r}{X} 40 V_s - Y V_s^2 - Z$$

$$\frac{dV_s}{dt} = V_s^2(0.4r - Y) + V_s\left(-0.8 r V_a - \frac{r}{X} 40\right) + 0.4 r V_a^2 + \frac{r}{X} 40 V_a - Z$$

Simplifying this expression by letting:

$$0.4r - Y = C_1$$

$$-0.8 r V_a - 40\frac{r}{X} = C_2$$

$$0.4 r V_a^2 + 40\frac{r}{X} V_a - Z = C_3$$

The above equation now becomes:

$$\frac{dV_s}{dt} = C_1 V_s^2 + C_2 V_s + C_3$$

Separating variables:

$$dt = \frac{dV_s}{C_1 V_s^2 + C_2 V_s + C_3}$$

Integrating both sides:

$$t = \frac{1}{\sqrt{Q}} \ln \frac{2 C_1 V_s + C_2 - \sqrt{Q}}{2 C_1 V_s + C_2 + \sqrt{Q}} + C$$

Where:

$$Q = C_2^2 - 4 C_3 C_1$$

Since the initial conditions are $v_s = 0$ when $t = 0$, the constant of integration (C) is equal to:

$$C = -\frac{1}{\sqrt{Q}} \ln \frac{C_2 - \sqrt{Q}}{C_2 + \sqrt{Q}}$$

Substituting this into the equation for "t" and simplifying gives:

$$t = \frac{1}{\sqrt{Q}} \ln \left[\frac{(2 C_1 v_s + C_2 - \sqrt{Q})(C_2 + \sqrt{Q})}{(2 C_1 v_s + C_2 + \sqrt{Q})(C_2 - \sqrt{Q})} \right]$$

$$t = \frac{1}{\sqrt{Q}} \ln \left[\frac{C_2^2 - Q + 4 C_1 v_s \sqrt{Q}}{2 C_1 C_2 v_s - Q - 2 C_1 v_s \sqrt{Q} + C_2^2} \right]$$

Transposing this into exponential form:

$$\left(\frac{1}{e^{-T\sqrt{Q}}} \right) \left(C_2 2 C_1 v_s - Q - 2 C_1 v_s \sqrt{Q} + C_2^2 \right) = C_2^2 - Q + 4 C_1 v_s \sqrt{Q}$$

Solving for "v_s":

$$\frac{2 C_1 C_2 v_s}{e^{-T\sqrt{Q}}} - \frac{Q}{e^{-T\sqrt{Q}}} - \frac{2 C_1 v_s \sqrt{Q}}{e^{-T\sqrt{Q}}} + \frac{C_2^2}{e^{-T\sqrt{Q}}} - C_2^2 + Q - 4 C_1 v_s \sqrt{Q} = 0$$

$$\frac{v_s (2 C_1 C_2 - 2 C_1 \sqrt{Q}) + C_2^2 - Q - C_2^2 e^{-T\sqrt{Q}} + Q e^{-T\sqrt{Q}} - 4 C_1 v_s \sqrt{Q} e^{-T\sqrt{Q}}}{e^{-T\sqrt{Q}}} = 0$$

$$v_s = \frac{Q - C_2^2 + C_2^2 e^{-T\sqrt{Q}} - Q e^{-T\sqrt{Q}} + 4 C_1 v_s \sqrt{Q} e^{-T\sqrt{Q}}}{2 C_1 C_2 - 2 C_1 \sqrt{Q}}$$

Determine the terminal velocity which the particles will reach by letting $t \rightarrow \infty$

$$\lim_{t \to \infty} v_s = \frac{Q - C_2^2}{2C_1C_2 - 2C_1\sqrt{Q}}$$

$$v_s = \frac{C_2^2 - 4C_3C_1 - C_2^2}{2C_1C_2 - 2C_1\sqrt{C_2^2 - 4C_1C_3}}$$

$$v_s = \frac{-2C_3}{C_2 - \sqrt{C_2^2 - 4C_1C_3}} \qquad (8)$$

The constants for the above equations are:

$$C_1 = \frac{0.2 A_p \rho_a}{mg} - \frac{f_s}{2D}$$

$$C_2 = \frac{-0.4 A_p \rho_a v_a}{mg} - \frac{20 A_p \mu_a}{mgd}$$

$$C_3 = \frac{0.2 A_p \rho_a v_a^2}{mg} + \frac{20 A_p \mu_a}{mgd} v_a - g \sin\theta$$

Derived assuming "C" = $0.4 + \frac{40}{RN}$ Valid for "RN" between $10^{0.5}$ and $10^{4.25}$.

Section IV

This section of the Appendix will deal with the development of the orifice equations. Fig. 39 will be used as a basis for the development of equations 14 and 15.

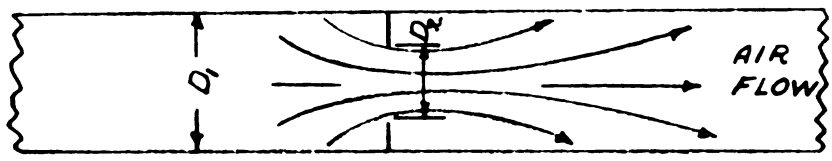

Fig. 39. Crossection of conveyor pipe near the orifice.

Writing the energy balance between points "1" and "2" (see Fig. 39) gives:

$$\frac{v_1^2}{2g} + \frac{P_1}{\rho_a} + Z_1 = \frac{v_2^2}{2g} + \frac{P_2}{\rho_a} + Z_2 \qquad (9)$$

Since the pipe lies in the horizontal plane, $Z_1 = Z_2$.

Collecting terms and assuming that $A_1 v_1 = A_2 v_2$:

$$H_1 - H_2 = \frac{v_2^2 - \left(\frac{A_2}{A_1}\right)^2 v_2^2}{2g}$$

This expression is valid only for pressure differentials less than ten inches of water, as was previously mentioned. Solving this equation for "v_2" gives:

$$v_2 = \sqrt{\frac{2g(H_1 - H_2)}{1 - \left(\frac{A_2}{A_1}\right)^2}}$$

Since the actual velocity at point "2" will never reach the above theoretical value due to frictional losses, it is necessary to introduce a velocity correction factor (C_v).

$$v_2 = C_v \sqrt{\frac{2g(H_1 - H_2)}{1 - \left(\frac{D_2}{D_1}\right)^4}} \qquad (10)$$

Substituting Q/A_2 for v_2 in equation 10 yields an expression for the flow rate in ft^3/sec.

$$Q = A_2 C_v \sqrt{\frac{2g(H_1 - H_2)}{1 - \left(\frac{D_2}{D_1}\right)^4}}$$

However, due to the reduced area of the stream at the pressure tap, another correction factor (C_A) must be included in the above equation. For convenience, "C_V" and "C_A" will be lumped into one coefficient - "C".

$$Q = C A_2 \sqrt{\frac{2g(H_1 - H_2)}{1 - \left(\frac{D_2}{D_1}\right)^4}} \qquad (11)$$

To reduce the number of steps required to calculate "Q", the pressure differential will now be converted from feet of air to inches of water.

"h" equals head in inches of water $= \dfrac{H \rho_a 12}{62.38}$

From the equation of a perfect gas: $\rho_a = \dfrac{W}{V} = \dfrac{P}{RT}$

So: $H = \dfrac{h\ 62.38\ T\ 53.3}{12\ P} = 276.8 \dfrac{T}{P} h$

In this expression, "T" and "P" are, respectively, the absolute temperature and pressure of the surrounding air.

Substituting this value of "H" into equation 11 gives:

$$Q = C A_2 \sqrt{\frac{2g\ 276.8 \frac{T}{P}(h_1 - h_2)}{1 - \left(\frac{D_2}{D_1}\right)^4}} \qquad (12)$$

This equation can be further simplified by assuming the pressure and temperature of the surrounding air to be, respectively, 29.92 inches of Hg and 50° F. Therefore:

T absolute $460 + 50 = 510°$ absolute.

P absolute $\frac{29.92}{12}$ 13.6 x 62.38 2117 #/ft.^{2}.

Assuming $T = 510^{\circ}$ absolute and $P = 2117$ #/ft.^{2}, equation 11 can be written as:

$$Q = \frac{65.6\ C\ A_2}{\sqrt{1 - \left(\frac{D_2}{D_1}\right)^4}} \sqrt{h_1 - h_2} \qquad (13)$$

The velocity of air can be found by substituting $v_1 A_1$ for Q in equation 13. This substitution yields:

$$v_1 = \frac{65.6\ A_2\ C}{A_1 \sqrt{1 - \left(\frac{D_2}{D_1}\right)^4}} \sqrt{h_1 - h_2}$$

Simplifying:

$$v_1 = \frac{65.6\ C}{\sqrt{\left(\frac{D_1}{D_2}\right)^4 - 1}} \sqrt{h_1 - h_2} \qquad (14)$$

For any given pipe and orifice, equation 14 reduces to:

$$v_1 = K \sqrt{\Delta h}$$

where $K = \dfrac{65.6\,C}{\sqrt{\left(\frac{D_1}{D_2}\right)^4 - 1}}$ and $\Delta h = h_1 - h_2$

The value of "C" given by Ref. 29 is 0.80.

For this specific installation, $D_1 = 3.89$ inches and $D_2 = 3.125$ inches, thus:

$$K = \frac{65.6 \times 0.80}{\sqrt{\left(\frac{3.89}{3.125}\right)^4 - 1}} = 44.25$$

Equation 14 now becomes:

$$v_1 = 44.25 \sqrt{\Delta h} \qquad (15)$$

The limitations on equation 15 are:

1. Valid only for this installation.
2. Derived assuming T = 50° F.
3. Derived assuming P = 2117 #/ft.^{2}.

Section V

The possibility of error due to the compressibility of the air in a long pipe will be examined assuming a pipe to be 150 feet long with steady state conditions existing. The static pressure loss along this pipe, and thus the head differential, will be assumed to be 15 inches of water.

If the temperature is assumed to remain constant, the following can be written:

$$P_1 V_1 = P_2 V_2$$

Where "P_1" will be assumed to equal 431 inches of water. This fixes "P_2" at 416 inches of water.

This gives a volume ratio of:

$$\frac{V_1}{V_2} = \frac{P_1}{P_2} = \frac{416}{431} = 0.966$$

Since volume is proportional to area for a given length of pipe:

$$\frac{H_1}{H_2} = 0.966 \qquad H_1 = 0.966\, H_2$$

Now since Q = VA:

$$V_2 = \frac{Q}{H_2} = \frac{Q}{H_1}(0.966) = 0.966\, V_1$$

So $V_2 = 0.966\ V_1$ with Δh equal to 15 inches of water.

Section VI

The possibility of error due to the loss of air through the bucket wheel feeder air vents will now be considered.

The volume of one chamber in the bucket wheel feeder is 0.0363 ft.^{3}. Since the paddle wheel rotates at 40 R.P.M., the air loss per minute is as follows:

air loss (#/min.) = .0363 x 6 x 40 = 8.71 ft.^{3}/min.

This accounts for the loss due to the rotation of the paddles. An additional loss of 3 ft.^{3}/min. will be added to account for any additional loss due to air leakage by the paddles. This gives a total loss of 11.71 ft.^{3}/min. By assuming the air velocity within the pipe to be 101 ft./sec., the air flow rate would be 500 ft.^{3}/min.

So:

$$\% \text{ loss} = \frac{11.71}{500} \times 100 = 2.35\%$$

REFERENCES

1. Albright, C. W., and others. "Pneumatic Feeder for Finely Divided Solids." Chemical Engineering. 56: 108-111. June, 1949.

2. Allen, J. R., and others. Heating and Air Conditioning. 6th ed., McGraw-Hill Book Company, N.Y., 1946.

3. Belden, D. H., and Kessel, L. S. "Pressure Drops." Industrial and Engineering Chemistry. 41: 1174-1178. June, 1949.

4. Berge, O. I. "Design and Performance Characteristics of the Flywheel Type Forage Harvester Cotterhead." Agricultural Engineering Journal. 32: 85-91. February, 1951.

5. Besley, H. E., and Humphries, W. R. "Machines Designed for Harvesting and Storing Grass Silage." Agricultural Engineering Journal. 22: 125-126. April, 1941.

6. Brown, A. I., and Marko, S. M. Introduction to Heat Transfer. 2nd ed., McGraw-Hill Book Company, N.Y., 1951.

7. Bryson, A. E. "An Experimental Investigation of Transonic Flow Past Two-Dimensional Wedge and Circular-Arc Sections." National Advisory Committee for Aernatuics. Technical Note 2560, Washington, November, 1951.

8. Challey, H. "The Pumping of Granular Solids in Fluid Suspension." Engineering. 149: 230-231. March, 1940.

9. Cramps, W. "Pneumatic Transport Plants." Chemistry and Industry. 44: 207-213. 1925.

10. Dallavalle, J. M. Micromeritics. 2nd ed., Pitman Publishing Corporation, N. Y., 1948.

11. Davis, R. F. "The Conveyance of Solid Particles by Fluid Suspension." Engineering. 140: 1-3. July 5, 1935.

12. Davis, R. F. "The Conveyance of Solid Particles by Fluid Suspension." Engineering. 140: 124-125. August 2, 1935.

13. Duffee, F. W. "Efficiently Filling the Silo." Agricultural Engineering Journal. 6: 4-12. January, 1925.

14. Duffee, F. W. "A Study of Factors Involved in Ensilage Cutter Design." Agricultural Engineering Journal. 7: 84-87. March, 1926.

15. Duffee, F. W. "Mechanizing Forage Crop Handling." Agricultural Engineering Journal. 20: 47-49. February, 1939.

16. Duffee, F. W. "New Developments in Forage Harvesting." Agricultural Engineering Journal. 24: 182-183. June, 1943.

17. Fanning, J. T. A Treatise on Hydraulic and Water Supply Engineering. 4th ed., D. Van Nostrand Publishers, N.Y., 1884.

18. "Fluid Mechanics." The Encyclopedia Americana. 11: 401b-401d.

19. Goldstein, S. Modern Developments in Fluid Mechanics. University Press, Oxford, England, 1938.

20. Harin, O. H., and Molstad, M. C. "Pressure Drop in Vertical Tubes in Transport of Solids by Gases." Industrial and Engineering Chemistry. 41: 1148-1160. 1949.

21. Jennings, M. "Pneumatic Conveying in Theory and Practice." Engineering. 150: 361-363. 1940.

22. Kleis, R.W. "Moving Feed From Storage to Feeding Point." Agricultural Engineering Journal. 35: 655. September, 1954.

23. Lapple, C. E., and Shepherd, C. B. "Calculation of Particle Trajectories." Industrial and Engineering Chemistry. 32: 605-616. May, 1940.

24. Lees, A. "Crop Moving by Air Force." Farmer and Stock Breeder. 62: 1493. 1948

25. Longhouse, A. D., and others. "The Application of Fluidization to Conveying Grain." Agricultural Engineering Journal. 31: 349 July, 1950.

26. Longhouse, A. D. "Performance Characterisitcs of Long Hay Blowers." Agricultural Engineering Journal. 30: 439-441. September, 1949.

27. Matheson, G. L., and others. "Dynamics of Fluid-Solid Systems." Industrial and Engineering Chemistry. 41: 1099-1104. 1949.

28. Miller, J. T. A Course in Industrial Instrument Technology. United Trade Press, London.

29. Ower, E. The Measurement of Air Flow. Chapman and Hall, Limited, London, 1927.

30. Pinkus, O. "Pressure Drops in the Pneumatic Conveyance of Solids." Journal of Applied Mechanics. 19: 425-431. December, 1952.

31. Rhodes, T. J. Industrial Instruments for Measurement and Control. McGraw-Hill Book Company, N.Y., 1941.

32. Segler, G. Pneumatic Grain Conveying. National Institute of Agricultural Engineering, Wrest Park, England, 1951.

33. Segler, G. "Calculation and Design of Cutterhead and Silo Blower." Agricultural Engineering Journal. 32: 661-663. December, 1951.

34. Sternbruegge, G. W. "Air Flow in the Main Duct of a Barn Hay-Drying System." Agricultural Engineering Journal. 27: 217-218. May, 1946.

35. Stewart, E. A. "Cutting Ensilage With Electric Motors." Agricultural Engineering Journal. 9: 175-179. June, 1928.

36. "The Pneumatic Transport of Grain." Engineering. 111: 205. February, 1921.

37. Vogt, E. G., and White, R. R. "Friction in the Flow of Suspensions." Industrial and Engineering Chemistry. 40: 1731-1738. 1948.

38. Whisler, P. A. "The Field Forage Harvester." Agricultural Engineering Journal. 28: 497-499. November, 1947.

39. Whisler, P. A., and Frushour, G. V. "Engineer Advance Art of Making Grass Silage." Agricultural Engineering Journal. 34: 315-318. May, 1953.

40. Zink, F. J. "Specific Gravity and Air Space of Grains and Seeds." Agricultural Engineering Journal. 16: 439-440. November, 1935.